



UNIVERSITAT
POLITÈCNICA
DE VALÈNCIA



ESCUELA TÉCNICA
SUPERIOR INGENIERÍA
INDUSTRIAL VALENCIA

INDUSTRIAL ENGINEERING MASTER THESIS

FEASIBILITY STUDY AND PROJECT OF A MULTIMEGAWATT PHOTOVOLTAIC PLANT CONNECTED TO THE SPANISH NATIONAL GRID

AUTHOR: ANGELA VENEZIA

SUPERVISOR: CARLOS ROLDAN BLAY

SUPERVISOR: CARLOS ROLDAN PORTA

Academic year: 2019-20

This elaborate is made available by Angela Venezia under terms and conditions applicable to Creative Commons Public License Attribution-NonCommercial-NoDerivatives 4.0 International (CC BY-NC-ND 4.0).
The full text is available at <https://creativecommons.org/licenses/by-nc-nd/4.0/>

Acknowledgments

I would like to thank my family and friends who supported me during my studies.

I also thank the “Universitat Politècnica de València” that hosted me for a year, showing me a different system from the Italian one. In particular, I am grateful to professor Carlos Roldán Blay and Carlos Roldán Porta who offered a subject to me and followed me in the course of the thesis.

Resumen

Este trabajo presenta el estudio de viabilidad y el proyecto para una instalación solar centralizada de 5 MWp con el objetivo de generar energía e inyectarla en la red. Esta instalación se encuentra en Chelva, Comunidad Valenciana, España. Los primeros capítulos están destinados a introducir todos los conceptos para comprender los resultados de la tesis presentando el estado del arte del sector fotovoltaico. Por lo tanto, los temas principales son las energías renovables, la energía solar fotovoltaica, las tecnologías de los módulos, el inversor y otros elementos de una instalación, desde cables hasta protecciones. Después de estos capítulos, el núcleo del proyecto se ocupa de los argumentos de las opciones de diseño. El emplazamiento de la instalación, la preparación del suelo y la elección de los diversos componentes se describen con justificación, resultados y cálculos de verificación cuando resulta necesario. Luego se estudian las protecciones y la puesta a tierra. Termina con una estimación de la producción y un análisis económico. Los apéndices muestran un código de MATLAB, planos de AutoCAD y los cálculos de conductores de manera extensa.

Palabras clave: instalación solar, energías renovables, módulos solares, estación MV, protecciones, producibilidad, análisis económico.

Abstract

This work presents the feasibility study and the project for a centralized 5 MWp solar installation with the aim of generating energy and injecting it into the grid. This installation is located in Chelva, Valencian Community, Spain. The first chapters are intended to introduce all the concepts for understanding the results of the thesis by presenting the state of the art of the photovoltaic sector. The main topics are therefore renewable energy, photovoltaic solar energy, module technologies, the inverter and other elements of an installation, from cables to protections. After these chapters, the heart of the project deals with arguments of the design choices. The installation site, the soil preparation and the choice of the various components are described with justification, results and verification calculations where necessary. Protections and earthing are then studied. It ends with a producibility and economic analysis. The appendices show a MATLAB code, AutoCAD drawings and the calculations of cable in an extensive manner.

Keywords: photovoltaic plant, renewable energy, solar modules, MV power station, protections, producibility, economic analysis.

Index

Acknowledgments.....	2
Resumen.....	3
Abstract	4
Table of Figures	9
List of tables	12
MEMORIA.....	13
0. Introduction.....	14
1. Introduction to renewable energy	15
1.1. Renewable energy.....	15
1.2. Renewables in Spain.....	16
2. Photovoltaic solar energy.....	17
2.1. Pre-Definitions.....	17
2.2. Solar radiation	17
2.2.1. Solar radiation meters.....	19
2.3. Solar radiation over the desired geographical point.....	20
2.4. Radiation on surfaces and Air Mass	21
2.5. Azimuth, solar altitude and declination angles	21
2.6. Correct placement of the panels.....	23
3. The solar panel	25
3.1. The photovoltaic effect	25
3.2. Technologies of the cells	27
3.3. The photovoltaic module	27
3.4. The Protection diodes	28
3.5. Standards of the modules	29
3.6. Equivalent circuit of a photovoltaic cell	29
3.7. Electrical parameters.....	31
3.8. Dependence of the I-V curve on environmental conditions	33
3.9. Strings, arrays and photovoltaic field.....	34
4. The photovoltaic inverter	36

4.1.	DC/DC converter.....	36
4.2.	DC/AC converter.....	36
4.2.1.	The stand-alone inverter.....	38
4.2.2.	The grid inverter.....	39
4.3.	Maximum power point.....	40
4.4.	Configurations of the system.....	41
5.	Coupling between inverter and photovoltaic field.....	43
5.1.	Inverter choice.....	43
5.2.	Configuration of the system.....	43
6.	Other elements of the photovoltaic field.....	46
6.1.	Solar string combiner boxes.....	46
6.2.	Support structures.....	46
6.3.	Electric cables.....	48
6.3.1.	General concepts.....	48
6.3.2.	Cables for photovoltaic installations.....	50
6.3.3.	Dimensioning of the cables.....	51
6.4.	Protections.....	55
6.4.1.	Protection against direct contacts.....	55
6.4.2.	Protection against indirect contacts.....	56
6.4.3.	Protection against overcurrent.....	56
6.4.4.	Protection against surge voltage.....	57
6.4.5.	Inverter and grid protection.....	57
6.4.6.	System grounding.....	58
7.	Producibility estimation and economic analysis.....	59
7.1.	Estimation of energy losses.....	59
7.2.	Calculation of the expected annual production.....	61
7.3.	Economic analysis.....	62
7.3.1.	Net present value, NPV.....	62
7.3.2.	Internal rate of return, IRR.....	63
7.3.3.	Discounted payback time, DPB.....	63
8.	Description of the position of the photovoltaic plant.....	64

8.1.	The location	64
8.2.	Place of installation	66
9.	Choice of plant components.....	72
9.1.	Choice of the solar module	72
9.2.	Choice of the inverter.....	75
9.3.	Choice of the configuration.....	77
9.4.	Choice of the solar string combiner box	79
9.5.	Choice of the support structure	80
10.	Photovoltaic field layout	81
10.1.	Calculation of the shadows	81
10.2.	Identification of the strings	83
10.3.	Low voltage connections	84
10.3.1.	Connection of modules	84
10.3.2.	Connection of modules-string combiner box.....	86
10.3.3.	Connection of string combiner box-inverter	89
10.3.4.	Calculation example	92
10.4.	Medium voltage connections.....	96
10.4.1.	Short circuit condition	97
10.4.2.	Thermal criterion.....	98
10.4.3.	Electrical criterion.....	98
10.5.	Ducts.....	99
11.	Protections and system grounding.....	101
11.1.	Protections	101
11.2.	System grounding.....	105
11.2.1.	Low voltage	105
11.2.2.	Medium voltage stations.....	105
11.2.3.	Common ground.....	106
12.	Producibility of the plant.....	110
	PRESUPUESTO	115
13.	Economic analysis.....	116
13.1.	Economic specifications	116

13.2. Economic indices	117
13.2.1. NPV	118
13.2.2. IRR.....	119
13.2.3. DPB	120
Conclusions.....	121
Appendix A	122
Appendix B	131
1. Electrical criterion	132
2. Thermal criterion.....	138
3. Choice of cable: modules-string combiner box.....	143
Appendix C	148
1. Electrical criterion	149
2. Thermal criterion.....	150
Appendix D	152
Bibliography.....	155
Software	156
PLANOS.....	157

Table of Figures

Figure 1: Subdivision of energy source (Source: [1]).....	15
Figure 2: Photovoltaic power installed in Spain from 2007 to 2019 (Source: [2])	16
Figure 3: Types of irradiance (Source https://images.app.goo.gl/inq6FuNUgCHnTMZt8)	18
Figure 4: Solar radiation spectrum: power value at different point of the atmosphere and spectrum subdivision (Source: https://i.stack.imgur.com/lqzTC.png).....	18
Figure 5: Pyranometer (Source: https://images.app.goo.gl/iyA7gALX7YyYnFv5)	19
Figure 6: Calibrated cells (Source: https://images.app.goo.gl/K5zQj7Uf6PL3qeU9).....	19
Figure 7: Pyrheliometer (Source: https://images.app.goo.gl/MbfQ887YNzqWXxnP7).....	20
Figure 8: Global horizontal irradiation (Source: https://images.app.goo.gl/s2QgUsJmZDSd7)	20
Figure 9: AM typical values (Source: https://images.app.goo.gl/vkNwixcHoP73s86WA)	21
Figure 10: Angles of azimuth and solar altitude (Source: https://images.app.goo.gl/6GZJA7G7spK5ZDbZ9)	22
Figure 11: Values assumed by the solar declination during the year (Source: https://images.app.goo.gl/njtJJ9PucQuc9eMv6)	22
Figure 12: Sun's path during the year (Source: https://images.app.goo.gl/Rn6odhywJTn4jJAt5)	22
Figure 13: Distance d between panels with different heights (Source: [1])	24
Figure 14: Structure of (a) undoped silicon (b) n-type silicon (c) p-type silicon (Source: https://images.app.goo.gl/NQATgFMTAZVk)	25
Figure 15: Photovoltaic effect (Source: https://images.app.goo.gl/wWG8i3c7MDMS2tVU6)	26
Figure 16: Polycrystalline, monocrystalline and amorphous panels (Source: https://images.app.goo.gl/GLwhm9QPGmoQnYK87)	27
Figure 17: Photovoltaic module structure (Source: https://images.app.goo.gl/x1GjbcHusWpX4vwS7)	28
Figure 18: Blocking and bypass diodes (Source: https://images.app.goo.gl/X2mm4gKSpNCf9new5). 29	29
Figure 19: Solar cell's electrical circuit (Source: https://images.app.goo.gl/9AT2Ytbf8dzqN5Z87)	29
Figure 20: Characteristic curve in absence of solar radiation (Dark) and with solar irradiance (of 400 and 800 W/m ²) (Source: https://images.app.goo.gl/BNrrHxnF6v6xssrz6).....	31
Figure 21: Current-voltage curve (I-V) of the solar cell (Source: https://images.app.goo.gl/jjFbsojQQ719H1r7).....	31
Figure 22: Power curve of the solar cell (Source: https://images.app.goo.gl/ahS1GMP4ZVRj8E3G9) .	32
Figure 23: Variation of the characteristic curve with irradiance and temperature (Source: https://images.app.goo.gl/ahS1GMP4ZVRj8E3G9)	33

Figure 24: Modules connected in series (Source: <https://images.app.goo.gl/sQNYkdGPftRJ7YWo9>) . 34

Figure 25: Modules connected in parallel (Source: <https://images.app.goo.gl/sQNYkdGPftRJ7YWo9>) 35

Figure 26: Hot spots seen with infrared rays (Source: <https://images.app.goo.gl/Rc61F3ZjZo4cYBYz5>) 35

Figure 27: Simplified layout of a solar system (Source: <https://images.app.goo.gl/pUwjDjWdrvcn4ZM37>) 37

Figure 28: European efficiency inverter curve (Source: <https://images.app.goo.gl/yHuL7Zioa3bTTbA66>) 38

Figure 29: Graphical representation of the algorithm disturbs and observes (Source: <https://images.app.goo.gl/M6Ud1cD5nCVVZFg49>) 40

Figure 30: Graphical representation of the method of incremental conductance (Source: <https://images.app.goo.gl/rJpZijgc5viaUAJHA>) 41

Figure 31: Configurations of the system: a) central inverter; b) String inverters; c) AC modules; d) Multi string inverters (Source: <https://images.app.goo.gl/mXZ1LUPiSauZeZ9bA>) 42

Figure 32: Operation zones of inverter and photovoltaic field (Source: <https://images.app.goo.gl/BLVW6Gd8nrrqzJ2Y9>) 44

Figure 33: Solar string combiner boxes (Source: <https://images.app.goo.gl/v4DHYSZ9Y4CZiM8g6>) .. 46

Figure 34: Installation on the ground, examples of adaptation to the place orography (Source: [8]) . 47

Figure 35: Two-axis solar tracking systems (Source: <https://images.app.goo.gl/y13A1nJJS9KmMyCs8>) 48

Figure 36: Characteristics of a photovoltaic cable (Source: https://www.google.com/url?sa=t&rct=j&q=&esrc=s&source=web&cd=6&ved=2ahUKEWjl1cCdyrr0AhVNCxoKHXztCPMQfjAFegQIARAB&url=http%3A%2F%2Fboj.pntic.mec.es%2Fcrodenas%2Fsolares%2Fut5%2FCables_General%2520cable.pdf&usq=AOvVaw0paOzVgXx283aDFbsueHms) 50

Figure 37: Photovoltaic energy diagram, from production to the measuring point (Source <https://images.app.goo.gl/QjocuTmC9M5g2r617>) 60

Figure 38: Position of the municipality of Chelva, Spain (Source: https://upload.wikimedia.org/wikipedia/commons/thumb/8/88/Spain_location_map.svg/260px-Spain_location_map.svg.png) 64

Figure 39: Position of Chelva in the comarca of Los Serranos (Source: <https://es.goolzoom.com/mapas/>) 64

Figure 40 : Chelva, average temperature and precipitation in the year (Source: <https://es.climate-data.org/europe/espana/comunidad-valenciana/chelva-274765/#climate-table>) 65

Figure 41: Cadastral reference Plot 806 of Polygon 57 (Source: [15]) 66

Figure 42: Litho-geological map of the installation site, located in the hexagon (Source: [17]) 67

Figure 43: Place of installation (Source: [16])	68
Figure 44: Elevation profile in an area of the plot (Source: [16]).....	68
Figure 45: Representation of the soil profiles and of the plot	69
Figure 46: Representation of the area of interest in the plot	69
Figure 47: No levelled area.....	70
Figure 48: Levelled area	70
Figure 49: Trinasolar TSM-DE15H(II) panel (Source: [18])	74
Figure 50: SMA MV Power Station 2500 (Source: [19])	75
Figure 51: PVGIS temperature data recorded from 2007 to 2016. (Source: [20]).....	77
Figure 52: SMA SSM-U-1615 and SSM-U-2415 (Source: [21])	79
Figure 53: Double pole structure with variable inclination (Source: [8]).....	80
Figure 54: Calculation of the distance between rows of modules in an inclined plane	81
Figure 55: Calculation of the distance between inverter and modules in an inclined plane.....	82
Figure 56: Identification of the strings	84
Figure 57: Series connection of modules: a) daisy chain and b) leapfrog wiring (Source: [22]).....	84
Figure 58: Connection with rows of inverted polarity modules	85
Figure 59: Examples of incorrect (left) and correct (right) connection of photovoltaic modules in series to avoid overvoltage (Source: [6]).....	85
Figure 60: Trinasolar TSM-DE15H(II) panel (Source: [18])	86
Figure 61 Series connection of modules: daisy chain without coiled cables (Source: [22])	86
Figure 62: TECSUN (PV) PV1-F 0,6/1 kV AC (1,5 kV DC) (Source: [23])	86
Figure 63: TECSUN (PV) S3Z2Z2-K 1,8/3 kV AC (Source: [23]).....	89
Figure 64: ARP1H5(AR)E cable (Source: [24]).....	97
Figure 65: Minimum external diameter of the duct as a function of the number and section of the conducting cables (Source: [25]).....	99
Figure 66: Admissible applied contact voltage values as a function of the current fault time (Source: [28])	108
Figure 67: Monthly energy output from fix-angle PV system (Source: [20])	114
Figure 68: Performance warranty of the modules (Source: [18])	117

List of tables

Table 1: IDAE table for the panel's optimal inclination angle (Source: [1])	23
Table 2: IDAE table for the maximum losses caused by orientation, inclination and shadow (Source: [1])	23
Table 3: k values according to the latitude of the place (Source: [1])	24
Table 4: Limits of efficiency with resistive loads (Source: [1])	38
Table 5: Different poses of the cables (Source: [10])	49
Table 6: Admissible current for copper conductors with an ambient temperature of 30 °C (Source: [10])	52
Table 7: Correction factors for ambient temperature different from 30 °C (Source: [10])	53
Table 8: Correction factors for cables buried directly in the ground or underground conductors for soil with resistivity different from 2,5 K·m/W (Source: [10])	53
Table 9: Correction factors for groups of various circuits or multipolar cables (Source: [10])	54
Table 10: Technical data of the selected modules (Source: [18])	73
Table 11: Technical data of the selected inverter (Source: [19])	76
Table 12: Study of the sizing of a connected PV system (Source: [6])	78
Table 13: Technical data of the selected solar string combiner box (Source: [21])	79
Table 14: Verification of the voltage drop for MV cables	99
Table 15: Calculation of ducts, diameter	100
Table 16: Calculation of ducts, length	100
Table 17: Calculation of ducts, final summary	100
Table 18: Calculation of Ptemp in the year	111
Table 19: Calculation of the PR parameter	113
Table 20: Calculation of monthly and annual producibility	114
Table 21: Costs of the various elements of the PV system	116
Table 22: Low voltage cable's price.....	117
Table 23: NPV calculation.....	118
Table 24: IRR calculation	119
Table 25: DPB calculation	120

MEMORIA

0. Introduction

This thesis develops the feasibility study and the design of a photovoltaic installation within the context of the Spanish electricity grid. This is a centralized 5 MWp solar installation located in the Spanish municipality of Chelva, in the Valencian Community. The first introductory chapters are preparatory to understanding the work done and the design choices. The first chapter introduces renewable energies with a nod to the Spanish solar market, a European country that hosts the plant and which is experiencing a second boom in this sector. Then the state of the art of the photovoltaic sector is presented starting from the basic concepts and definitions, such as solar radiation and astronomical angles. In fact it is important to know the technical language in order to describe the optimal orientation of the panels. The following sections deal with the two main elements of the photovoltaic installation:

- the solar cell, the various technologies of the photovoltaic modules and their possible series and parallel connections to form a solar field;
- inverters to transform the direct current produced by the panels into alternates. The characteristics, the various possible configurations of this component and its use in the search for the point of maximum producible power are presented.

For the system to work properly, inverters and modules must interact correctly. There are conditions to be respected expressed in terms of voltage and maximum/minimum current and calculable from the values present in the datasheets. These conditions are translated into a maximum number of panels connected in series and parallel. One chapter is dedicated to other elements present in the photovoltaic field, such as string combiner boxes, module support structures and electrical cables. The choice of cables is also subject to constraints translated into the verification of the thermal and electrical criteria. Final components of the plant are the electrical protections of the system. The last theoretical chapters concern producibility and some terms necessary for an economic analysis. After the theoretical analysis, the practical project is described, starting from the choice of the terrain. It is a plant located in the Chelva area, characterized by little exploited agricultural land. With the help of the cartography of the area and the MATLAB software, the volume of the soil to be removed to level the area and the average final inclination of the soil are then obtained. The script is shown in Annex A. The choice of the various elements of the system is then discussed: panels, inverters, string combiner boxes, support structures. To choose them correctly, reference is made to the theoretical notions and they adapt to the case under exam. In addition, the layout of the system and the connection cables are presented. Having this latter part of the extended calculations, it is decided to insert them entirely in the annexes B and C. Later, the system protections are analysed. Many protective elements are verified because included in other components, that is the inverter and string combiner boxes. Besides, grounding is calculated. The earthing of the low voltage side and of the MV station are studied. The possibility of having a common grounding is calculated and verified. Finally, the last chapters concern the producibility and the study of the plant from an economic point of view. In this way the profitability of the project can be determined. Annex D presents tables for calculating the price of low voltage cables. This work also includes AutoCAD drawings, inserted at the end, that give an idea of location, layout and other details of the photovoltaic plant.

1. Introduction to renewable energy

This first paragraph introduces the concept of renewable energy. It is analysed how photovoltaic solar energy plays a fundamental role among these. The advantages and disadvantages of this energy source are listed. Finally, the current situation of the renewable Spanish sector is presented.

1.1. Renewable energy

Renewable energies are energies that are present in nature and that have virtually unlimited possibilities of use. The term renewable energy encompasses several energy sources that in theoretically do not run out over time. These sources represent an excellent option to the conventional ones (non-renewable) because they would minimally affect the environment. The most important renewable energies are organized in the following scheme.

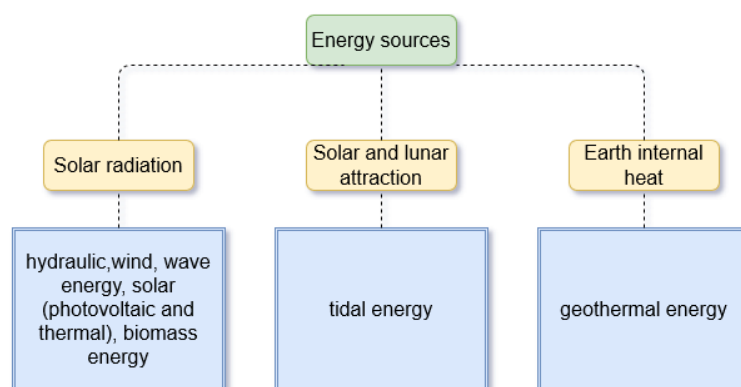


Figure 1: Subdivision of energy source (Source: [1])

As can be seen, most renewable energies have solar radiation as a source of direct (photovoltaic or thermal) or indirect (hydraulic, wind, etc.) energy. Solar energy is one of the most important energy alternatives today, in fact it offers several advantages such as:

- It employs an inexhaustible natural resource: the sunlight.
- It is a clean energy that does not generate emissions of polluting gases or any other waste.
- It is an ideal solution in order to have electricity in isolated areas.
- It is the only renewable energy that can be installed on a large scale within urban areas.
- For grid-connected installations, there are public subsidies and production premiums.
- The panels and the supporting structure can be finally disassembled and used again

But there are some disadvantages too:

- The visual impact of solar farms, which often need larger areas
- Energy is produced with daylight and it depends on the degree of insolation
- The installations prices are high, especially when compared to other types of installations that generate the same power
- Investment's return period of the is about ten years long.
- Due to solar cells low efficiency, there is poor performance, in many cases less than 40 %

- The waiting time of small and medium-sized photovoltaic installations for companies' homologation. [1]

1.2. Renewables in Spain

In Spain nowadays there is one of the best European solar energy markets. This goal was not achieved gradually but it was a consequence of two PV installation boom. The first boom dates to 2008 after an installation of more than 2 MW, from an installing capacity of 512 MW to 2718 MW. This was possible thanks to government subsidies (Royal Decree (RD) 436/2004 and RD 661/2007). These subsidies were then limited by the RD 1578/2008 because of the financial burden leading to the installation boom. The following period was characterized by cuts and regulatory obstacles in the photovoltaic sector. The restart occurred in 2017, thanks to two large-scale energy auctions that established to install a capacity of 8 GW in the renewable sector by the beginning of 2020. The second boom occurred in 2019, this time characterized by an installation of 3,9 GW. As a result of this change, Spain is closer to meeting its 2020 binding targets for renewable energy production set by Europe under Directive 2009/28 EC. [2]

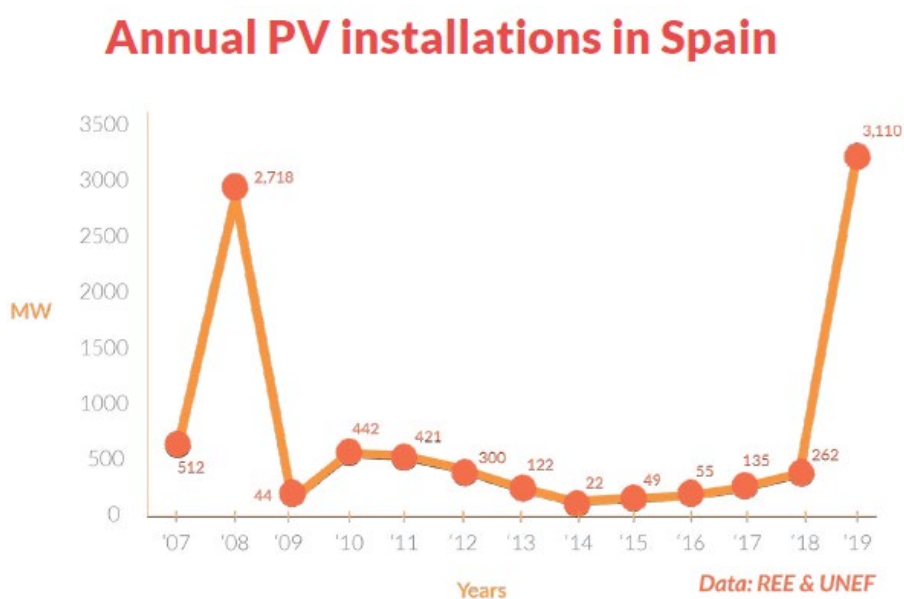


Figure 2: Photovoltaic power installed in Spain from 2007 to 2019 (Source: [2])

After analysing the main advantages and disadvantages and the situation of the photovoltaic sector in Spain, the photovoltaic technology is studied in detail to understand its operation.

2. Photovoltaic solar energy

Starting from this chapter, the state of the art of the photovoltaic sector is discussed. Firstly, panels' geographical position and location relative to the sun are considered, in order to improve their performance. Therefore, the definitions of radiation, irradiance, irradiation are presented. To achieve maximum solar radiation, it is necessary to study the irradiation at the point of the installation (in terms of latitude and longitude) and how the radiation varies on surfaces. The concept of air mass (AM), the azimuth, solar and declination angles are then defined. Eventually, the concepts of optimal orientation inclination and losses due to shadows are applied to define the correct placement of the panels.

2.1. Pre-Definitions

In photovoltaic systems the incident solar energy is turned into electricity. Consequently, knowing solar radiation means knowing the available energy. The following terms are usually used:

- Solar radiation: energy from the Sun in the form of electromagnetic waves.
- Irradiance: incident power density on a surface, measured in kW/m^2
- Irradiation: incident energy on a surface, measured in kWh/m^2 or MJ/m^2

Briefly, irradiance is the instantaneous value and irradiation is the value during a time of radiation, both for a surface of 1 m^2 . [1] [3]

2.2. Solar radiation

The concept of solar radiation is taken up by specifying the values assumed by encountering the Earth's atmosphere. Irradiance is defined with respect to its incidence and the wavelength. Finally, some methods for measuring solar radiation are presented.

The Sun releases an energy that is called solar radiation. The solar irradiance that is received over a surface perpendicular to the Sun outside the Earth's atmosphere can be considered constant and roughly equal to 1367 W/m^2 . Due to the rotation and shifting of the Earth around the Sun, and due to the diffusion effects of the Earth's atmosphere, the irradiance received by the Earth's surface presents variations. The final value on Earth's surface is 1000 W/m^2 by convention. There are three types of incident irradiance:

- Direct irradiance: it is the one received directly from the Sun.
- Diffuse irradiance: it is the one that is received from the Sun after being diverted by atmospheric dispersion and it arrives from all directions (clouds, sky).
- Reflected or albedo irradiance: it is the one that has been reflected by the soil.

The sum of the three results in the global solar constant or solar irradiance and the reference value is 1000 W/m^2 (achieved on clear days).

In the following image the types of incident irradiance are represented.

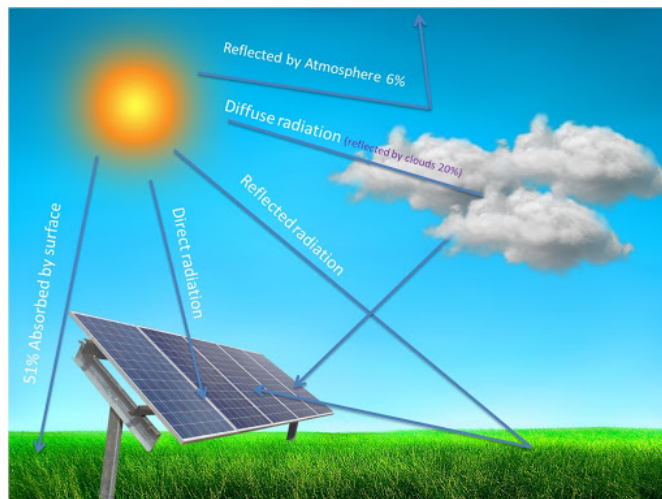


Figure 3: Types of irradiance (Source <https://images.app.goo.gl/inq6FuNUgCHnTMZt8>)

Analysing the radiation with respect to the wavelength, it reaches the Earth in the following percentages:

- 7 % ultraviolet
- 47 % visible light
- 46 % infrared radiation

In the following image the spectral irradiance (irradiance referred to the wavelength) for every wavelength is represented. It can be observed the decrease in the power value as it passes through the atmosphere and the spectrum subdivision into ultraviolet (UV), visible, infrared light.

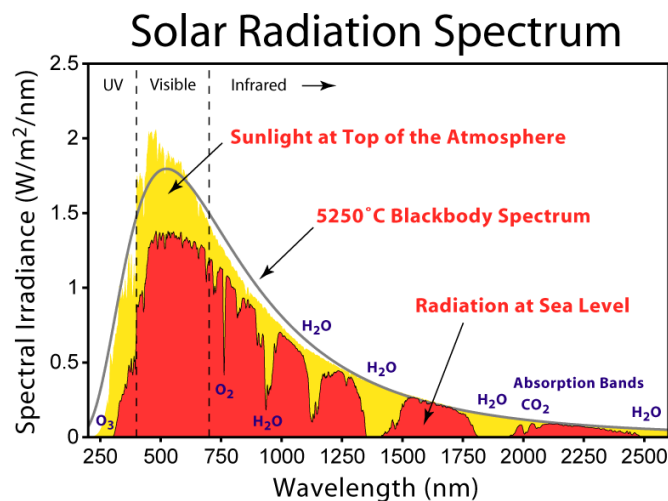


Figure 4: Solar radiation spectrum: power value at different point of the atmosphere and spectrum subdivision (Source: <https://i.stack.imgur.com/lqzTC.png>)

Solar cells capture most visible light, as ultraviolet arrives in small amounts and the infrared has low energy. The various module technologies are distinguished by the spectral operating zone. Crystalline silicon modules operate around a wavelength $\lambda=1,1 \mu\text{m}$ while amorphous silicon is characterized by $\lambda=0,6 \mu\text{m}$. [1] [3] [4]

2.2.1. Solar radiation meters

Although there are several ways of measuring solar radiation, pyranometer and cells of equivalent technology are usually used. Direct solar radiation can be measured using pyr heliometer.

Pyranometers are instruments that measure global irradiance with hemispheric symmetry. There are two types of Pyranometers, the first is the thermopile type while the second has small photovoltaic cells. The former is more precise and more expensive; it is based on the thermoelectric effect: the radiation received is absorbed by a black surface, which heats a set of thermocouples producing a voltage proportional to the irradiance. The detector element of the pyranometers is a thermoelectric cell consisting of several thermocouples in series. It provides a voltage proportional to the overall incident irradiance. The latter uses small photovoltaic cells or photodiodes as irradiance sensors. In this case the current is proportional to the received irradiance. Both sensors must be calibrated regularly.



Figure 5: Pyranometer (Source: <https://images.app.goo.gl/iyA7gALX7YyYnFv5>)

Cells of equivalent technology (CTE) or calibrated reference cells are suitable to verify the correct functioning of the photovoltaic modules. They are the same type as the ones to evaluate. Normally these cells are calibrated in specialized laboratories under standard solar spectrum conditions. They can give different measurements if they operate with different spectra, as accessed with photovoltaic modules. These are lower-precision meters than the previous ones but, given their low cost, they are ideal as proofs of the proper functioning of the facilities.

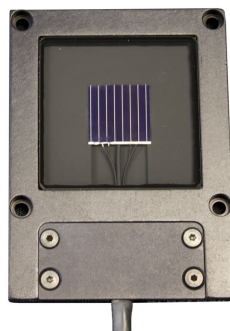


Figure 6: Calibrated cells (Source: <https://images.app.goo.gl/K5zQJj7Uf6PL3qeU9>)

The pyr heliometer is an instrument that focuses directly on the Sun to measure direct radiation. A movement system is necessary to follow the Sun with great precision. They are high precision instruments that can be used for the calibration of pyranometers. [1] [3]



Figure 7: Pyrheliometer (Source: <https://images.app.goo.gl/MbfQ887YNzqWXxnP7>)

2.3. Solar radiation over the desired geographical point

Knowing the geographical coordinate of latitude and longitude, which allow to define the exact situation of any point on Earth, it is possible to find out the solar irradiation at the point of the installation.

The latitude is the meridian arc that goes from the equator (maximum circle perpendicular to the earth's axis) to the point where its value is estimated. It has a value between -90° and 90° and it is measured as a positive angle from the equator (latitude of 0°) to the north, as a negative angle from the equator to the south.

The longitude is the arch of the equator that goes from the Greenwich meridian to the upper meridian of the place. It has a value between -180° and 180° and it is measured as a positive angle from the Greenwich meridian (longitude of 0°) to west, as a negative angle from the Greenwich meridian to east.

In the figure below, for example, the world solar map of the annual global radiation is shown on a plane with optimal inclination. [1]

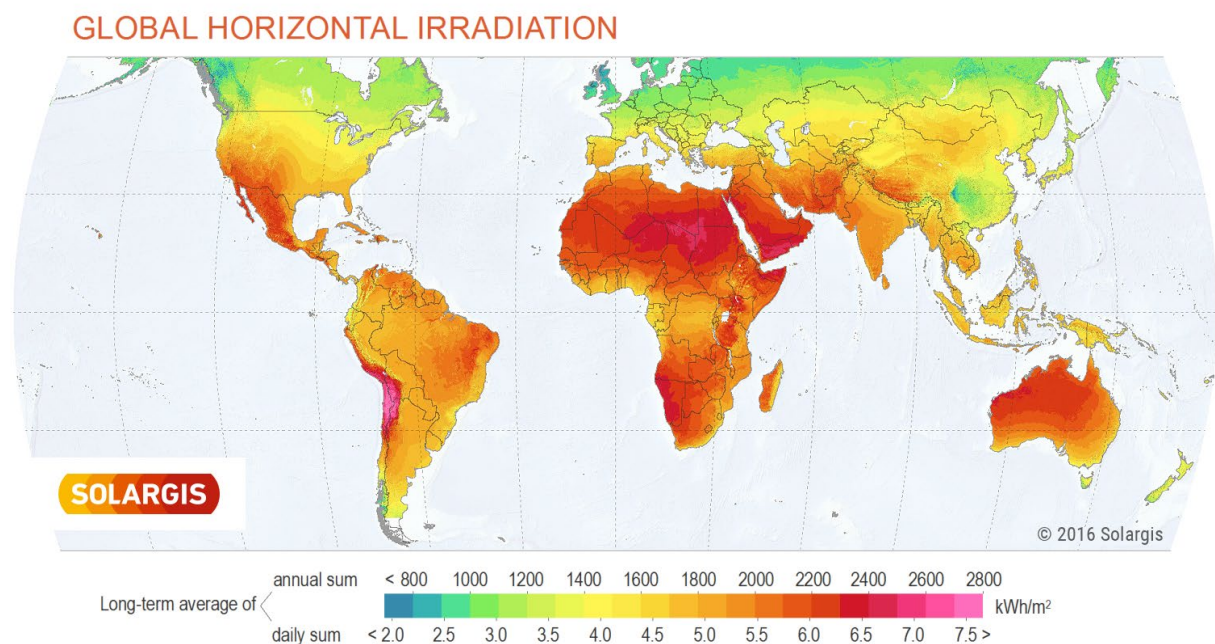


Figure 8: Global horizontal irradiation (Source: <https://images.app.goo.gl/s2QgUsJmZDSd7>)

2.4. Radiation on surfaces and Air Mass

Radiation is maximum when the Sun's rays strike vertically. When the rays arrive inclined, the same amount of solar energy extends over a larger surface and therefore the same point receives less solar radiation. The Earth's rotational motion makes the rays arrive perpendicular to noon and with more inclination in the morning and afternoon. Also, the rays arrive more inclined and, therefore, with less energy at the high latitudes (closer to the poles).

Linked to the concept of inclination is the air mass (AM), thickness of air which solar radiation must go through. The layer of atmosphere increases with the proximity of the Sun to the horizon. Consequently, the losses due to atmospheric gases increase. The ideal value of AM is the unit, that is when the ray arrives vertically. It means that the Sun is at zenith (point right above the head of the observer). Outside the AM atmosphere is equal to zero. The electrical values of the solar panels are given by agreement for an AM=1,5 corresponding to an angle of $48,18^\circ$. In formulas AM is:

$$AM = \frac{1}{\cos\theta} \quad (1)$$

Where θ is the angle between the sun's ray and the perpendicular.

In the following figure the main values of AM are represented. [1]

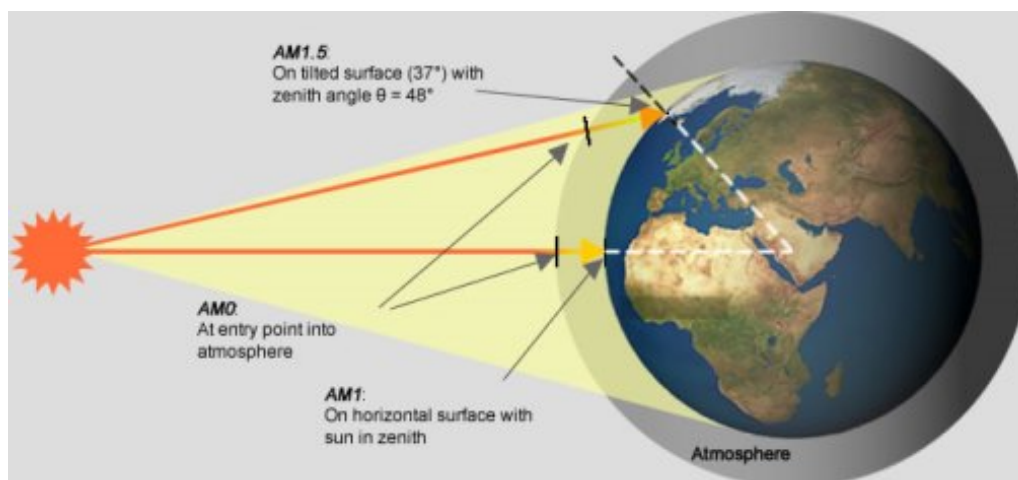


Figure 9: AM typical values (Source: <https://images.app.goo.gl/vkNwixcHoP73s86WA>)

2.5. Azimuth, solar altitude and declination angles

The azimuth angle is formed by the North-South line and the solar ray projection on the horizontal plane. At dawn it is -90° since the sun's rays are in the East and form this angle with the South. At 12:00 it is zero because the Sun is above the Southern line. Maximum radiation will be achieved here and it is the best orientation for the panels.

Solar altitude is the angle that formed by the solar ray with the horizontal plane. It varies throughout the year by the movement and inclination of the Earth.

The angles of azimuth and solar altitude are represented in the following figure.

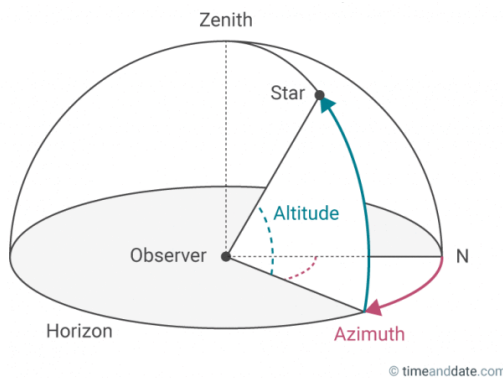


Figure 10: Angles of azimuth and solar altitude (Source: <https://images.app.goo.gl/6GZJA7G7spK5ZDbZ9>)

The inclination of the Earth is calculated as the angle that the Sun forms with the plane of the equator and it is called solar declination (δ). The solar declination assumes variable values during the year, values between $-23,45^\circ$ (winter solstice) and $23,45^\circ$ (summer solstice) as shown in the picture.

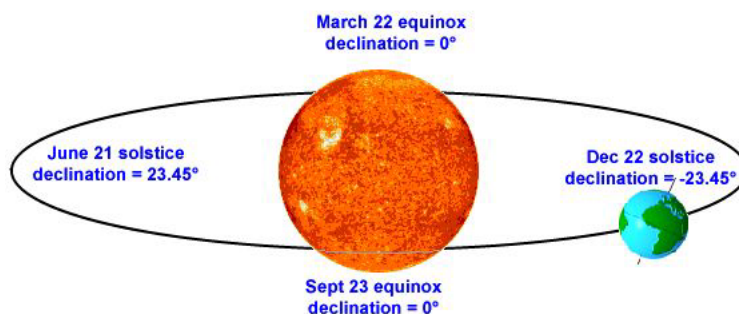


Figure 11: Values assumed by the solar declination during the year (Source: <https://images.app.goo.gl/njtJ9PucQuc9eMv6>)

It is possible to observe the effect of the variation of the declination on Earth with a geocentric perspective. The Sun's paths are illustrated in the following picture. Solar altitude reaches its maximum value in the summer solstice and its minimum in winter solstice. In winter the shadows are bigger due to the greater inclination of the sun's rays. [1]

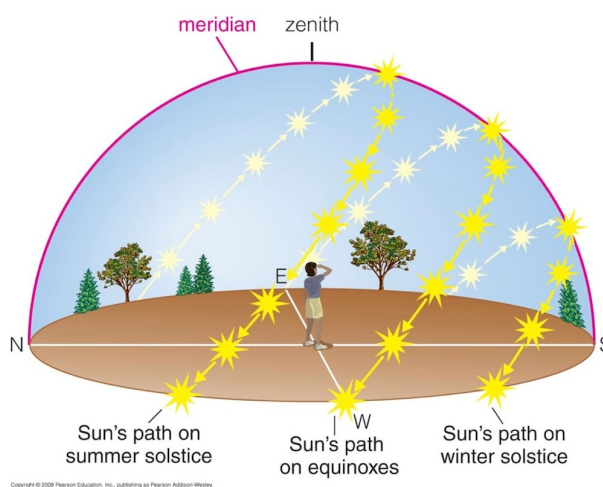


Figure 12: Sun's path during the year (Source: <https://images.app.goo.gl/Rn6odhywJTn4jJA5>)

2.6. Correct placement of the panels

In order to obtain the maximum amount of irradiation in the Northern Hemisphere, the panels are oriented towards the South.

For an optimal inclination of the panels, it is important that the rays touch the module perpendicularly at noon. The solar radiation reaches perpendicular between the Tropics of Cancer and Capricorn (that is, with a deviation of 23,45° to the equator). It is possible to achieve the perpendicularity at another latitude tilting the panels the angle of latitude including the δ (the $\pm 23,45^\circ$). Therefore, the inclination is calculated as:

$$\beta = \Phi - \delta \quad (2)$$

Where:

- β is the inclination of the panels
- Φ is the latitude
- δ is the angle of decline and it changes during the year

In order to avoid changing the inclination of the panels periodically (in the case of fixed installation) the panels can be tilted according to their use. The inclination should be chosen following the Institute for Energy Diversification and Savings (IDAE) table which indicates the optimal angle in two options: a homogeneous production throughout the year or a higher production in summer or wintertime.

Period of utilization	β_{opt}
Winter	$\Phi + 10^\circ$
Summer	$\Phi - 20^\circ$
Annual	$\Phi - 10^\circ$

Table 1: IDAE table for the panel's optimal inclination angle (Source: [1])

The shadow produces losses of solar radiation uptake as well.

The IDAE allows losses of 20 % for autonomous installations (layout of panels) and up to 10 % for shadow. The sum of the two must not exceed 20 %. In the case of installations to grid the permissible values are in the following table.

	Orientation and inclination	Shadow	Total
General	10 %	10 %	15 %
Overlap	20 %	15 %	30 %
Architectural integration	40 %	20 %	50 %

Table 2: IDAE table for the maximum losses caused by orientation, inclination and shadow (Source: [1])

The difference between overlap and integration is that the first goes parallel to the structure of the building and the second replaces elements of the construction.

Since the losses caused by the presence of shadow are remarkable, considering a minimum distance in the positioning of panel files should be taken into account.

The distance d between rows of h -high modules that can produce shadows must ensure that they do not do so in a minimum of four hours of Sun around noon of the winter solstice (season with greater shadows). This minimum distance d_{min} is calculated:

$$d_{min} = h \cdot k \tag{3}$$

$$k = \frac{1}{\tan(61^\circ - \text{latitude})} \tag{4}$$

k is a coefficient without units, in the following table some of its values are shown according to the latitude of the place.

Latitude	29°	37°	39°	41°	43°	45°
k	1,600	2,246	2,475	2,747	3,078	3,487

Table 3: k values according to the latitude of the place (Source: [1])

If the panels are at different heights, h is the difference in heights between the top of one module and the bottom of the next, as shown in the following figure. Measurements are made on the base plane of the module affected by the shadow. [1] [5]

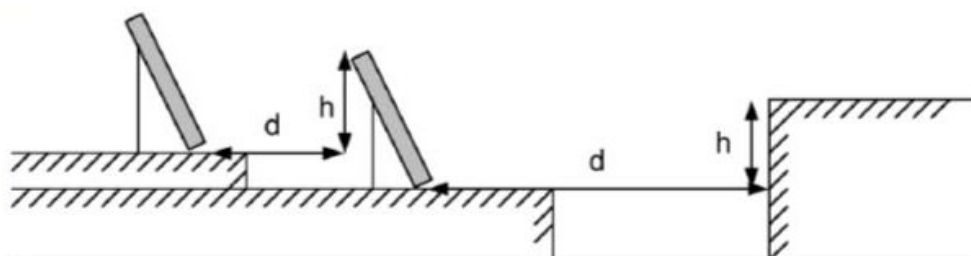


Figure 13: Distance d between panels with different heights (Source: [1])

After presenting the photovoltaic solar energy and positioning the panels optimally, we move in the following chapter to deal in detail with the technologies and the operation of a solar panel.

3. The solar panel

This chapter deals with the core unit of the photovoltaic system, the solar cell. Its physical operation and some technologies present on the market are introduced. The module's component parts and its standards are described. Then, the equivalent circuit of the photovoltaic cell and the characteristic curves, analysing the dependence on irradiance and temperature. Finally, the composition of photovoltaic modules in series and parallel leads to the definition of string, array and photovoltaic field.

3.1. The photovoltaic effect

Currently the type of photovoltaic cell that dominates the market is the crystalline silicon semiconductor cell. In order to understand the principle of functioning of this cell, and therefore the direct conversion of solar radiation into electricity, it is useful to analyse some physical principles that are at the basis of this phenomenon.

Silicon atoms, semiconductor material that forms solar panels, have 4 electrons in their last layer. These join the other atoms around forming groups of 8 electrons and create a crystalline net. This crystal is stable and does not allow the passage of current, but by adding a small amount of Boron and Phosphorus (which have 3 and 5 electrons), two zones are created, in which one (P zone) is missing and in the other one (N zone) has extra electrons inside the crystalline network.

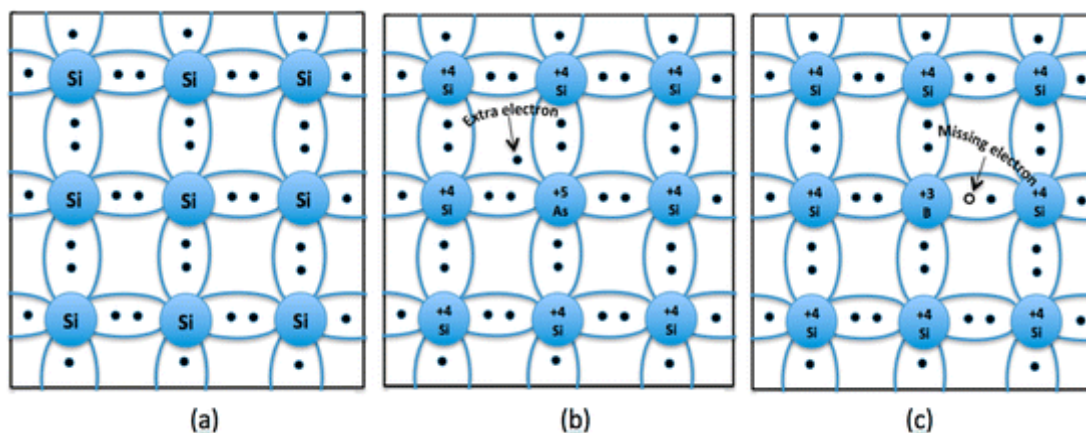


Figure 14: Structure of (a) undoped silicon (b) n-type silicon (c) p-type silicon (Source: <https://images.app.goo.gl/NQATgFMTAZVk>)

By joining the two zones, holes and electrons are free to move in the grid by diffusion. A union of electrons-holes is created in the centre (the gap is the lack of electron), which causes a permanent electric field (the N loses electrons and remains with positive charge and the P in reverse) and avoids the passage of current. The N layer receives the sun's rays and is thinner than the other. Sunlight is formed by photons that have an energy capable of ripping off the electrons. Photons break the electron-bond gap, the electronic field separates them by taking the electrons to the N layer and the holes to the P layer. If an external conductor is put, the electric current flows from P to N. It is the photovoltaic effect.

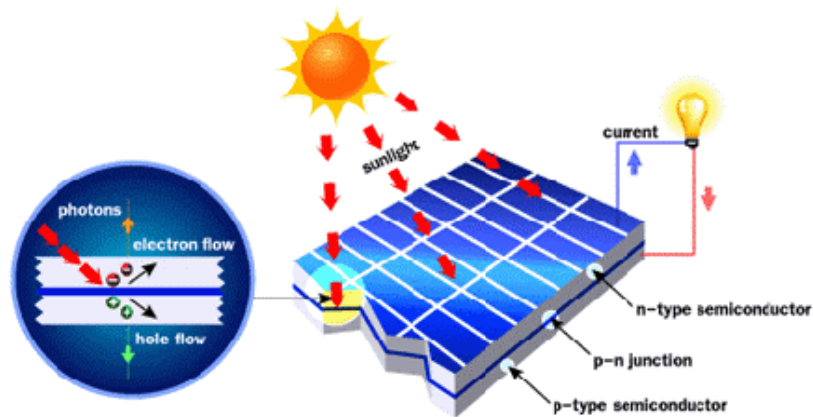


Figure 15: Photovoltaic effect (Source: <https://images.app.goo.gl/wWG8i3c7MDMS2tVU6>)

As said before, sunlight is made up of photons. These photons have different energies corresponding to the different wavelengths of the solar spectrum. When photons hit a PV cell, they can be reflected, absorbed, or passed through. Only absorbed photons can generate electricity. When a photon is absorbed, its energy is transferred to an electron of a cell atom.

The minimum energy that photons have to produce an electric current is called energy gap or forbidden bandwidth (E_g). In formulas:

$$E_{ph} = h \cdot \nu = h \cdot \frac{c}{\lambda} \geq E_g \quad (5)$$

Where:

- E_{ph} is the photon's energy, measured in Joules
- E_g is the energy gap, measured in Joules
- $h = 6,626 \cdot 10^{-34} Js$ is the Planck constant
- ν is the frequency measured in Hertz
- $c = 3 \cdot 10^8 m/s$ is the light speed
- λ is the wavelength, measured in meters

The optimal value of E_g is about 1,5 eV. In Silicon the link break occurs at 1,1 eV. In contrast, Gallium Arsenide produces 1,4 eV which is better, but more expensive. All materials can be studied in terms of energy gap. On the one hand, the insulators have a high energy gap, the electrons need a large amount of energy to reach the conduction band. They are therefore not suitable materials to conduct. If the materials used for the panels were insulating, there would be no conduction. The conductors, on the other hand, are characterized by a high number of electrons which already have got the energy necessary to reach the conduction band thus giving rise to an electrical flow. If the materials used in the panels have an E_g lower than the photon, there is energy left over from the photons and that dissipates in the form of heat (not interesting). Semiconductor materials are used to make the panels. They are a sort of halfway between insulators and conductors. The breaking energy of their atoms is similar to the one of the photons. [1] [3]

3.2. Technologies of the cells

There are three main cells' technologies, classified according to their crystalline structure:

- Monocrystalline silicon. It has a completely ordered structure. Its uniform behaviour makes it good conductor. It is difficult to manufacture. It is obtained from pure molten silicon and doped with boron. The colour is dark blue and metallic gloss. Performance is over 19 % in business models.
- Polycrystalline silicon. Formed by a group of Silicon crystals: it has a structure arranged by separate regions. Irregular links of crystalline borders decrease cell performance. It is obtained in the same way as monocrystalline silicon, but with fewer crystallisation phases. They look like an amalgam of crystals (different shades of blue and grey with a metallic sheen). The yield does not exceed 15 % in commercial models. The cost of manufacturing this type of cells is lower than before.
- Amorphous silicon. The ordered crystalline structure has disappeared, and the silicon has been deposited to form a thin layer. It contains many structural defects and links. Its manufacturing process is simpler than the previous ones and less expensive. Its colours are brown and dark grey. Calculators and other small objects are used. The yield does not exceed 9 % in commercial models. [1] [4]



Figure 16: Polycrystalline, monocrystalline and amorphous panels (Source: <https://images.app.goo.gl/GLwhm9QPGmoQnYK87>)

3.3. The photovoltaic module

Solar cells usually are not employed alone because of their small power and fragility. Cells with similar characteristics are generally connected in series to form photovoltaic modules (or photovoltaic panels) with rigidity and protection suitable for outdoor operation. The serial connection is made by joining the negative (top) and the positive (bottom) of two adjoining cells. Many modules are formed by 36 cells (voltage approximately 18-21 V that is 0,5-0,6 V/cell). There are also modules of 60 cells.

Although cells differ greatly with technology considered both as a visual aspect and as a construction process, the parts of a photovoltaic module are the same.

In general terms, it can be observed:

- An aluminium frame
- An outer cover made of tempered glass (4 or 5 mm) resistant to impacts and transmitting solar radiation. The glass should be smooth on the outside and not retain dirt.
- Two encapsulating layers protecting cells and interconnecting contacts. The materials (silicone, EVA¹) must have a good transmission to the solar rays.
- Back sheet or Tedlar² (trade name): usually white in colour, as it reflects the incident radiation that passes through the cells. Currently, in facades of buildings, also tempered glass.
- Electrical contacts. They are placed in one or two outdoor connection boxes, with screw contacts, connector... Inside there is the protection diode by-pass to avoid problems with shadows. [1] [3]

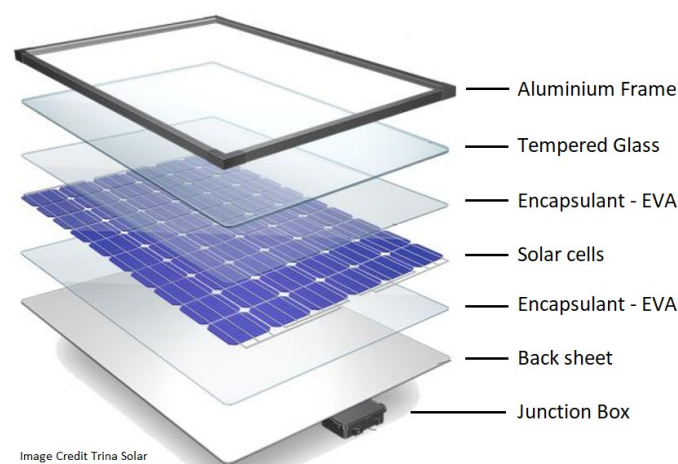


Figure 17: Photovoltaic module structure (Source: <https://images.app.goo.gl/x1GjbcHusWpX4vwS7>)

3.4. The Protection diodes

Solar panels can have two types of diodes:

- a) Blocking diode (outside the panel). One is placed on each row of modules. It prevents the current from going from the battery (or the net) to the panels when there is no solar radiation; it also prevents one row of modules from discharging into another because of a breakdown.
- b) Bypass diode. If one part of the panel is covered by shade, it stops generating current and becomes a charge, it consumes in the form of heat the current coming from the other cells. It is known as Hot-Spot. Materials can be set on fire (especially in panels with a voltage of 24 V or more). In order to avoid this sort of accident, bypass diodes are placed in the junction box. The shaded part, when it becomes a charge, changes its polarity. When the diode detects this change it causes the current to pass through it (instead of through the cells).

¹ EVA (Ethylene Vinyl Acetate) is a type of rubber that is worn to prevent air and moisture from entering.

² TEDLAR is polyvinyl fluoride (PVF). It protects cells from the degrading effects of ultraviolet radiation and serves as an electrical insulator

The two types of diode are shown in the following figure.

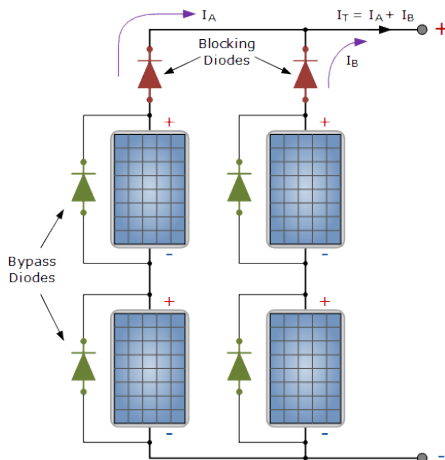


Figure 18: Blocking and bypass diodes (Source: <https://images.app.goo.gl/X2mm4gKSpNCf9new5>)

3.5. Standards of the modules

The photovoltaic modules in production have to be carefully controlled because of the problems of inequality. In fact, the energy produced depends on the minimum value of current (in the most frequent case of cell connection in series) or voltage (in the case of parallel connection). The standard according to which photovoltaic panels are approved is EN 61215. In this way the client has the guarantee that the acquired modules have a correct level of qualification. Tests done include:

- Measurements under standard operating conditions (radiation of 1000 W/m², temperature of 25 °C and AM=1,5)
- Low irradiance operations
- Outdoor exposure test and hot spot formation resistance
- Resistance to ultraviolet (UV) and hail radiation
- Moisture/freezing test
- Mechanical load test, terminal robustness torsion test. [1]

3.6. Equivalent circuit of a photovoltaic cell

From an electrical point of view, all cell types when illuminated by the Sun have a behaviour that can be described with the following equivalent circuit.

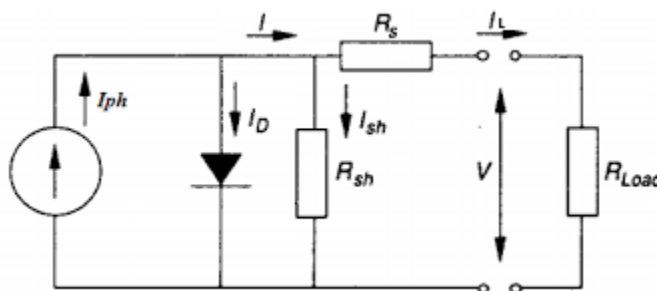


Figure 19: Solar cell's electrical circuit (Source: <https://images.app.goo.gl/9AT2Ytbf8dzqN5Z87>)

Consequently, a solar cell behaves like a diode with a parallel current source. In lack of irradiance, the current generator disappears in the equivalent circuit. This circuit is described by the following equations:

$$I = I_{ph} - I_D \quad (6)$$

Where:

- I_{ph} is the photovoltaic current
- I_D is the current in the diode

$$I_D = I_0 \cdot \left(e^{\frac{qV}{mkT}} - 1 \right) \quad (7)$$

Where:

- I_0 is the reverse current
- $q = 1,6022 * 10^{-19} C$ is the electron charge value
- V is the applied voltage
- m It is an ideal factor that varies between 1 and 2
- $k = 1,3806 * 10^{-23} J/K$ is the constant of Boltzman
- T is the absolute temperature, measured in Kelvin

The other components of the solar cell are resistance series R_s and parallel resistance R_{sh} . The first is due to the resistance of the material volume, the interconnections and the resistance between the metal contacts and the semiconductor. The second is due to the non ideality of the p-n junction and to the union's impurities. The current I_L coming out of the cell is therefore: [3]

$$I_L = I_{ph} - I_D - I_{sh} = I_{ph} - I_0 \cdot \left(e^{\frac{qV}{mkT}} - 1 \right) - \frac{V}{R_{sh}} \quad (8)$$

3.7. Electrical parameters

In order to get the characteristic current-voltage curve (I-V) of the solar cell, start from the characteristic curve of a diode. This is the curve of the cell in the absence of solar radiation. The cell lighting adds a photogenerated current to this curve, shifting it downwards (fourth quadrant).

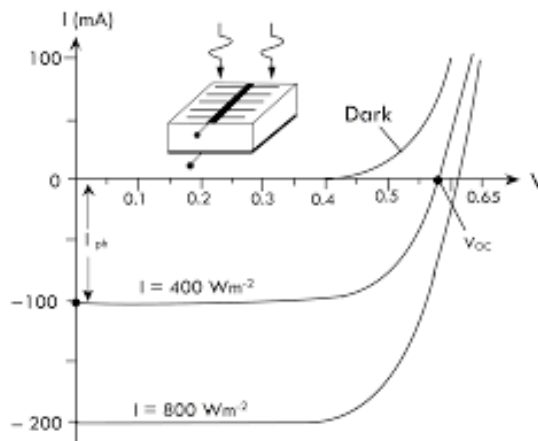


Figure 20: Characteristic curve in absence of solar radiation (Dark) and with solar irradiance (of 400 and 800 W/m²) (Source: <https://images.app.goo.gl/BNrrHxnF6v6xssrz6>)

By convention, this resultant curve is represented in the first quadrant, as in the following image.

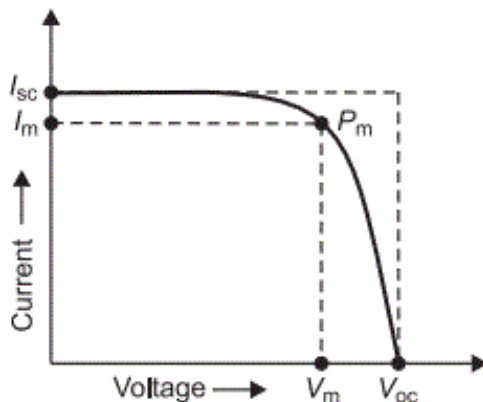


Figure 21: Current-voltage curve (I-V) of the solar cell (Source: <https://images.app.goo.gl/jiIfBsojQQ719H1r7>)

The electrical parameters represented in the characteristic I-V curve are analysed.

- Short-circuit current (I_{sc}): it occurs at zero voltage and is the one measured by putting the ammeter directly at the output of the cell or panel. It mostly depends on the technology and light radiation.
- Open circuit voltage (V_{oc}): it exists when charges are not connected. It is the maximum that a cell can give. It mostly depends on temperature. Its value is around 0,5 V.
- Peak power (P_m): is the greatest power a cell can supply and is defined by the point of the I-V curve at which the maximum value is achieved, the remaining points of the curve generate lower values. This highest point corresponds to a specific current I_m and voltage V_m .

Being:

$$P_m = V_m \cdot I_m \quad (9)$$

In the catalogues there are also the subscript “MPP”, “MPPT” or “max” indicating the maximum value, for example P_{MPP} , P_{MPPT} or P_{max} . It is measured in Wp (Peak Watt). The power curve as a function of the voltage is then represented.

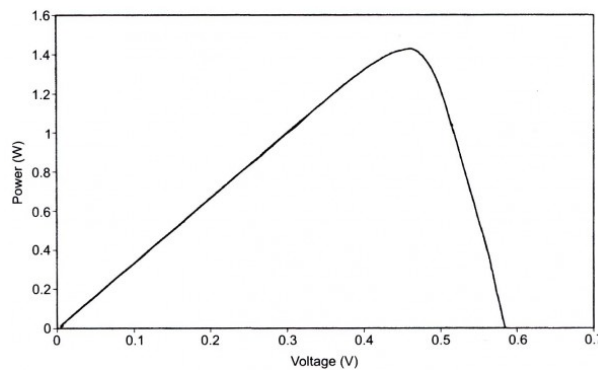


Figure 22: Power curve of the solar cell (Source: <https://images.app.goo.gl/ahS1GMP4ZVRj8E3G9>)

It is useful to define the following parameters:

- The form factor (FF) is a measure of the quality of the junction and the serial strength of the cell. It has this expression:

$$FF = \frac{V_m \cdot I_m}{V_{oc} \cdot I_{sc}} \quad (10)$$

- The FF improves for high R_{sh} values and low R_s values. The parallel resistance is related to the slope of the I-V curve around the I_{sc} , while the resistance series is related to the slope in V_{oc} .
- Conversion efficiency. It is the ratio between the power supplied by the cell or panel per surface and the standard irradiance.

$$\eta_g = \frac{P_m}{P_{inc}} = \frac{P_m}{S \cdot G^*} \quad (11)$$

Being:

- η_g the efficiency
- P_{inc} the incident power
- P_m the peak power
- S the surface area
- $G^* = 1000 \text{ W/m}^2$ the standard irradiance

For laboratory monocrystalline silicon cells, the efficiency is about 22 % or 24 % and decreases up to 15 % in commercial cells of the same type. [1] [3]

3.8. Dependence of the I-V curve on environmental conditions

The characteristic current-voltage curve (I-V) of the solar cell depends on temperature and irradiance variations.

When incident irradiance varies, carrier generation also varies, resulting in a change in the current and output voltage. The short circuit current varies linearly with irradiance, while the open circuit voltage is less affected by a logarithmic dependence. The main effect of the increase in cell temperature is a reduction in the open circuit voltage. The short circuit current increases by a very small proportion. The variations of the cell parameters are different for each technology and for each manufacturer.

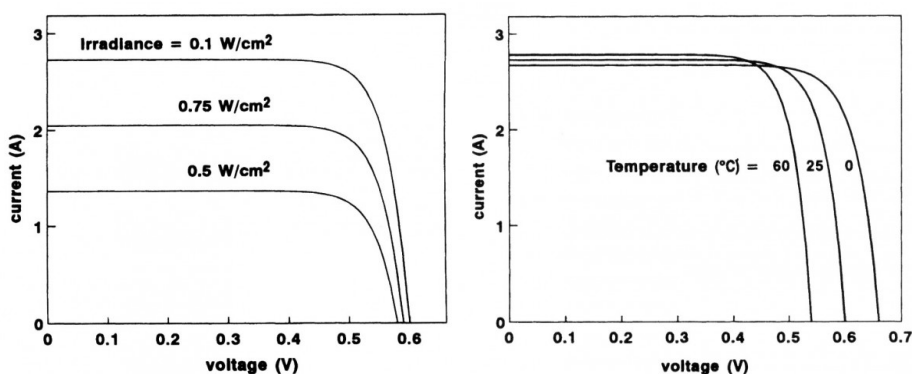


Figure 23: Variation of the characteristic curve with irradiance and temperature (Source: <https://images.app.goo.gl/ahS1GMP4ZVRj8E3G9>)

From the figures it can be deduced that an increase in irradiance at the same temperature is favourable for photovoltaic conversion. But if the increment in irradiance is caused by an increase in temperature, there is a reduction in the maximum final power. In fact, the short circuit current increases in value but is unable to recover the losses due to the decrease in open circuit voltage. Consequently, a temperature increment is not favourable for photovoltaic conversion.

Analytical formulas, presented below, may be used to describe the variation of short circuit current I_{sc} , open circuit voltage V_{oc} and maximum power P_m with irradiance G and cell temperature T_c ($T_c = T_a + 0,03 \cdot G$; T_a is the environment temperature).

In the following expressions, the values with an asterisk indicate the values under standard STC conditions. it is recalled that $G^* = 1000 W/m^2$ and $T_c^* = 25 °C$ are the irradiance and temperature in STC.

$$I_{sc} = I_{sc}^* \cdot \frac{G}{G^*} + \alpha \cdot (T_c - T_c^*) \quad (12)$$

$$V_{oc} = V_{oc}^* + \frac{mkT}{q} \cdot \ln \frac{G}{G^*} - \beta \cdot (T_c - T_c^*) \quad (13)$$

Their expression and typical values are indicated.

$$\alpha = \frac{1}{I_{SC}} \cdot \frac{\partial I_{SC}}{\partial T} \approx 0,0006 \text{ } ^\circ\text{C}^{-1} \quad (14)$$

$$\beta = \frac{1}{V_{oc}} \cdot \frac{\partial V_{oc}}{\partial T} \approx -0,003 \text{ } ^\circ\text{C}^{-1} \quad (15)$$

As illustrated, in literature there are different equations for the open circuit voltage. For example, an expression can be found with a second logarithmic term that considers low irradiance effects.

To describe the maximum power variation, the efficiency η_g defined as the maximum power P_m related to the incident power on the cell P_{inc} is used.

$$\eta_g = \eta_g^* \cdot [1 - \gamma \cdot (T_c - T_c^*)] \quad (16)$$

γ is the coefficient of variation of P_m with temperature. Its expression and typical value are reported. [3]

$$\gamma = \frac{1}{P_m} \cdot \frac{\partial P_m}{\partial T} \approx -0,0045 \text{ } ^\circ\text{C}^{-1} \quad (17)$$

3.9. Strings, arrays and photovoltaic field

When cells are associated in series, the same current circulates through them and the resulting voltage is the sum of the voltages of each. The I-V curve of the module is obtained from the curve of a cell: for serial connection, the voltages are added; for parallel connection the currents are added. Photovoltaic modules can also be connected in series forming a string; the string then can be connected in parallel to form an array. The set of all the arrays forms a photovoltaic field.

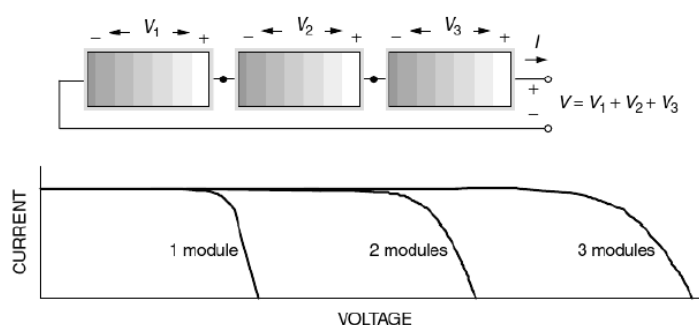


Figure 24: Modules connected in series (Source: <https://images.app.goo.gl/sQNYkdGPftRJ7YWo9>)

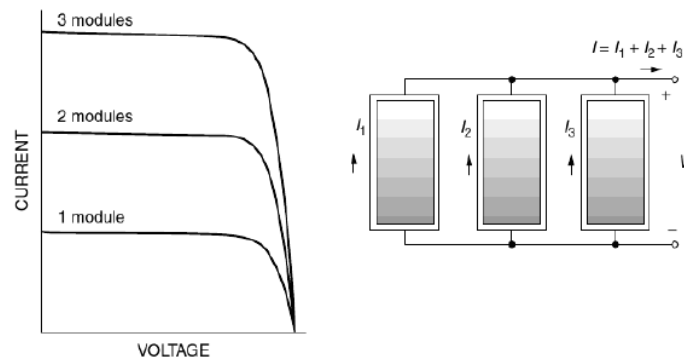


Figure 25: Modules connected in parallel (Source: <https://images.app.goo.gl/sQNYkdGPftRJ7YWo9>)

When the I-V characteristics of the cell that make up a module or the modules that form a string are not identical, then mismatch problems appear. The result is a power module (or string) lower than the power sum of each of the individual cells (or modules). These losses are called mismatch losses. Analysing the case of serial connection with mismatch, it is observed that some cells are generating power and others are dissipating it. In the worst case there is only one shaded or with construction defects cell, that dissipates the power generated by all the other cells. This dissipation takes the form of heat and the cell is at risk of irreversible damage. This phenomenon is known as hotspot formation. A solution to the formation of hot spots is the inclusion of bypass diodes to the cell or module connection circuit. These diodes offer an alternative way for the current to flow through them when there is a shaded cell in the circuit that is acting as a power sink. In normal operation the diodes are polarized in reverse and do not lead current, only when a cell or a group of cells are shaded the diode is polarized directly and leads current. In practice, putting a diode per cell is very expensive and they are usually placed in groups of cells within each module. Bypass diodes are usually incorporated into the photovoltaic module junction boxes. A similar phenomenon occurs when many cells or modules are connected in parallel, where blocking diodes are needed to prevent the formation of hot spots and the recirculation of currents between different branches. [3]

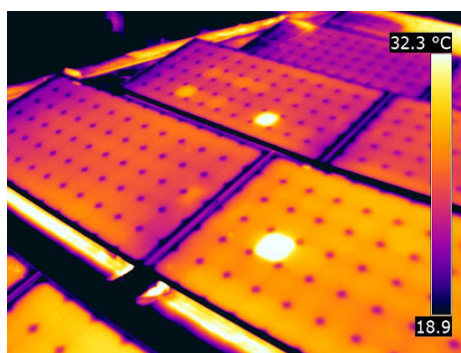


Figure 26: Hot spots seen with infrared rays (Source: <https://images.app.goo.gl/Rc61F3ZjZo4cYBYz5>)

To use the direct current produced by the photovoltaic panels, there are devices that transform the values produced into the desired ones, whether they are continuous or alternate. These are the continuous-continuous (chopper) or continuous-alternate (inverter) converters, topic of the next chapter.

4. The photovoltaic inverter

This chapter deals with converters, essential elements for transforming direct current from the photovoltaic field. If working in DC there is a voltage different from the nominal voltage (panels and batteries) a continuous-continuous converter is used. If the consumption or part works with alternating values a continuous-alternating converter should be employed. Among the latter, we distinguish the stand-alone inverters, which converts direct current into alternating current, and the grid inverter, which converts direct current into alternating current and injects it into the electricity grid. After presenting the main characteristics of the converters, the search for the maximum power point is presented. Finally, the possible configurations of inverters and photovoltaic field are analysed.

4.1. DC/DC converter

The primary function of DC/DC converters is converting an input power into an output power with the highest possible efficiency. To allow it, it is important matching the input values with the maximum power point of the generator (treated in the paragraph: 4.3. Maximum power point). Its specifications are as follows:

- Rated input voltage
- Rated output voltage
- Rated output power
- Performance

Different DC/DC converter typologies can be found in the literature, however, the most used can be grouped into one of the following types:

- Voltage reducing converters
- Elevation voltage converters
- Reducer converters/ voltage lifts
- Cúk type converters
- Full Bridge Converters

A DC/DC converter is based on the use of one or more switch devices, such as MOSFETs, in which the average output voltage can be controlled for a given value of the input voltage, depending on the opening and closing times of the switch. Whatever the type of converter is used, a modulation circuit is needed to follow the maximum power point and keep the voltage of the generator stable at this point. Currently, the performance of these devices is very high (90-95 %). [1] [3]

4.2. DC/AC converter

The overall performance of a power inverter is based on power semiconductor switch with a controlled cycle of opening and closing, generating variable pulse waves (the more pulses, the less harmonic distortion and the closer to the pure sine wave). The power semiconductors commonly used in photovoltaic inverters are thyristors and power transistor. Inverters used in photovoltaic applications can be grouped or divided into two main categories: stand-alone inverters and the grid inverters. The former can be used as a voltage or a current source, so they can be used in both standalone and grid-

connected applications. The latter can operate as a current source, so it can be used in grid-connected applications. This inverter operates at a fixed output frequency (50 Hz). By analysing the DC side, inverters can be connected to a battery system with a defined voltage, as in the case of stand-alone inverters, or directly to the photovoltaic generator, as in the case of inverters for connection to the grid; in the latter the range of variation of the input voltage is greater. The inverters of direct connection to a photovoltaic generator also have monitoring of the maximum power point of the photovoltaic generator. Due to their high production cost, photovoltaic solar energy inverters need to be reliable and high performance (even at very low power levels). The return on inverters must be above 90 %, considering 94 % a normal value (referring to sine wave inverters). In the most common applications, sinusoidal inverters controlled with the pulse width modulation (PWM) technique are used. This technique involves comparing a high-frequency (usually isosceles) triangular waveform called a "carrier" with a sinusoidal waveform called "modulation".

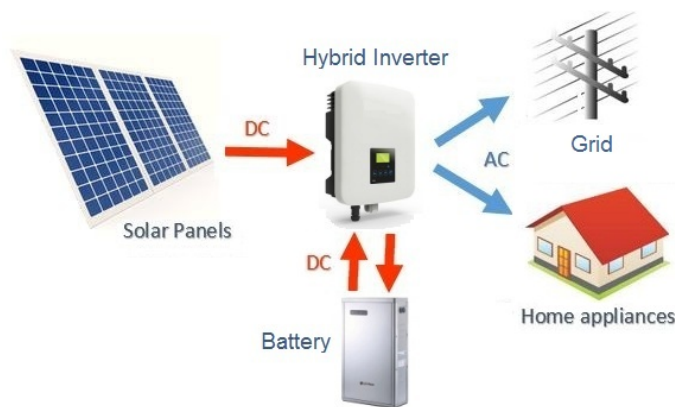


Figure 27: Simplified layout of a solar system (Source: <https://images.app.goo.gl/pUwjDjWdrvcn4ZM37>)

They are characterized by:

- Nominal input voltage. Range in which they can work.
- Rated power. Range in which higher efficiency is achieved.
- Efficiency:

$$\eta = \frac{\text{input power}}{\text{output power}} \quad (18)$$

Here it is remarked the inverter's behaviour for powers other than the nominal one. The biggest difference is in case of working with low power because losses and consumption affect more. It is common to define a standard or European performance or European performance based on one at specific nominal power values:

$$\eta_{EU} = 0,03\eta_{5\%} + 0,06\eta_{10\%} + 0,13\eta_{20\%} + 0,1\eta_{30\%} + 0,48\eta_{50\%} + 0,2\eta_{100\%} \quad (19)$$

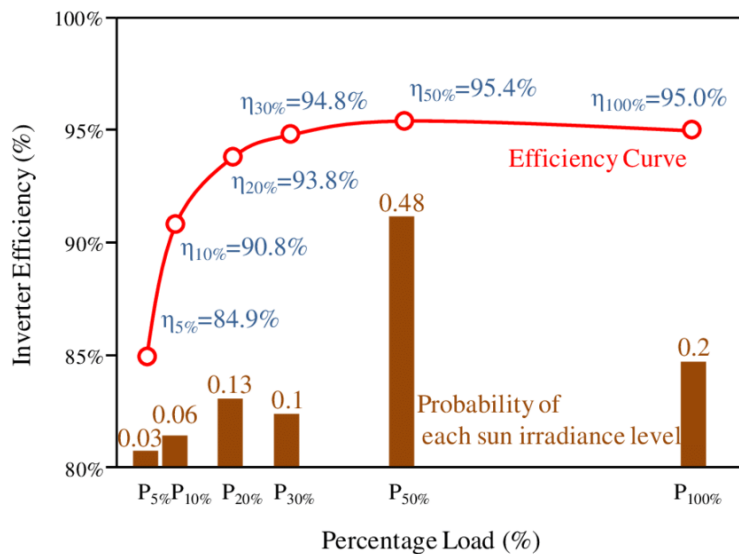


Figure 28: European efficiency inverter curve (Source: <https://images.app.goo.gl/yHuL7Zioa3bTTbA66>)

- Overload. Supports powers several times higher than nominal for a short period of time, to create the current; for example, in engines;
- Signal type. There are two classifications: sinusoidal (the grid) and modified (or trapezoidal). Resistive devices are not affected by the type of wave. Electronics depends on the voltage variation in their circuits and if there are sudden changes in voltage consequently there may be overheating and breakdowns. Trapezoidal inverters are worse at overcharging. This means that in a starter engine they can heat up more than normally. [1] [3]

4.2.1. The stand-alone inverter

The stand-alone inverters usually operate connected to a battery system to supply the AC charges of the installation. In addition to the characterisation aspects, the technical requirements to be considered recommended by the IDAE are:

- Sinusoidal wave, except if less than 1 kVA and does not cause damage to load
- Voltage and frequency output in margins: $V_{nom} \pm 5\%$ and $50\text{ Hz} \pm 2\%$
- Shielded from input voltage outside operating range; AC output short circuit; overloads exceeding permitted duration and limits.
- Inverter self-consumption less than or equal to 2 %
- Efficiency with resistive loads shall be higher than the limits of the following table. [1]

Wave	Power	Efficiency at 20 % of the nominal power	Efficiency at nominal power
Sinusoidal	$P_{nom} < 500\text{ VA}$	>80 %	>70 %
	$P_{nom} > 500\text{ VA}$	>85 %	>80 %
No sinusoidal	$P_{nom} < 1\text{ kVA}$	>85 %	>80 %

Table 4: Limits of efficiency with resistive loads (Source: [1])

4.2.2. The grid inverter

Inverters for connection of photovoltaic systems to the electric grid are electronic power devices linked directly to a PV generator (DC side) and to the electric grid (AC side). They are mainly used to transform the DC energy produced by the PV generator and inject it into the electrical grid. To optimize the efficiency of the PV generator, they follow the maximum power point (treated in the paragraph: 4.3. Maximum power point). In addition, they must work with maximum performance generating energy with a certain quality (low harmonic distortion, high power factor, low electromagnetic interference) and meet certain safety standards (for people, equipment, electrical grid).

They must incorporate protections against:

- AC short circuits
- Voltage and grid frequency out of range
- Over voltages, by varistors or similar
- Grid disturbances such as micro cuts, pulses, cycle defects

The electrical characteristics are:

- Activation at powers greater than 10 % and withstand 30 % spikes
- Performance greater than 92 % from 50 % rated power
- Minimum protection degree IP20 for indoor and inaccessible places, IP30 for indoor and outdoor accessible places and IP65.

Beyond the specific requirements for operation in connection with the grid, the photovoltaic inverter must also operate within voltage ranges and output, which coincide with those defined for the stand-alone inverter, as well as they do not affect the harmonic distortion of the voltage wave of the grid. Besides, it is usually a regulatory requirement that grid inverters have galvanic insulation (or equivalent) between the grid and the photovoltaic installation. This isolation can be by low frequency or high frequency transformers. Related to the harmonic content of the current to the use (or not) and type of galvanic insulation, there is the undesirable effect of injection to the DC current grid. The adverse effect of DC current injection into the power grid can cause saturation in the transformers, resulting in high currents in the primary winding; it can determine protection fuses to burst and thus a general fall in the grid in a given sector. In addition, the transformer's performance and lifetime are reduced. DC current also generate cathodic corrosion in the wiring. To add to this, the protective function of type A differentials is negatively affected and differentials type B (sensitive to DC and AC currents) need to be used instead of A's.

Another important aspect is the prevention of the phenomenon called island operation. If the power company disconnects a local stretch of electricity grid where a photovoltaic inverter is operating, (for example, to carry out maintenance work) for safety reasons, it is important to avoid that the inverter is automatically disconnected before a specified number of grid cycles. Although the real possibility of this to happen is very low, inverters must incorporate methods to detect downstream power grid disconnection. Several studies have been carried out to assess the probability and associated risk of the island operation. These studies conclude that, in cases of low-density PV systems in a grid section, the probability of island mode operation is poor. However, in cases of high densities of PV systems, the inverters must incorporate island-mode operation prevention techniques in order not to increase

the risk of an electrical shock accident. Finally, the inverter must reconnect automatically once the causes for its disconnection have disappeared. [1] [3]

4.3. Maximum power point

Unlike stand-alone inverters, which are usually connected to a battery, tracking the maximum power of the photovoltaic generator is a distinguishing aspect between different models of inverters connected to the electricity grid. Its stability and performance are the elements that define the amount of energy injected into the grid. It is common for the monitoring performance of the maximum power point to be at 97 % for powers greater of 10 % of than the nominal power, being able to reach 99 % for powers greater of 30 % than the nominal power.

The DC power that the inverter can obtain from a photovoltaic generator depends on the working point on the I-V curve. The maximum power depends on the environmental conditions, irradiance and temperature. The inverter should always operate at the maximum power point of the photovoltaic generator. Because a maximum power point search algorithm is necessary, a maximum power tracking performance can be defined, such as the quotient between the energy obtained and the energy that would be obtained in the ideal tracking.

$$\eta_{TR} = \frac{P_{cc}}{P_m} \quad (20)$$

Where P_{cc} is the power at a given instant and P_m is the maximum power of the photovoltaic generator for a given irradiance condition and operating temperature. There is a single point on the I-V curve (the maximum power point) at which the generator produces the maximum power.

The inverter, in order to operate at this point, needs an algorithm, in which the operating voltage of the PV generator is controlled. There are different types of algorithms: perturbation and observe, incremental conductance, capacity, constant voltage, temperature corrected voltage, diffuse logic... However, one of the most used algorithms in inverters of connection to the grid is that of perturbation and observe. In this method the operating voltage ΔV is modified and the power increase ΔP is measured. In the case of a positive increase, the voltage raises and vice versa.

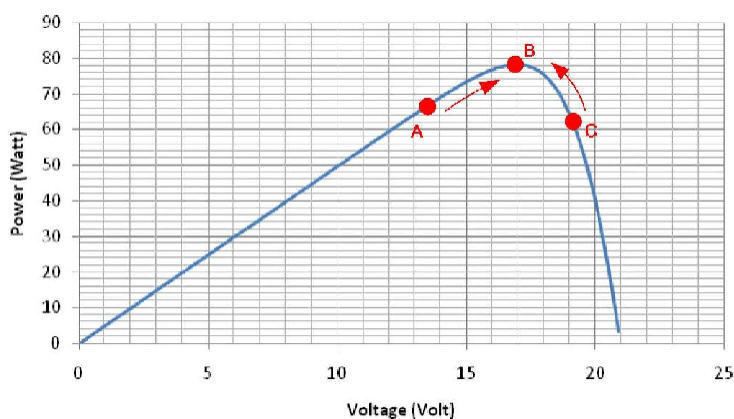


Figure 29: Graphical representation of the algorithm disturbs and observes (Source: <https://images.app.goo.gl/M6Ud1cD5nCVVZFg49>)

The method of incremental conductance consists of measuring the value $\Delta P/\Delta V$. If this derivative is positive, then it is necessary to increase the value of the voltage. If the derivative is negative, the value of the voltage is decreased.

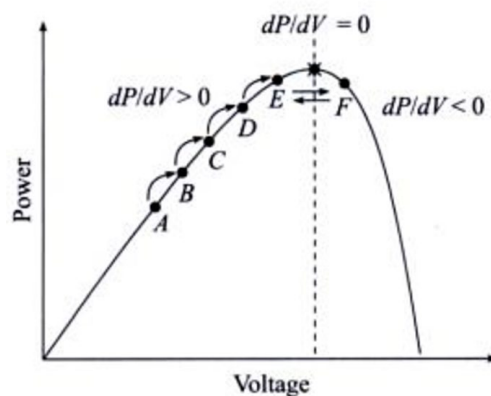


Figure 30: Graphical representation of the method of incremental conductance (Source: <https://images.app.goo.gl/rJpZijgc5viaUAJHA>)

Although these algorithms seem easy to implement, they could produce some difficulties; for example, they can cause a decrease in the tracking performance (in specific circumstances). At very low levels of irradiance the power curve becomes flat; consequently, it becomes more difficult to discern the location of the maximum power point. In the case of sudden variations of irradiance (as happens on cloudy and clear days), erratic follow-up behaviour may occur. Besides, When the irradiance increases, the voltage reference could continue to change to values opposite to the voltage of the maximum power. These problems can be corrected by including different voltage values' disturbance times, depending on the evolution of the power variation over time, or by performing alternating variations of voltage disturbances.

An alternative method of monitoring is setting the working voltage to a value related to the open circuit voltage of the photovoltaic generator and then modifying that value according to the operating temperature. This simple method does not follow the maximum power point, but the results are good. [1] [3]

4.4. Configurations of the system

Inverters can be classified into:

- a) Central inverters: usually used in large PV installations, where the PV generator is connected in parallel branches and the DC/AC conversion is centralised in a single inverter. Grid-switched inverters are based on IGBTs with PWM control.
- b) String inverters: based on a modular concept, in which several branches of a generator FV are connected to inverters in the power range of 1 to 3 kW.
- c) Inverters integrated in photovoltaic modules or AC modules: they are an integrated combination of a single PV module and an inverter.
- d) Multi string inverters: they have in a single unit several DC/DC converters in a single unit, with their respective maximum power point trackers, which supply power from a common DC/AC

inverter to all of them. Using this system, it is possible to connect to the same inverter series of modules with different nominal data, sizes or technologies; even series with different installations and orientations or with different shades degrees, each series working at its maximum power point.

The string inverter is employed to connect to the grid a photovoltaic installation to the grid, in order to get for building integration. The string inverter and the central inverter are both valid for grid-connected photovoltaic power plants. The reduction of DC wiring, associated with the string inverters along with their modularity, is a factor factors that face the simplicity and higher performance of the large central inverters. Some inverters have a DC/DC voltage booster/reducer converter that attacks the inverter input allowing to extend the DC voltage operating range. In other cases, the inverter attacks a 1: N ratio transformer that raises the output AC voltage. [1] [3]

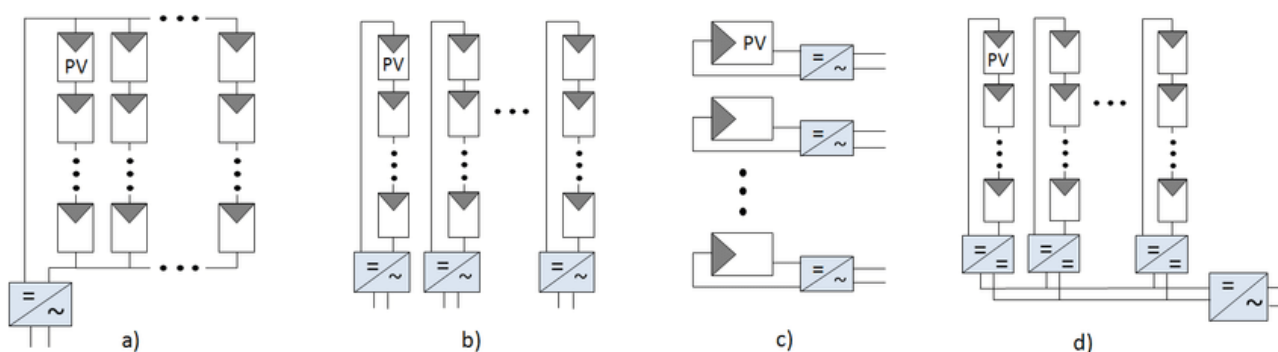


Figure 31: Configurations of the system: a) central inverter; b) String inverters; c) AC modules; d) Multi string inverters
 (Source: <https://images.app.goo.gl/mXZ1LUPiSauZeZ9bA>)

After describing separately the photovoltaic modules and the inverter, it is necessary to define the coupling conditions that allow to obtain a system working properly. This is therefore the subject discussed in the next chapter.

5. Coupling between inverter and photovoltaic field

This chapter deals with the coupling between inverter and photovoltaic modules, in order to obtain a configuration physically achievable. It is then explained how to correctly choose the size of the inverter and, starting from its technical data, get to the number of panels in series and parallel of the installation.

5.1. Inverter choice

Choosing the inverter, starting from the nominal power, is important for a correct array - inverter coupling. There is a relationship between the peak power of the photovoltaic field P_{A-MPP} and the maximum power of the inverter P_{DC-max} , given by the following formula:

$$P_{DC-max} = f \cdot P_{A-MPP} \quad (21)$$

f is a sizing factor of the inverter that considers various conditions, such as solar radiation and exposure. For example, if the geographical area of installation is Northern Europe (less radiation) or if the exposure is not optimal, f has a value of about 0.7; in southern Europe it usually assumes a unitary value.

5.2. Configuration of the system

The choice of the inverter is important in order to define the number of panels in series and parallel to the photovoltaic field. In phase of planning, it must refer to the values of maximum DC voltage, maximum incoming current and to the range MPPT. All these data are in the catalogue of the inverter.

A correct coupling between photovoltaic field and inverter means that:

- 1) The maximum voltage of the photovoltaic field $V_{A-OCmax}$ (i.e., string) must be less than the maximum continuous voltage of the inverter V_{DC-max} . If this does not occur, the inverter can be damaged.
- 2) The minimum voltage of the photovoltaic field $V_{AMPP-min}$ must be greater than the minimum voltage MPPT of the inverter $V_{MPP-min}$. If this does not occur, the inverter does not work properly.
- 3) The maximum voltage of the photovoltaic field $V_{A-MPPmax}$ must be lower than the maximum MPPT voltage of the inverter $V_{MPP-max}$. If this does not occur, the inverter does not work properly.
- 4) The maximum current of the photovoltaic field I_{A-max} , sum of the current of all the arrays, must be less than the maximum continuous current of the inverter I_{DC-max} . If this does not occur, the inverter can be damaged.

These limits are shown in the figure below.

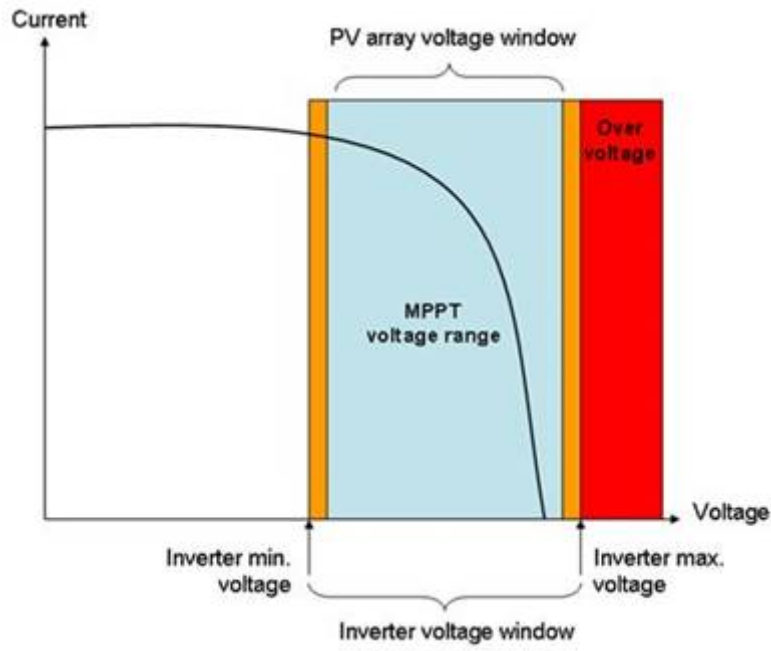


Figure 32: Operation zones of inverter and photovoltaic field (Source: <https://images.app.goo.gl/BLVW6Gd8nrrqzJ2Y9>)

These conditions can be translated into mathematical expressions to be applied to any new configuration realizable. Therefore, the following formulas can be obtained:

- 1) The maximum voltage of the photovoltaic field $V_{AOC-max}$ is produced in open circuit V_{A-OC} , with the maximum irradiance G_{STC} and the minimum ambient temperature T_{MIN} .

$$V_{A-OCmax} = V_{A-OC}(G_{STC}, T_{MIN}) = N_{S-M} \cdot V_{M-OC}(G_{STC}, T_{MIN}) \leq V_{DC-max} \quad (22)$$

Where N_{S-M} is the maximum number of modules in series and V_{M-OC} is the open circuit voltage of the module in the working conditions dictated by the place of installation. This parameter is obtained with the catalogue open circuit voltage V_{oc} and a correction given by the following formula

$$V_{M-OC}(G_{STC}, T_{MIN}) = V_{oc} + \beta \cdot (T_{MIN} - 25) \quad (23)$$

Where β is the coefficient of variation of V_{oc} with temperature

- 2) The minimum voltage of the photovoltaic field is reached at the maximum ambient temperature of operation T_{MAX} (the influence of irradiation is neglected)

$$V_{A-MPPmin} = V_{A-MPP}(G_{STC}, T_{MAX}) = N_{S-m} \cdot V_{m-MPP}(G_{STC}, T_{MAX}) \geq V_{MPP-min} \quad (24)$$

Where N_{S-m} is the minimum number of modules in series and V_{m-MPP} is the minimum voltage MPPT. This parameter is obtained with the catalogued MPPT voltage V_{MPP} and a correction given by the following formula

$$V_{m-MPP}(G_{STC}, T_{MAX}) = V_{MPP} + \beta \cdot (T_{MAX} - 25) \quad (25)$$

T_{MAX} depends on the ambient temperature of the installation site T_{envMAX} and the NOCT (nominal operating Cell Temperature) data of the catalogued photovoltaic module. In formulas

$$T_{MAX} = T_{envMAX} + G_{STC} \cdot \frac{NOCT - 20}{800} \quad (26)$$

- 3) The maximum MPPT voltage of the photovoltaic field is considered at the minimum operating temperature of the modules

$$V_{A-MPPmax} = V_{A-MPP}(G_{STC}, T_{MIN}) = N_{S-M} \cdot V_{M-MPP}(G_{STC}, T_{MIN}) \leq V_{MPP-max} \quad (27)$$

Where V_{M-MPP} is the maximum MPPT voltage. This parameter is obtained with the catalogued MPPT voltage V_{MPP} and a correction given by the following formula:

$$V_{M-MPP}(G_{STC}, T_{MIN}) = V_{MPP} + \beta \cdot (T_{MIN} - 25) \quad (28)$$

- 4) The maximum current of the photovoltaic field is produced in case of maximum ambient temperature.

$$I_{A-max} = N_{P-M} \cdot I_{M-SC}(T_{MAX}) \leq I_{DC-max} \quad (29)$$

Where N_{P-M} is the maximum number of modules in parallel and I_{M-SC} is the short circuit current of the module in the working conditions dictated by the installation site. This parameter is obtained with the short circuit current given by catalogue I_{sc} and a correction given by the following formula:

$$I_{M-SC}(T_{MAX}) = I_{sc} + \alpha \cdot (T_{MAX} - 25) \quad (30)$$

Where α is the coefficient of variation of I_{sc} with temperature.

These equations allow to determine the number of modules in series and parallel for a correct functioning of a photovoltaic installation. The solution can be a result of various iterations and is not unique. [1] [6]

The photovoltaic field just defined consists of a series of accessories such as supports, solar string combiner boxes, and electrical cables, of which functions are explained in the next chapter.

6. Other elements of the photovoltaic field

A photovoltaic field is incomplete and cannot operate without a series of structural and electrical accessories, presented below. The solar string combiner boxes protect, monitor and link the cables coming from the strings. The support structures, supporting elements that allow the correct positioning of the panel, are then described. The following subject is the electrical cables that carry the current in the system. Finally, the electric protections allow to operate in the safety of people and system components.

6.1. Solar string combiner boxes

The solar string combiner boxes, or junction boxes, are elements located between the modules and the inverter. They normally are in the shade under the support structures. They reduce the number of total string cables presenting several cables inputs, usually 16, 24 or 32, and only one cable output. The inputs can be used entirely or partially, depending on the configuration to obtain. The total number of solar string boxes that can be connected to an inverter depends on the number of DC inputs of the inverter. In addition to the number of strings, the rated voltage and current are the main parameters. Among the electrical components of the solar string combiner box, many models have built-in fuses to protect the strings. The fuses, even though they are not incorporated, must be present to operate in safety. Another important element is the DC power disconnect switch, through which the solar string combiner boxes can disconnect the photovoltaic subfield from the inverter. Some solar string combiner boxes are equipped with devices capable of measuring electrical parameters, such as voltage and current, and therefore assessing correct operation. [7]



Figure 33: Solar string combiner boxes (Source: <https://images.app.goo.gl/v4DHYSZ9Y4CziM8g6>)

6.2. Support structures

The photovoltaic modules are mounted on stable, rigid and durable support structures. They are usually constructed with hot-dip galvanised steel, aluminium or stainless-steel profiles. In addition, they must withstand atmospheric agents. Some aspects of common meteorological phenomena should be considered during the design process. In particular:

- Rain in photovoltaic systems is beneficial as it helps to clean up dust and impurities accumulated on the surfaces of modules. Besides, on hot days, it causes a drop in temperature and better performance when the Sun comes back. But drainage is necessary in the area where the solar panels are located, in order to avoid possible flooding and, consequently, corrosion and deterioration of the equipment. Usually in the frame of the panels there are holes for the drainage, in order to expel accumulated water.
- The hail is dangerous because it can cause many damages to the structure although it is unlikely to break the glass of the solar panel. In fact, Solar panels are normally subjected to rigorous tests before being approved. But, to minimise the risk of a solar collector being broken by hail, tempered glass panels are better and more resistant.
- The wind can cause problems depending on its speed and surface. A quite strong wind can make the module and support fly away, with the consequent loss of the component and the possible material and personal damage. The most dangerous wind in the Northern Hemisphere, being the modules oriented towards the South, is the one heading towards the Equator. To prevent the wind from blowing the modules, the supporting structure must exert a force towards the ground, equal to or greater than the one the wind is capable of exerting on the collectors. In the case of several modules in the support structure, the action of the wind can be minimized, leaving gaps between the modules and separating them from the ground, reducing the pressure exerted.
- Snow does not pose any danger to the integrity of the solar modules. It can reduce the efficiency since snow, being solid, accumulates in the place where it falls. In order to avoid snow piles, the supporting structure can be raised so that it accumulates outside the photovoltaic modules.

The support structure can be described as an auxiliary element. Besides its support function, it always gives the panel the most suitable inclination to optimize the energy efficiency. The structures can be classified firstly according to the place of installation of the photovoltaic modules or, secondly, according to the type of movement of the structure.

The most common system found in the installations is a fixed support. This is further classified by ground, wall or roof mounting. Depending on the latitude of the installation and the desired application, the panels are equipped with the most suitable inclination to capture the greatest possible solar radiation. The inclination is very easy to apply in the installations on the ground and is adaptable to the place orography. In the case of ceilings or walls, architectural restrictions should also be considered.

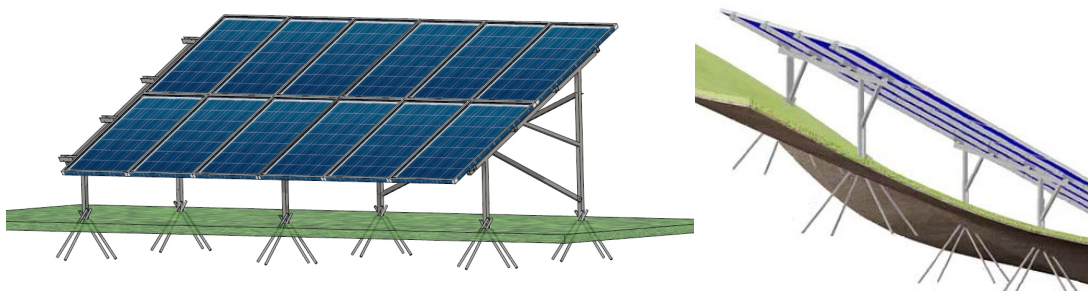


Figure 34: Installation on the ground, examples of adaptation to the place orography (Source: [8])

Solar tracking systems are mobile structures. The modules are placed on them in order to optimize the incidence of solar rays at any time and thus increase the uptake. They look for the optimal position of the panels in relation to the Sun. Depending on their moving parts and the arrangement of the panels on them, they are distinguished in:

- One-axis solar tracking systems: rotation of the support is done by means of a single axis, vertical, horizontal or oblique. This type of tracking is the simplest and cheapest. They can follow either the Sun's inclination or azimuth
- Two-axis solar tracking systems: with this system it is already possible to fully monitor the Sun in altitude and in azimuth and it will always be possible to obtain the greatest uptake of the perpendicular incised radiation. It is estimated that these systems can achieve a greater 30 per cent increase in the energy collected. It is necessary to assess the cost of the tracking system and the gain from increased energy to determine its profitability. [1] [3]

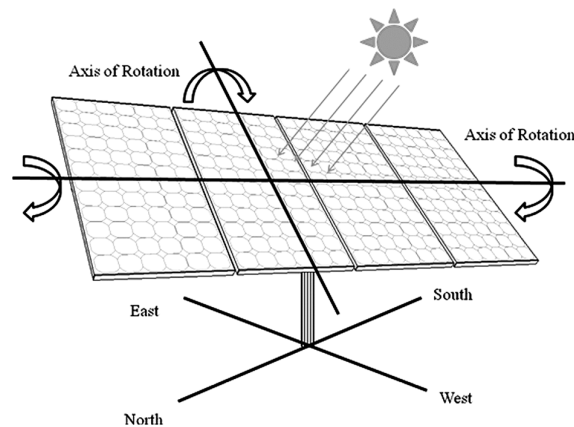


Figure 35: Two-axis solar tracking systems (Source: <https://images.app.goo.gl/y13A1nJJS9KmMyCs8>)

6.3. Electric cables

The cable is an electrical element that allows to transport the current produced by the photovoltaic field to the inverter and from this to the transmission grid. In the next paragraph some general notions on cables are provided, and after the PV cables and their sizing are analysed.

6.3.1. General concepts

Three components can be distinguished in a cable: the conductor, the insulator and a protection conduit. Moreover, there are cables without insulation, used in the overhead lines, called bare electric cables. The various parts of a cable are then analysed. [6] [9]

- As far as the conductor is concerned, copper and aluminium are the most used materials. The choice of the conductor material shall consider the voltage level of the system, the cost of the element and the application for which it is intended. A further distinction is due to the number of conductors: if there is only one conductor in the coating, it is called a unipolar cable, otherwise it is multipolar.

- The insulation consists of impregnated paper or extruded materials. These include PVC (polyvinyl chloride), PE (polyethylene) and its derivatives, EPR (ethylene propylene rubber) and butyl rubber.
- The outer sheath can be made of aluminium, lead, PVC and provides mechanical and weather protection

Cables can have different poses and each pose has an identifying letter and number. The following table shows some poses taken from UNE 60364 and whose description has been translated.

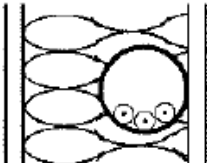
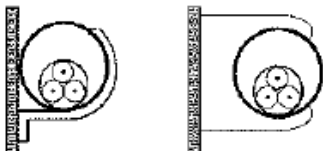
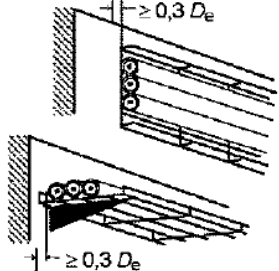
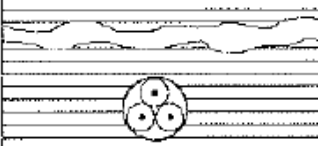
	Types of installation	Definition
A1		Insulated conductors or unipolar cables in tube inside a wall thermally insulating
B2		Multipole cable in a tube on, or separated from, wooden or masonry wall less than 0,3 times the diameter of the tube
C		Unipolar or multipolar cables: fixed directly under a wooden or masonry ceiling
E or F		Unipolar or multipolar cables: on supports or grids in route horizontal or vertical
B1		Insulated conductors or single-core cable on channels embedded in the floor
D1		Multipole cable in tube or closed conduit
D2		Single-core or multi-core cables with sheath on the floor: without additional mechanical protection

Table 5: Different poses of the cables (Source: [10])

6.3.2. Cables for photovoltaic installations

There are two types of cables in a photovoltaic installation. Firstly, from the modules to the inverter there are cables carrying a direct current. Secondly, after the inverter we have AC cables.

DC cables used in photovoltaic installations shall meet the following requirements:

- Resistant to humidity, UV rays, working temperature up to 120 °C
- Ambient temperature of the installation from 90 °C to -40 °C
- Section from 4 mm² to 35 mm² in the spaces between panels and panels to the CC junction box and from 16 mm² to 300 mm² in the section from junction box to inverter with armature option for mechanical protection.
- Conductors must be made of copper (IDAE)
- High security to protect in case of fire when there is a deck of cables
- Suitable for use in Class II equipment
- Cover colours are red (positive) and black (negative)
- Average service life of 25 years
- If outdoors, protection against rodents

In alternating current, the same conductors are used for connection installations, insulated with thermostable material such as XLPE, EPR with fireproof polyolefin cover. [1] [5]

Below there is a graphic summary of these characteristics, present in a data sheet of a cable for solar installations.

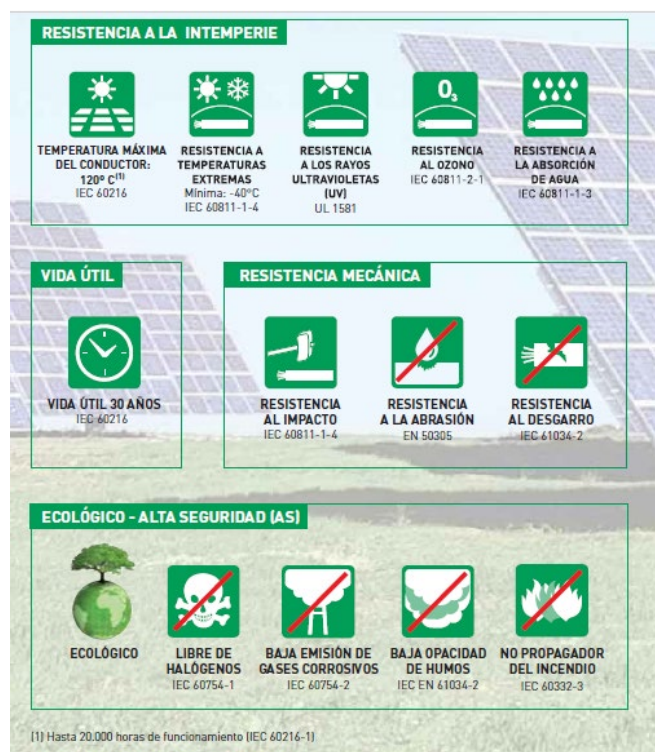


Figure 36: Characteristics of a photovoltaic cable (Source: https://www.google.com/url?sa=t&rct=j&q=&esrc=s&source=web&cd=6&ved=2ahUKEwj11cCdyrroAhVNCxoKHXztCPMQFjAFegQIARAB&url=http%3A%2F%2Fboj.pntic.mec.es%2Fcrodenas%2Fsolares%2Fut5%2FCables_General%2520cable.pdf&usg=AOvVaw0paOzVgXx283aDFbsueHms)

6.3.3. Dimensioning of the cables

To correctly choose a cable, the first thing to do is calculating the operational current. IDAE states that "electric conductors shall have the appropriate section to prevent voltage falls and heatings". Then, applying the thermal and electrical criteria, a section of the cable suitable for carrying this current is defined.

The technical instruction ICT BT 40 reports that "connection cables shall be dimensioned for an intensity not less than 125 % of the maximum intensity of the generator". The formula is as follows:

$$I_b = m \cdot 1,25 \cdot I_{sc} \quad (31)$$

Where:

- I_b is the operational current
- I_{sc} is the short circuit current of the photovoltaic module, in standard conditions
- m is the number of subfield strings: it assumes unitary value in the stroke between strings and combiner box or in the case of direct connection between strings and inverter.

The multiplication constant considers cases of temperature drops below 25 °C and cases where irradiation is greater than 1000 W/m². Under these conditions, the current is higher.

This current shall be lower than the cable flow rate I_z :

$$I_b \leq I_z \quad (32)$$

The flow rate calculation according to standard UNE 60364-5-52 which gives the following formula, allows the thermal criterion to be applied.

$$I_z = I_o \cdot k \quad (33)$$

Where:

- I_z is the chosen cable flow rate in non-standard conditions
- I_o is the maximum flow rate in standard cable conditions, obtainable from tables depending on the installation, section, insulation and circuit (single phase or two-phase). Below is the table of reference for copper conductors in the air. There are corresponding tables for aluminium and for underground cables

Método de referencia de la tabla B.52.1	Número de conductores cargados y tipo de aislamiento											
		3 PVC	2 PVC		3 XLPE	2 XLPE						
A1		3 PVC	2 PVC		3 XLPE	2 XLPE						
A2	3 PVC	2 PVC		3 XLPE	2 XLPE							
B1				3 PVC	2 PVC		3 XLPE		2 XLPE			
B2			3 PVC	2 PVC		3 XLPE	2 XLPE					
C					3 PVC		2 PVC	3 XLPE		2 XLPE		
E						3 PVC		2 PVC	3 XLPE		2 XLPE	
F							3 PVC		2 PVC	3 XLPE		2 XLPE
1	2	3	4	5	6	7	8	9	10	11	12	13
Tamaño (mm ²) Cobre												
1,5	13	13,5	14,5	15,5	17	18,5	19,5	22	23	24	26	-
2,5	17,5	18	19,5	21	23	25	27	30	31	33	36	-
4	23	24	26	28	31	34	36	40	42	45	49	-
6	29	31	34	36	40	43	46	51	54	58	63	-
10	39	42	46	50	54	60	63	70	75	80	86	-
16	52	56	61	68	73	80	85	94	100	107	115	-
25	68	73	80	89	95	101	110	119	127	135	149	161
35	-	-	-	110	117	126	137	147	158	169	185	200
50	-	-	-	134	141	153	167	179	192	207	225	242
70	-	-	-	171	179	196	213	229	246	268	289	310
95	-	-	-	207	216	238	258	278	298	328	352	377
120	-	-	-	239	249	276	299	322	346	382	410	437
150	-	-	-	-	285	318	344	371	395	441	473	504
185	-	-	-	-	324	362	392	424	450	506	542	575
240	-	-	-	-	380	424	461	500	538	599	641	679

Table 6: Admissible current for copper conductors with an ambient temperature of 30 °C (Source: [10])

- k is a correction coefficient to use if the cable is not in standard condition. This coefficient derives from the product of other k_i coefficients, which consider firstly the type of laying, secondly the temperature of the surrounding medium (air or ground), and eventually the presence of adjacent cables. Besides in the case of underground cables there is a correction coefficient for thermal resistivity different from 2,5 K·m/W. In the photovoltaic field there is also a coefficient that considers the exposure to the Sun and assumes value 0,9 in the case of direct exposure and 0,91 in the case of exposed canal. Some tables are necessary to identify these coefficients.
 - ✓ The first table considers when the ambient temperature is different from 30 °C in the air. A corresponding table is used when the temperature of the soil differs from 20 °C.

Temperatura ambiente °C	Aislamiento			
	PVC	XLPE y EPR	Mineral ^a	
			Cubierta de PVC o cable desnudo y accesible 70 °C	Cable desnudo e inaccesible 105 °C
10	1,22	1,15	1,26	1,14
15	1,17	1,12	1,20	1,11
20	1,12	1,08	1,14	1,07
25	1,06	1,04	1,07	1,04
30	1,00	1,00	1,00	1,00
35	0,94	0,96	0,93	0,96
40	0,87	0,91	0,85	0,92
45	0,79	0,87	0,78	0,88
50	0,71	0,82	0,67	0,84
55	0,61	0,76	0,57	0,80
60	0,50	0,71	0,45	0,75
65	–	0,65	–	0,70
70	–	0,58	–	0,65
75	–	0,50	–	0,60
80	–	0,41	–	0,54
85	–	–	–	0,47
90	–	–	–	0,40
95	–	–	–	0,32

Table 7: Correction factors for ambient temperature different from 30 °C (Source: [10])

- ✓ Another table gives the coefficient to the variation of the thermal resistivity of the soil

Resistividad térmica K·m/W	0,5	0,7	1	1,5	2	2,5	3
Factor de corrección para cables en conductos enterrados	1,28	1,20	1,18	1,1	1,05	1	0,96
Factor de corrección para cables enterrados directamente	1,88	1,62	1,5	1,28	1,12	1	0,90

Table 8: Correction factors for cables buried directly in the ground or underground conductors for soil with resistivity different from 2,5 K·m/W (Source: [10])

- ✓ The following tables concern the correction factor for various cables in the same channel. In fact the presence of more cables increases the temperature.

Punto	Disposición	Número de circuitos o de cables multipolares								
		1	2	3	4	6	9	12	16	20
1	Agrupados en el aire, en una superficie, empotrados o en el interior de una envolvente	1,00	0,80	0,70	0,65	0,55	0,50	0,45	0,40	0,40
2	Capa única sobre muros, suelos o bandejas no perforadas	1,00	0,85	0,80	0,75	0,70	0,70	–	–	–
3	Capa única fijada directamente al techo	0,95	0,80	0,70	0,70	0,65	0,60	–	–	–
4	Capa única sobre bandejas perforadas horizontales o verticales	1,00	0,90	0,80	0,75	0,75	0,70	–	–	–
5	Capa única sobre bandeja de escalera, soportes o bridas de amarre, etc.	1,00	0,85	0,80	0,80	0,80	0,80	–	–	–

A) Cables multipolares en conductos individuales				
Número de cables	Distancia entre conductos ^a			
	Nula (conductos en contacto)	0,25 m	0,5 m	1,0 m
2	0,85	0,90	0,95	0,95
3	0,75	0,85	0,90	0,95
4	0,70	0,80	0,85	0,90
5	0,65	0,80	0,85	0,90
6	0,60	0,80	0,80	0,90
7	0,57	0,76	0,80	0,88
8	0,54	0,74	0,78	0,88
9	0,52	0,73	0,77	0,87
10	0,49	0,72	0,76	0,86
11	0,47	0,70	0,75	0,86
12	0,45	0,69	0,74	0,85
13	0,44	0,68	0,73	0,85
14	0,42	0,68	0,72	0,84
15	0,41	0,67	0,72	0,84
16	0,39	0,66	0,71	0,83
17	0,38	0,65	0,70	0,83
18	0,37	0,65	0,70	0,83
19	0,35	0,64	0,69	0,82
20	0,34	0,63	0,68	0,82

Table 9: Correction factors for groups of various circuits or multipolar cables (Source: [10])

The current is then obtained from the Table 6 and the various corrective factors from the tables present in the standard. The current I_z obtained must be greater than the one calculated (I_b). Otherwise it is necessary to choose an I_o corresponding to a greater section until it is verified the inequality of Equation (32).

Besides, the cable, whose current I_o allows to verify the thermal criterion, must have appropriate electrical parameters (resistance) to satisfy the electrical criterion of the voltage drop. In fact, a cable can only be installed if it meets both criteria. Otherwise, it is necessary to proceed checking up a larger section.

The technical instruction ICT BT 40 states that "the voltage drop between the generator and the interconnection point to the Public Distribution Grid or to the indoor installation shall not exceed 1,5 % for the nominal intensity". The voltage drop must be distributed over the paths from the generating field to the inverter and, then from this to the consumption or interconnection point (standalone or grid installation). [1] [6] [10]

The formulae for the calculation of the voltage drop are given below.

- Direct current lines:

$$\Delta V = \frac{2 \cdot r \cdot L \cdot m \cdot I}{V} \cdot 100 \tag{34}$$

- Alternating current lines:

$$\Delta V = \frac{2 \cdot L \cdot m \cdot I \cdot (r \cdot \cos\Phi + x \cdot \sin\Phi)}{V} \cdot 100 \quad (35)$$

- Three-phase alternating current lines:

$$\Delta V = \frac{\sqrt{3} \cdot L \cdot m \cdot I \cdot (r \cdot \cos\Phi + x \cdot \sin\Phi)}{V} \cdot 100 \quad (36)$$

Specifying the terms in the photovoltaic field there are:

- ΔV is the voltage drop in %
- V, I are the MPP tension and current of the string
- $\cos\Phi$ is the power factor
- L is the length of the cable in meters
- r, x are the resistance and the reactance of the cable to the temperature of interest
- m is the number of subfield strings: it assumes unitary value in the stroke between strings and combiner box or in the case of direct connection between strings and inverter.

6.4. Protections

The protective elements prevent damage to cables, appliances and people. Large intensities can cause fire (on wires), damage to appliances or produce electrical shocks to people. The protections will avoid direct and indirect contacts, short circuits, overloads and overvoltages. The definitions of these terms are provided in the following paragraph; then they are analysed in the photovoltaic context.

1. A direct contact occurs when a person touches a point of the installation directly under voltage (conductors, windings).
2. Indirect contact occurs when a person makes contact with a under tension installation's mass as a result of an isolation failure. This is an element outside the electrical circuit which, under normal conditions, should not have voltage, but which has acquired it accidentally.
3. A short circuit occurs when two or more points of the installation with different electrical potential reach each other.
4. An overload occurs when a permanent operating current circulates through the installation and is greater than the nominal design current of the installation.
5. An overvoltage occurs when between two points of the installation there are higher voltages than in normal operation. [1] [3]

6.4.1. Protection against direct contacts

Protection against direct contact means taking measures in order to protect people from reaching active electrical parts. (UNE 60364, ITC-BT-24). Measures are taken to avoid contact, as the following:

- Insulation protection of active parts
- Protection by barriers or envelopes
- Protection through obstacles

- Out-of-range protection by remoteness
- Additional protection by residual differential current devices

Eventually, the active parts are considered protected from obstacles, if they are resistant, and suitably fixed; besides, they should meet the following requirements:

- Obstacles' external surfaces of obstacles must have a minimum degree of protection of IP2XX
- Easily accessible surfaces (within reach of the person) must have an IP4XX degree of protection

According to the UNE-EN 60529 standard, the protection's degrees of the low voltage electrical equipment enclosures are indicated by the IP symbol, then followed by three digits:

- The first figure indicates the degree of protection of people against contacts with parts in tension or moving parts, besides the protection of the material against penetration of solid and dust.
- The second one reports the degree of protection of the material against the penetration of liquids
- The last one illustrates indicates the degree of protection of the material against any mechanical damage. [3]

6.4.2. Protection against indirect contacts

Protection measures against indirect electrical contacts are included in the Spanish "Reglamento Electrotécnico Para Baja Tensión" (REBT, Low Voltage Electrotechnical Regulation). In particular in its complementary technical instruction ITC-BT-24 and UNE 60364. This protection is achieved through the application of one of the following measures:

- Protection by automatic interruption of the power supply
- Class II equipment or equivalent insulation protection
- Protection in non-conductive locations
- Protection by non-grounded local equipotential connections
- Protection by electrical separation

Protection by automatic interruption of the power supply mainly depends on the Ground Connection Scheme: TT, TN, IT scheme. Choosing one or another is connected to different aspects: the country, the continuity of service required, the flexibility of the extension of the installation, the maintenance of the installation. Whichever scheme exists in an installation, the standards require that:

- Each mass is connected to a ground outlet through the protection conductor
- Simultaneously accessible masses are connected to the same ground
- A cutting device automatically disconnects any part of the installation where a dangerous contact voltage can be generated
- The cutting time of this device is less than the defined maximum time. [3]

6.4.3. Protection against overcurrent

The maximum current in the solar field is the short circuit current of the panel, I_{sc} . If in the generator there are m parallel branches and a short circuit occurs, the current will have a value of:

$$I_{sc,tot} = (m - 1) \cdot I_{sc} \quad (37)$$

In the parallel connection, the tension is the same. If one row lowers its tension, the others make a quick escape of intensity to equalize. This can cause damage in the lower voltage row. To avoid this, in a group of 3 or more strings, in each one of them there are blocking diode, fuses or magnetothermics. The reverse diode carried by the panels serves a group of two rows because it supports 1,5 times its I_{sc} . Then in the following paragraph, the 3 possible elements are presented.

- a) Blocking diodes: they prevent the passage of the reverse current. They are calculated to withstand $2 \cdot I_{sc}$ of a panel and a voltage of $1,2 \cdot V_{oc,string}$ (open short circuit of the string). The disadvantage is that they have a consumption and are only recommended when access is difficult or there are partial shades. The advantage is that they do not have to be replaced like fuses.
- b) Fuses: they are dimensioned to support between 1,25 and 2 times the I_{sc} and a voltage of $1,2 \cdot V_{oc,string}(T_{min})$. The drawback is that the cartridge must be replaced, but they dissipate less power than the diodes, about 0,2 V compared to 0,6 V. The general switch or disconnecter, located at the output of the solar group, must be disconnected before opening the fuses. It is dimensioned to support $1,5 \cdot I_{sc}$ and at the voltage of $1,2 \cdot V_{oc,string}$.
- c) Magnetic thermal circuit breakers: they must be in continuous. They are dimensioned to act as maximum $1,5 \cdot I_{sc}$ of a panel and at the voltage of $1,2 \cdot V_{oc,string}$. [1]

6.4.4. Protection against surge voltage

There are transient overvoltages due to atmospheric discharges to be diverted to the ground. The dischargers and earthing of about 10Ω are used, causing the lightning current to discharge by it. Due to their large size, solar fields are exposed to atmospheric problems. External protection against lightning (lightning rod) and internal protection against overvoltages are commonly used. In addition, there are permanent overvoltages, which cause a minor voltage surge, but their duration is not known. They originate from grid voltage variations or neutral failure. DC surge protections are installed in the generator junction box or at the inverter input. In the AC side, they are placed between the inverter and the protection and measurement box. After detecting them, the installation must disconnect automatically as overvoltages can cause premature aging of the equipment, overheating, fire. This type of protection is usually carried by the inverter in the alternating part, to avoid interference with the distribution grid and vice versa. [1]

6.4.5. Inverter and grid protection

There are at least the following protections

- Protection for maximum and minimum frequency (50,5 and 48 Hz) and voltage (1,15 and 0,85 the rated voltage) interconnection. Maximum frequency reconnection shall be made for a value less than or equal to 50 Hz.
- Overvoltages, with varistors or similar.
- Grid failures such as micro short circuits, cycle defect, grid absence and return.

- General switch. With insulation for protection and safety against electrical risk. A magnetothermics with the short circuit current higher than the one indicated by the distributor at the connection point.
- Differential automatic switch
- Automatic interconnection switch. [1]

6.4.6. System grounding

It consists of electrically joining metal masses with earth to obtain protection against direct contacts and atmospheric discharges, avoiding the potential difference between different masses or between these and the earth. The earth conductor connects all the panels' frames between itself and the structure. The structures are connected with a naked conductor.

In the IDAE it is explained that, from 48 V, the panels frames, the support structure and the metal masses are grounded. Panels usually work insulated from the soil, floating. In an IT distribution scheme, if there is a defect of a conductor with a metal mass, it does not circulate current to the ground because the circuit is not closed; but a second failure can create dangerous tensions in the masses. For voltages greater than 24 V there will be an isolation monitoring or leak detector to intervene in the installation before the second failure. In large installations the installation will be stopped after the first failure as a prevention to major currents. This protection may be incorporated in the inverter.

For the AC part, Royal Decree 1699/2011 indicates that the land of the installation is different from that of the grid. The land of the paper distributor is not to be altered. It is necessary to ensure that no defects are transferred to the grid with isolation transformer or similar. [1]

After describing a photovoltaic solar field in all its components, the causes of energy losses can be estimated. From these losses an estimation of the producibility can be made. Finally, some useful terms are presented for an economic analysis. These are therefore the topics of the next chapter.

7. Producibility estimation and economic analysis

This chapter deals with the estimate of the energy produced by a photovoltaic system connected to the electricity grid. The different energy loss factors are presented with relative values based on experimental data. One of the numerous existing methods for calculating the energy fed into the grid is described. Finally, some useful terms are presented for an economic analysis.

7.1. Estimation of energy losses

When dimensioning a photovoltaic system, it is important to consider the different energy profiles of the diverse components of the system, with respect to their nominal values. The loss factors are then analysed and they can depend on:

1. Orientation: photovoltaic modules are usually mounted on fixed structures (although they can also have solar monitoring on one or two axes). The inclination and orientation of the photovoltaic modules must be optimized according to periods of higher or lower consumption. While the optimal orientation is towards the observer (South in the Northern Hemisphere and North in the Southern Hemisphere), the inclination is of the order of the latitude of the place plus a correction to maximize the energy uptake in the period of the year wanted. This correction results in an energy loss that generally does not exceed 5 % of the optimum.
2. Shading of the photovoltaic generator. The partial or total shading of the generator during the day, originated by the near presence of houses, buildings, trees...may represent a considerable energetic loss source of energetic losses, despite having passing diodes. A typical value is 10 %.
3. Dust and localized dirt. The dust and the dirt accumulated on the surface of the modules can cause between 4 and 15 % energy losses. This effect depends on the angle of the inclination and the frequency of rainfall.
4. Effect of temperature. Usually the power of the modules is given in standard conditions of measurement, STC, referring to 1000 W/m² of irradiance and 25 °C of the cell's temperature. This value is the peak power, that is the nominal power for which you pay when you buy a panel. Power is proportional to increase of irradiance and to decrease of temperature.
5. Rated power. Not all modules have the same rated power assigned by the manufacturer due to the manufacturing processes. Usually the manufacturer ensures that the power of a certain module is in a range of ±10-15 % of the rated power.
6. Mismatch losses. They are lost from the zoning of slightly different power photovoltaic modules to form a photovoltaic generator. The physical cause that causes them is the connection of modules in series with different short-circuit currents: the "worst" module will limit the current of the series. Similarly, for the voltage of the parallel module connection. In general, the power of a photovoltaic generator is lower (or ideally equal) than the sum of the powers of each module of the modules that make it up. These losses can be reduced with the proper use of passing diodes.
7. Conversion. The grid-connected photovoltaic inverter is an electronic device with certain losses in its switching components. It is important to select the inverter power according to the power of the photovoltaic generator. There are also losses in the transformer.

8. Loss by tracking performance of the point of maximum power. The grid inverter operates directly connected to the photovoltaic generator and has an electronic device for tracking the point of maximum power of the generator. The control algorithms of this device can vary between different models and manufacturers. It is possible to characterize the inverter by a yield curve of the point of maximum power defined as the quotient between the energy that the inverter can extract from the generator and the energy that would be extracted in an ideal follow-up.
9. Loss in the cables. It is necessary to carry out an adequate dimensioning, that is the calculation of the section, of the wiring of the installation to imitate the falling ohmic. It is essential to remember that in medium-power and low-voltage systems the currents handled can considerably grow up, requiring cables of large sections. [3]

The following diagram shows the path of photovoltaic energy from production to the measuring point.

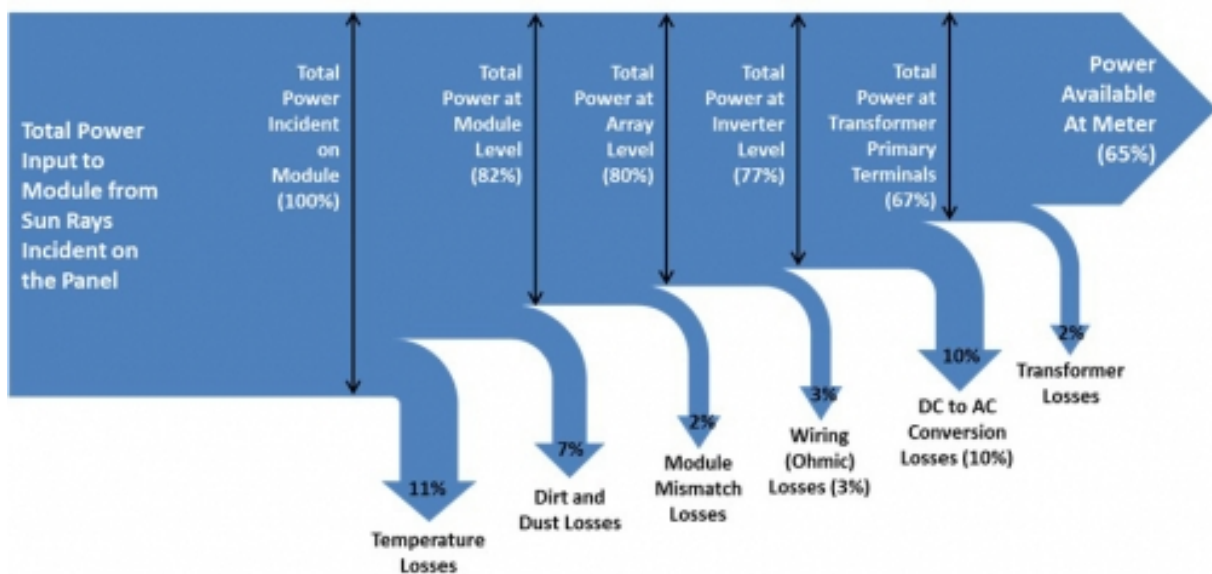


Figure 37: Photovoltaic energy diagram, from production to the measuring point (Source <https://images.app.goo.gl/QjocuTmC9M5g2r617>)

7.2. Calculation of the expected annual production

The study of producibility is presented according to the method proposed in chapter 7 of the “Pliego de condiciones” of the IDAE. Typical values are assumed for some parameters because real data are not accessible for the academic nature of the work. Normally this type of calculation is done with simulation programs firstly because real information is available and secondly because from this study comes an economic evaluation. Moreover, when evaluating the production of a photovoltaic system, discrepancies may arise between the model's predictions and the measurements of the energy input. This depends, for example, on the component, and specifically on the way it has been installed; anyway, there may not be reasonable reasons for this discrepancy.

The first information necessary for this calculation is the input data, is defined below.

$G_{dm}(0)$: monthly and annual average value of daily irradiation on a horizontal surface, in $kWh/(m^2 \cdot day)$, obtained from one of the following sources:

- State Meteorological Agency.
- The State Autonomous Body.
- Other data sources of recognised creditworthiness, or those expressly identified by IDAE.

$G_{dm}(\alpha, \beta)$: average monthly and annual value of the daily irradiation on the generator plane in $kWh/(m^2 \cdot day)$, obtained from the previous one, and in which the shaded losses have been discounted if they exceed 10 % per year. The parameter α represents the azimuth and β the inclination of the generator.

PR: energy efficiency of the installation or performance ratio. Efficiency of the installation in real working conditions.

$$PR(\%) = (100 - A - P_{temp}) \cdot B \cdot C \cdot D \cdot E \cdot F \quad (38)$$

This formula considers:

- A : dispersion of parameters between modules (0,02), dust and dirt (0,03), angular and spectral reflectance (0,03), shadow factor ($< 0,1$)
- B : Cabling efficiency and continuous protections (0,985-0,99)
- C : alternating wiring efficiency (0,98-0,995)
- D : coefficient for plant shutdown losses (0,95)
- E : energy efficiency of the inverter ($> 0,9$)
- F : losses due to errors in the monitoring of the maximum power point (0,9-0,95)
- P_{temp} : dependence on efficiency with temperature (0,08)

The estimate of the injected energy shall be made according to the following equation. [1]

$$E_p = \frac{G_{dm}(\alpha, \beta) \cdot P_{MPPT-PV} \cdot PR}{G_{STC}} \quad (39)$$

Where:

- $P_{MPPT-PV}$ = Peak power of the generator
- $G_{STC} = 1000 \text{ W/m}^2$

7.3. Economic analysis

The profitability analysis is intended to determine the feasibility of carrying out the designed project, by calculating and analysing the economic parameters NPV (net present value), IRR (internal rate of return), DPB (discounted payback time).

Before doing this analysis making this reflection, cash flows must be identified over time. The "overnight cost" hypothesis is often used in the investment in power plants. Completing a plant "overnight" means not considering interests during its construction.

To calculate the present value f_o of a future amount of money f_n the discounting factor $(1 + r)^{-1}$ is used: this parameter is necessary because money has a variable value over time. To express it for a number of years n , the following formula can be used. [11]

$$f_o = \frac{f_n}{(1 + r)^n} \quad (40)$$

7.3.1. Net present value, NPV

The NPV is the algebraic sum of all discounted cash flows of the project under analysis. By calculating the NPV, it is possible to compare two or more investments to each other, considering that the investment with the highest NPV in the pre-established year is more convenient. In general, a project is economically viable if it has a positive or zero NPV. [11]

The general equation is:

$$NPV = \sum_{k=0}^n \frac{f_k}{(1 + r)^k} \quad (41)$$

Where:

- k is indicative of the time interval of cash flows
- f_k is the positive or negative cash flow at time k , $f_k = f_k^+ - f_k^-$
- r is the discount rate

Considering the overnight cost hypothesis, the following formula is obtained:

$$NPV = -I_0 + \sum_{k=1}^n \frac{f_k}{(1 + r)^k} \quad (42)$$

Where:

- I_0 it is the initial investment

7.3.2. Internal rate of return, IRR

IRR is mathematically defined as that discount rate which renders the NPV null. This financial index allows to evaluate the returns from an investment. A project is economically viable if the IRR is higher than a threshold rate or more generally, higher than the discounting rate used in the calculation of the NPV. [11]

The general equation is:

$$NPV = \sum_{k=0}^n \frac{f_k}{(1+r)^k} = 0; \quad IRR = r \quad (43)$$

7.3.3. Discounted payback time, DPB

The DPB defines the period of time necessary to the algebraic sum of all discounted positive cash flows to be equal (or greater) to the one of the negative of the project under analysis. So, it represents the time that it takes to recover the investment. [11]

The general equation is:

$$\sum_{k=0}^n \frac{f_k^-}{(1+r)^k} \leq \sum_{k=0}^{n^*} \frac{f_k^+}{(1+r)^k}; \quad n^* = DPB \quad (44)$$

This chapter concludes the theoretical aspect of this thesis. After the first part, the practical project is described, starting from the choice of the terrain.

8. Description of the position of the photovoltaic plant

This chapter features the site of photovoltaic installation, located in Chelva. The area is presented in terms of climate, mainly temperature and rainfall. Then the type of terrain in the installation area is described. A MATLAB calculation is proposed to determine the correct soil preparation.

8.1. The location

The Spanish municipality of Chelva is presented in terms of geographical location and climate, useful parameters for the correct positioning of the panels. Its geographic coordinates are:

- Latitude: 39° 45' N
- Longitude: 1° 00' W
- Altitude above sea level: 483 m

Chelva is the main city in the comarca of Los Serranos in the Valencian Community. The town, in the middle of the mountains, has an area of about 192 km² and less than 2000 inhabitants. The following images show the location.



Figure 38: Position of the municipality of Chelva, Spain (Source: https://upload.wikimedia.org/wikipedia/commons/thumb/8/88/Spain_location_map.svg/260px-Spain_location_map.svg.png)



Figure 39: Position of Chelva in the comarca of Los Serranos (Source: <https://es.goolzoom.com/mapas/>)

Chelva has a BSk climate according to the Köppen-Geiger system. According to this system, the parameters for determining the climate of an area are the average annual temperature, monthly rainfall, and, finally, the seasonality of precipitation. BSk identifies a place with a dry Mediterranean climate, meaning that it is in a transition zone between a Mediterranean climate and a desert climate with little annual rainfall. The meteorological data collected between 1982 and 2012 are reported in detail.

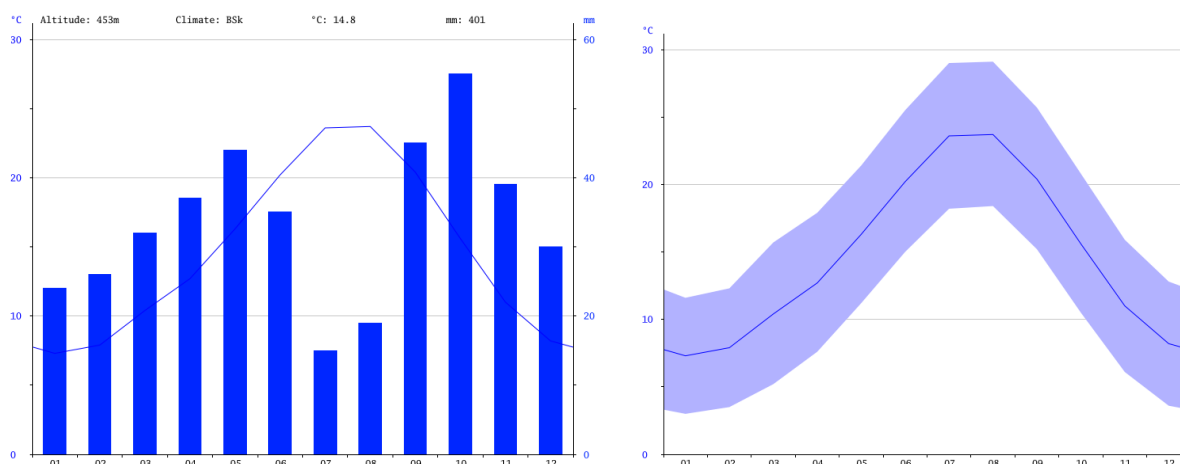


Figure 40 : Chelva, average temperature and precipitation in the year (Source: <https://es.climate-data.org/europe/espana/comunidad-valenciana/chelva-274765/#climate-table>)

In Chelva, the average annual temperature is 14,8 °C. The precipitation is 401 mm per year. The driest month is July, during which there are 15 mm of precipitation. The greatest amount of precipitation occurs in October, with an average of 55 mm with an average of 23,7 °C, August is the warmest month. The coldest month of the year is January, with 7,3 °C in the middle of January. [12] [13] [14]

8.2. Place of installation

The area is required not to be of cultural (historical heritage) or environmental (floristic or faunal nature reserves) interest. A suitable area is met by inserting these constraints in the cartographic viewer of the Valencian community.

The installation is projected in the Polygon number 57 of latitude coordinates 39,64°, -1,05° of longitude. The use of only one Plot (number 806) is required, whose characteristics and cadastral references are presented below. [15] [16]

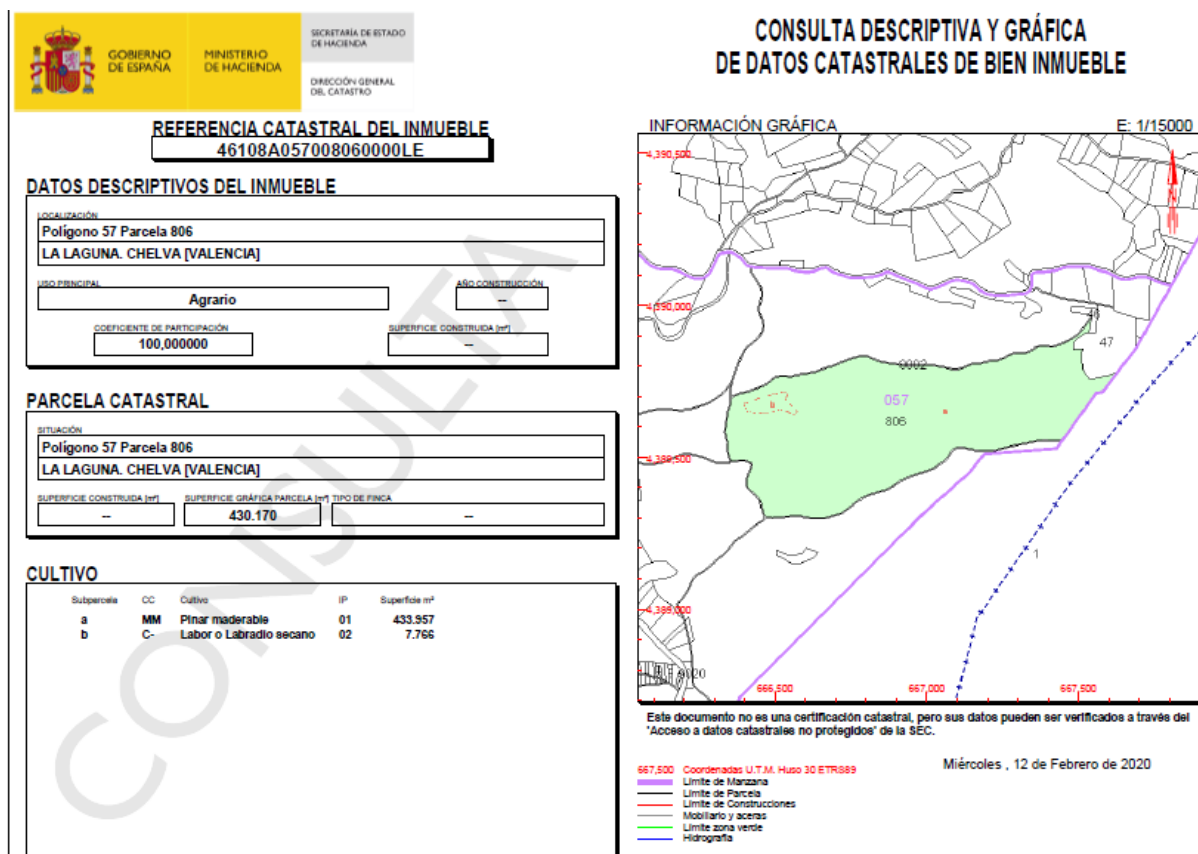


Figure 41: Cadastral reference Plot 806 of Polygon 57 (Source: [15])

These zones are also reported in the AutoCAD drawings (number 1 and 2).

The land can be studied from a litho-geological point of view with data provided by the geological and mining institute of Spain (IGME).

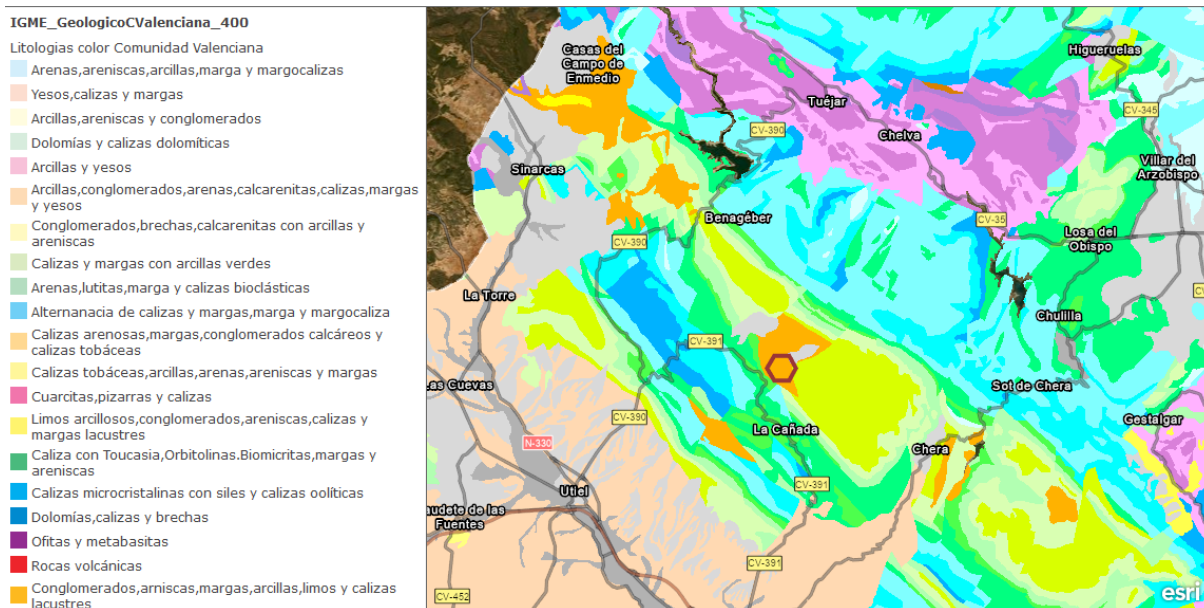


Figure 42: Litho-geological map of the installation site, located in the hexagon (Source: [17])

The cadastral data classify the land as agricultural, principally consisting of clay, therefore the municipality must carry out the appropriate procedures to make the land buildable.

The total land area is 433957 m². It is not necessary to use the entire surface for an installation of 5 MWp, it is estimated that 75000 m² are enough as shown in the calculation.

A first approximate value valid for both monocrystalline and polycrystalline technology is 10 m²/ kWp. For a 5 MWp installation, considering only the panels, it is obtained an area A equal to:

$$A = 5000 \text{ kW}_p * \frac{10 \text{ m}^2}{\text{kW}_p} = 50000 \text{ m}^2$$

This surface is increased by a factor of 50 % to consider electrical (cabins) and functional (passageways) accessories. Finally, a plot of land of about 78000 m² is then prepared for an additional margin. The northern part of the plot has been chosen because it has an optimal North-South orientation and, being at the top, it is less exposed to the shadow problem. Regarding the most significant technical characteristics of this part, it should be noted that it has a height around 920 m high. As regards the inclination, this is a very variable value and for this reason an average value is provided after the preparation of the soil. The chosen section is represented, with an area of 78081 m², in the map viewer.

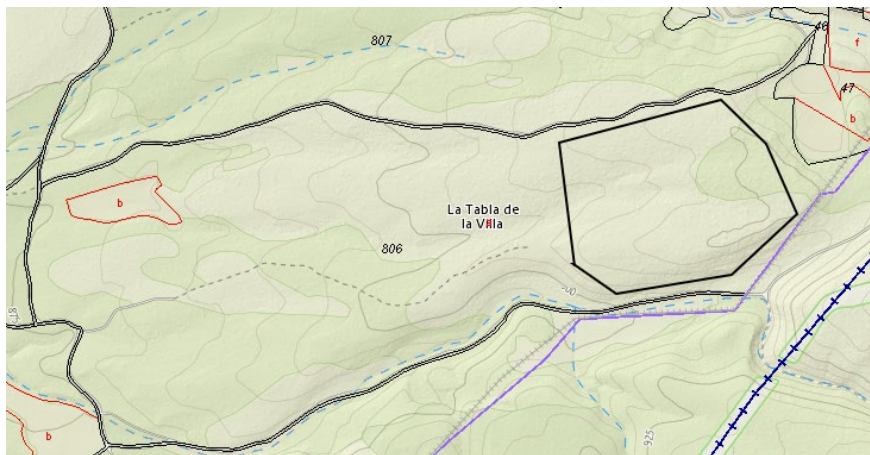


Figure 43: Place of installation (Source: [16])

This lot is also indicated in the AutoCAD drawing number 3.

The next step is the preparation of the soil. The main purpose is to avoid troughs, that are areas at lower height, in the main north-south inclination. In fact, placing a panel in a hollow involves its total or partial shading. The result is a levelling in the North-South direction.

This study involves the combined use of the cartographic viewer of the Valencian community and the software MATLAB. Then the various passages are explained and presented graphically.

With the aid of the map viewer, the elevation profile of the plot is obtained at various points.

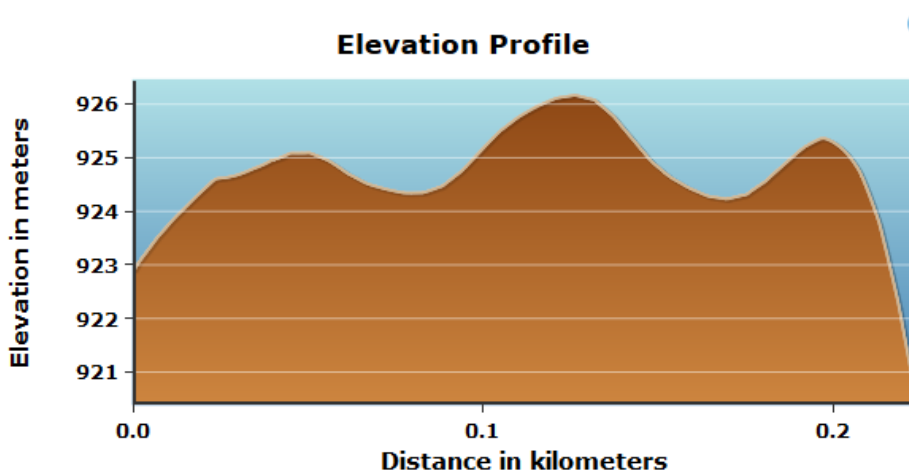


Figure 44: Elevation profile in an area of the plot (Source: [16])

These data are passed to a MATLAB script that reports in three dimensions the various profiles.

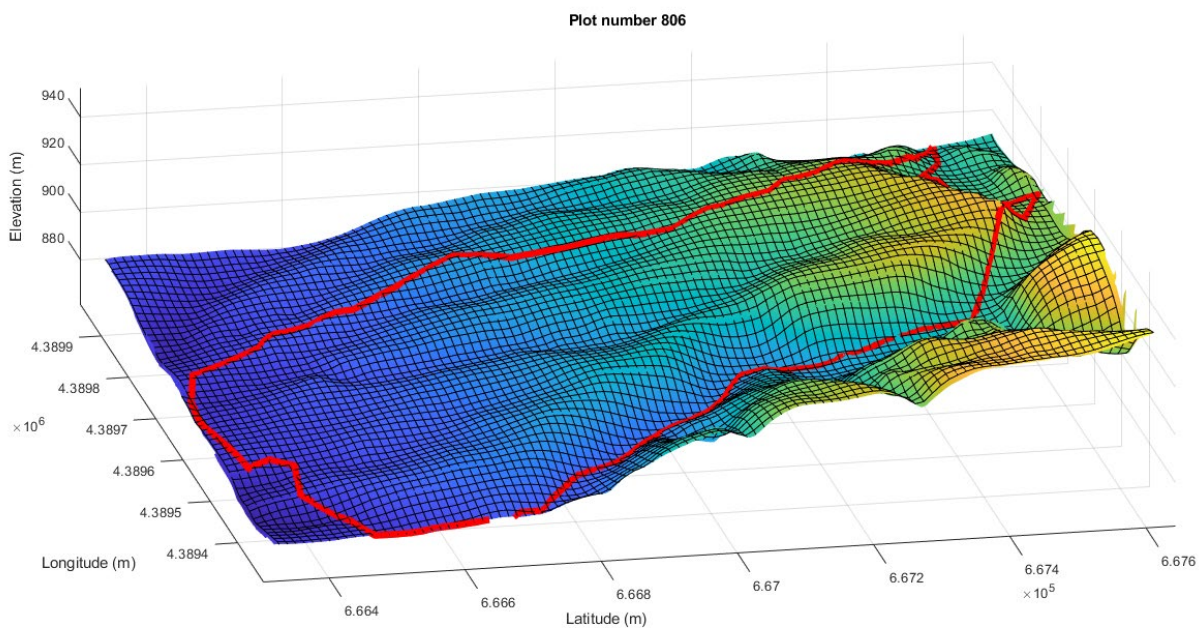


Figure 45: Representation of the soil profiles and of the plot

The area of interest in the plot can be identified.

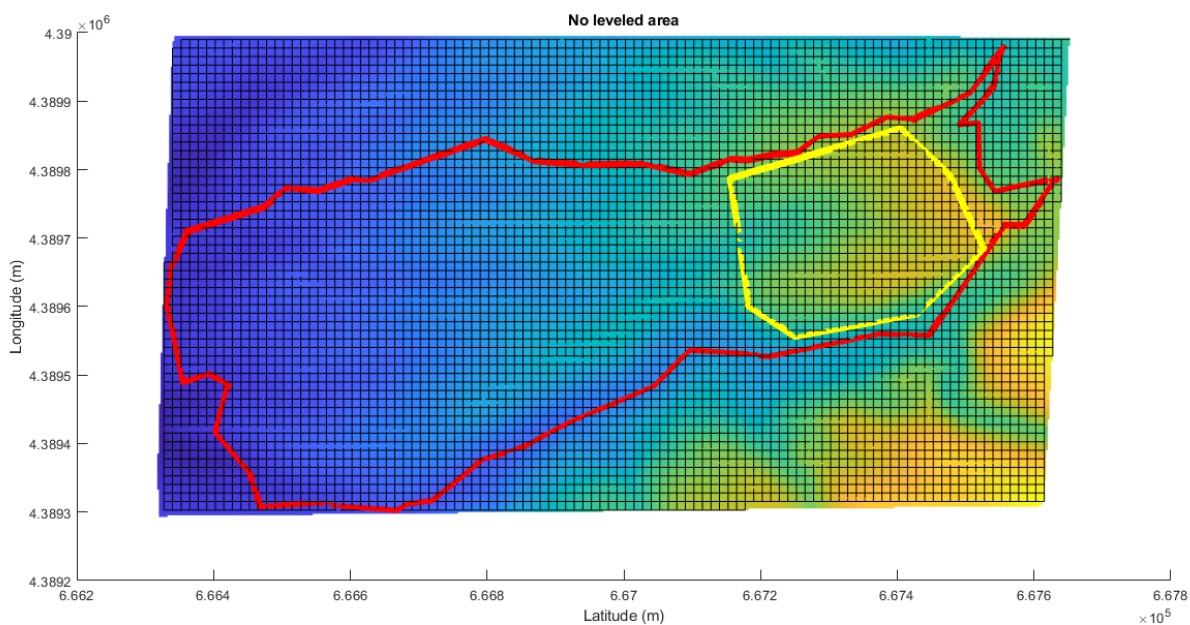


Figure 46: Representation of the area of interest in the plot

Besides, the script allows to level the soil in the desired direction, in this case North-South. The following images represent the area before and after levelling.

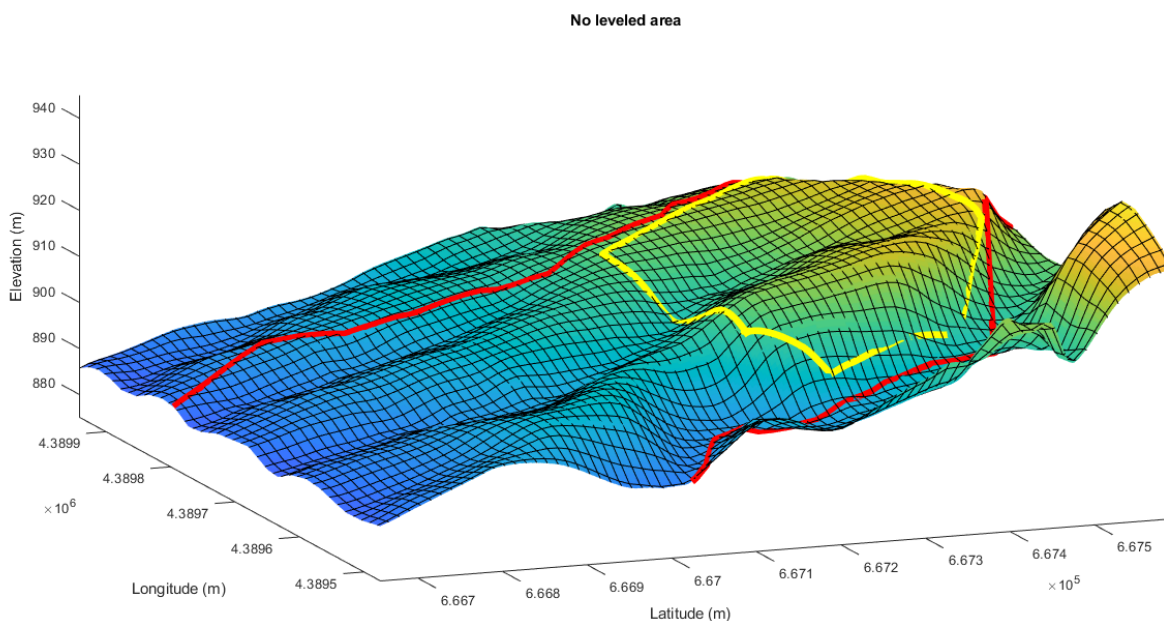


Figure 47: No levelled area

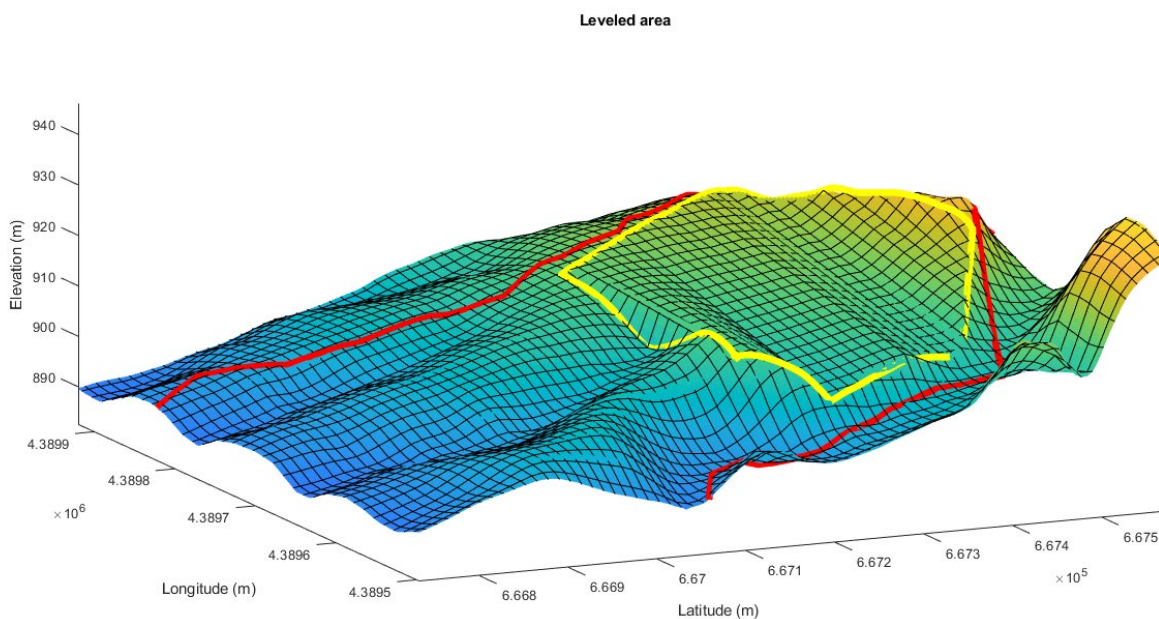


Figure 48: Levelled area

Using the MATLAB script, the North-South inclination of the area of interest is obtained. Eliminating the numerical error data, given from the points of the perimeter of the area considered, the inclination of the land is of 7°.

With a volumetric calculation it is possible to determine the amount of soil to add or subtract to the original volume, in order to allow this levelling. In this specific case, it must be removed a volume equal to:

$$V = 267240 \text{ m}^3$$

The removed soil is placed into another area in the same parcel.

Finally, the perimeter of the affected area is exported in AutoCAD, turning it into polyline. In this software, the study has been continued with the configurations of panels and inverters.

For further details on the MATLAB script, see annex A where it is reported in its entirety.

The next chapter discusses the choice of the various components of the photovoltaic system.

9. Choice of plant components

This chapter presents the main elements of the system, the photovoltaic module, the inverter, the string monitor and the support structure. Besides the correct coupling between modules and inverters is calculated.

9.1. Choice of the solar module

The choice of the basic element of a photovoltaic system, the solar panel, requires the comparison of the various technologies present on the market. In particular, this analysis takes into account technical, economic and functional characteristics. The following table shows a selection of some models of brands that are currently competitive on the market. This first selection considers comparable models by price, derived from a market survey referring to a palette of 30 modules.

Brand	Trinasolar	Trinasolar	QCELLS	SunPower
Model	TSM-PD14	TSM-DE15H(II)	Q.PEAK DUO-G6	SPR-MAX3-400
Solar Technology	Polycrystalline	Monocrystalline	Monocrystalline	Monocrystalline (high efficiency)
Price	0,42 €/Wp	0,46 €/Wp	0,58 €/Wp	0,83 €/Wp
ELECTRICAL CHARACTERISTICS (STC)				
Peak Power P_{max}	340 W	400 W	355 W	400 W
Power Output Tolerance	0/+5 %	0/+5 %	0/+5 %	0/+5 %
Module Efficiency η_m	17,5 %	19,7 %	19,8 %	22,6 %
Maximum Power Voltage V_{MPP}	37,8 V	41,1 V	34,38 V	65,8 V
Maximum Power Current I_{MPP}	8,99 A	9,74 A	10,33 A	6,08 A
Open Circuit Voltage V_{oc}	46,2 V	50,4 V	40,98 V	75,6 V
Short Circuit Current I_{sc}	9,42 A	10,18 A	10,84 A	6,58 A
Maximum System Voltage V_{DC}	1000 V	1500 V	1000 V	1000 V
Max Series Fuse Rating I_R	15 A	20 A	20 A	20 A
TEMPERATURE COEFFICIENTS				
NOCT ³	44 ± 2 °C	41 ± 3 °C	43 ± 3 °C	44 ± 2 °C
Operational Temperature	-40/+85 °C	-40/+85 °C	-40/+85 °C	-40/+85 °C
Temperature Coefficient of P_{max}	-0,41 %/°C	-0,36 %/°C	-0,36 %/°C	-0,29 %/°C
Temperature Coefficient of V_{oc}	-0,32 %/°C	-0,26 %/°C	-0,27 %/°C	-0,233 %/°C

³ Nominal Operating Cell Temperature

Temperature Coefficient of I_{sc}	0,05 %/°C	0,04 %/°C	0,04 %/°C	0,044 %/°C
MECHANICAL SPECIFICATION				
Solar Cells	72	144 (half cells)	120 (half cells)	104
Junction box	IP67/68; 2 diodes	IP68; 2 diodes	IP67; 2 diodes	IP68; 3 diodes
Cables	1200 mm	N 140 / P 285 mm	1150 mm	1200 mm
Connector	Trina TS4	Trina TS4	MC4	MC4
Module Dimensions	1960x992x40 mm	2024x1004x35 mm	1740x1030x32 mm	1046x1690x40 mm
Weight	22,5 kg	22,8 kg	19,9 kg	19 kg
Glass	High Transmission	High Transmission	Anti-reflection	Anti-reflection
Max. Load, Pull/Push	2400/5400 Pa	2400/5400 Pa	4000/5400 Pa	2400/5400 Pa

Table 10: Technical data of the selected modules (Source: [18])

It is noted that the modules have a high unit power, in accordance with the current trend of use of these modules in high power installations. This choice involves a smaller number of modules with the same installed power, and therefore lower transport, installation and maintenance costs. Moreover, always analysing from the economic point of view, the difference in price between two modules of the same company distinct for a 10 % in nominal power is minimal. The Trinasolar and SunPower monocrystalline modules are the most rated modules among the reported proposed. Another energy reflection can be made by observing the efficiency. The SunPower company maintains the world record for module efficiency, as confirmed by the numerical data in the table. The other monocrystalline models are not in the lead but have a high performance. In fact, they are part of the high efficiency models that use the PERC (Passivated emitter and rear Cell) technology able to better exploit the solar radiation with the passivation of the back layer of the module. This allows an increase of the possibility of photon recombination and the increase of the internal reflection at the junction. Among the electrical characteristics, the maximum system voltage of the Trinasolar monocrystalline is different from the others; a greater value of this parameter allows to have strings with more modules. Consequently, this implies a smaller quantity of strings and fewer accessory elements (electrical panels, cables). By analysing the temperature characteristics, a lower coefficient of power loss in absolute value means less losses when temperature changes and therefore greater stability. Again, monocrystalline modules have the best characteristics. In the mechanical characteristics, the greater dimensions and weight in the Trinasolar modules can be observed. These parameters affect the design of the support structures and the installation. The economic analysis shows that polycrystalline technology is still the most cost-effective technology on the market, especially in the case of large installations. This is due to the lower cost of producing the technology. However, in recent years the economic gap between the two technologies has narrowed, thus opening the possibility for monocrystalline to be considered also for installations of great installed power.

To compare the numbers, in the hypothesis of considering the estimate for 30 panels for an installation of 5 MWp, in the case Trinasolar polycrystalline and monocrystalline the amount for the modules would be respectively of 2,1 M€ and 2,3 M€. The 200000 € difference halves going to consider support

structures, as shown with the following calculation. For an installation of 5 MWp 14706 polycrystalline modules or 12500 monocrystalline modules are required. With a typical price for a structure of 42 €/module you get exactly:

$$\Delta C_{structure} = 42 \cdot (14706 - 12500) = 92652 \text{ €}$$

In order to choose the technology, over the technical-economic aspect, the good functioning of the cell can be considered. On the one hand, it is well known that the monocrystalline solar panel is more productive in case of low temperatures and does not resist to overheating. Polycrystalline, on the other hand, is more suitable in warm climates, resists overheating and is preferable in case of not optimal exposure. In conclusion, considering the technical-functional aspects, the monocrystalline technology is chosen. Among the three models proposed, Trinasolar TSM-DE15H(II) is chosen because it is the most convenient. Another not insignificant considerable advantage is the maximum system voltage. The number of total panels needed can be calculated:

$$N_{panels} = \frac{P_{installed}}{P_{panel}} = \frac{5000000 \text{ W}_p}{400 \text{ W}_p} = 12500 \text{ panels} \quad (45)$$

The panel is represented in the following image.

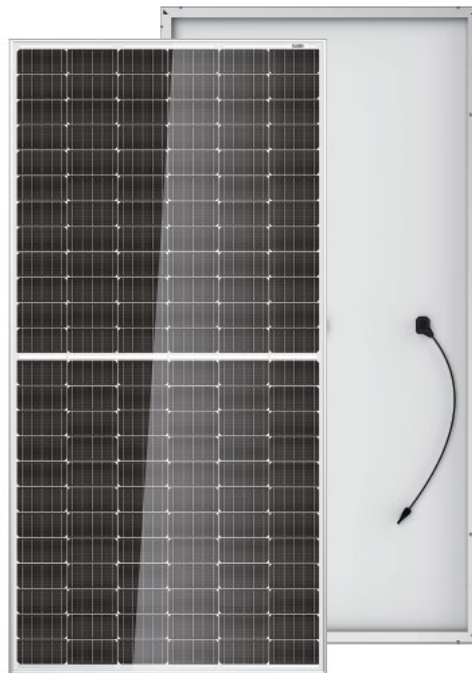


Figure 49: Trinasolar TSM-DE15H(II) panel (Source: [18])

9.2. Choice of the inverter

The choice of the inverter concerns the choice of size and configuration. As for the connection to the grid, it is three-phase in a system with installed power greater than 5 kWp. Regarding the size of the inverter, referring to formula (21)

$$P_{DC-max} = f \cdot P_{A-MPP} \quad (21)$$

A unit sizing factor of the inverter is considered because the installation is in Southern Europe and has an optimal orientation towards South. Consequently, the sum of the nominal power of the inverters of the plant is greater/equal than 5 MWp. The final value may be slightly different, for example, for the sum of standard inverter power.

For the choice of configuration, the two main schemes used, centralized inverter and the presence of more inverters are compared. It must be considered that a single centralized inverter is characterized by a greater simplicity and a greater efficiency. Moreover, it has the advantage of a smaller investment: the price of an inverter is less than that of the sum of inverters of smaller size, at the same total power. The cost of transport and assembly is also lower. The main disadvantages include:

- the reliability of operation of the whole plant, as a failure or the need for maintenance would stop production
- the longest cable length from the modules
- the presence of many modules leads to a difficult extraction of the maximum power for the high probability of mismatching

Conversely, in the case of string inverters, there is a more complex total structure and a higher total cost for inverters. Moreover, it increases the reliability of the plant. Finally, a configuration with two inverters of high power in parallel is chosen to have a compromise between cost, simplicity and reliability of the structure. The model chosen is SMA MV Power Station 2500, power station that incorporates a 2500 kW inverter, a medium voltage transformer and a medium voltage switchgear. Being a compact unit, it incorporates all the necessary elements and it can connect directly to the grid. Some technical specifications and image of the power station are presented below. [6]



Figure 50: SMA MV Power Station 2500 (Source: [19])

Technical Data	SMA MV Power Station 2500
Inverter selected	SC 2500-EV
Input (DC)	
Number of MPPT	1
MPP voltage range V_{DC} (at 25°C / at 35°C / at 50°C)	850 V to 1425 V / 1200 V / 1200 V
Min. input voltage $V_{DC, min}$ / Start voltage $V_{DC, Start}$	778 V / 928 V
Max. input voltage $V_{DC, max}$	1500 V
Max. input current $I_{DC, max}$ (at 35°C / at 50°C)	3200 A / 2956 A
Max. short-circuit current rating	6400 A
Number of DC inputs	24 double/32 single pole fused
Number of DC inputs with optional DC coupled storage	18 double pole fused
Max. number of DC cables per DC input (for each polarity)	2 x 400 mm ²
Available DC fuse sizes (per input)	200, 250, 315, 350, 400, 450, 500 A
Output (AC)	
Nominal AC power at $\cos \phi = 1$ (at 35°C / at 50°C)	2500 kVA / 2250 kVA
Nominal AC current $I_{AC, nom} = \text{Max. output current } I_{AC, max}$	2624 A
Max. total harmonic distortion	< 3 % at nominal power
Nominal AC voltage range	6,6 kV to 35 kV
AC power frequency	50 Hz / 47 Hz to 53 Hz
Power factor at rated power/ displacement power factor adjustable	1/0,8 overexcited to 0,8 underexcited
Transformer connection group	Dy11
Transformer cooling system	ONAN
Max. current output at 33 kV	44 A
Open -circuit transformer losses	2,5 kW
Short -circuit transformer losses	23,2 kW
Efficiency	
Max. efficiency / European efficiency	98,6 % / 98,3 %
Protective Devices	
Input-side disconnection point	DC load-break switch
Output-side disconnection point	AC circuit breaker
DC overvoltage protection	Surge arrester, type I
AC overvoltage protection (optional)	Surge arrester, class I & II
Resistance to voltaic arcs, medium voltage distribution room	IAC A 20 kA 1 s
General Data	
Dimensions-with integrated oil collector tank (W / H / D)	6058 mm / 2896 mm / 2438 mm
Weight	< 16 t
Self-consumption (max. / partial / average load)	< 8,1 kW / < 1,8 kW / < 2,0 kW
Self-consumption (standby)	< 370 W
Max. operating height above sea level	1000 m
Features	
DC connection	Cable terminals
AC connection	External cone angled connector
Communication	Optional

Table 11: Technical data of the selected inverter (Source: [19])

9.3. Choice of the configuration

To find the configuration of the photovoltaic system, the equations of paragraph 5.2 Configuration of the system are implemented in an Excel sheet. To highlight the equations, the minimum and maximum ambient temperature data are inserted, derived with PVGIS data recorded from 2007 to 2016 in the photovoltaic site.

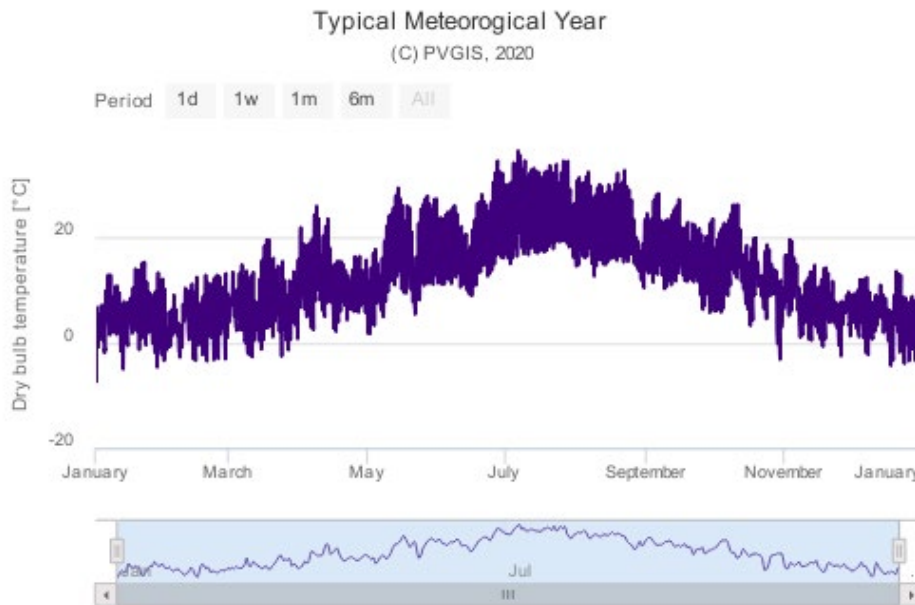


Figure 51: PVGIS temperature data recorded from 2007 to 2016. (Source: [20])

The minimum temperature, in January, is $-7,37^{\circ}$; the maximum temperature, in July, is $36,58^{\circ}$. The temperature extremes of -15°C and $+40^{\circ}\text{C}$ have been selected for precaution. For a safety margin, therefore:

$$T_{MIN} = -15^{\circ}\text{C} \quad (46)$$

$$T_{envMAX} = 40^{\circ}\text{C} \quad (47)$$

The last value is brought back to the maximum temperature with the formula (25)

$$T_{MAX} = T_{envMAX} + G_{STC} \cdot \frac{NOCT - 20}{800} = 40 + 1000 \cdot \frac{41 - 20}{800} = 66,25^{\circ}\text{C} \quad (48)$$

The analysis, shown in the following table, is carried out for one of the two power stations, to which half of the photovoltaic modules are assigned. The analysis is identical for the other station.

Module: Trinasolar TSM-DE15H(II)			
Peak Power	400	Wp	
Power Output Tolerance	"+0 % / +5 %"		
Length	2,024	m	
Width	1,004	m	
Surface	2,032	m ²	Output
Module Efficiency	19,7 %		Output
Weight	22,8	kg	
Cells Quantity	144		
Short Circuit Current I _{sc}	10,18	A	
Open Circuit Voltage V _{oc}	50,4	V	
Maximum Power Current I _m	9,74	A	
Maximum Power Voltage V _m	41,1	V	
Temperature Coefficient of P _m	-0,36 %	/°C	
Temperature Coefficient of I _{sc}	0,00407	A/°C	
Temperature Coefficient of V _{oc}	-0,131	V/°C	
Fill Factor FF	78,0 %		Output
Mechanical Load	11,2	kg/m ²	Output
Inverter: SMA SC 2500-EV			
Rated Power Pac	2500000	VA	
Range MPPT (V)	850	1425	
Maximum Voltage V _{dc}	1500	V	
Maximum Current I _{dc}	3200	A	
Efficiency	98,5 %		
Grid Voltage V _{ac}	400V-50 Hz		
Power Factor PF	1		
Contribution to short circuit current		A	
Photovoltaic array			
Number of modules	6250		
Number of modules/strings	25		
Number of strings	250		Output
Array total power P _{m(a) tot}	2500000	Wp	Output
Total surface	12701	m ²	Output
Total weight	142500	kg	Output
Nominal string voltage V _n	1028	V	Output
Nominal open circuit string voltage V _{oc}	1260	V	Output
Maximum open circuit voltage V _{A-OCmax}	1391	V	Checked
Minimum voltage V _{A-MPPmin}	892	V	Checked
Maximum voltage V _{A-MPPmax}	1159	V	Checked
Maximum Current I _{A-max}	2587	A	Checked
Ratio P _{inv} / P _{m tot} (0,9 - 1,1)	100,0 %		Checked

Table 12: Study of the sizing of a connected PV system (Source: [6])

After a series of iterations, the ideal configuration in 250 strings of 25 modules each is identified for each inverter. As a result, the photovoltaic field is sized with a 100 % exploitation of the inverters.

9.4. Choice of the solar string combiner box

The configuration chosen includes 24 elements, 12 for each inverter. In detail there are 16 elements with 24 inputs (SSM-U-2415) and 8 elements with 16 inputs (SSM-U-1615). The inputs are occupied entirely, except 2 elements with 16 inputs, of which only 10 will be used. Besides this model provides the optional option of built-in fuses and Ethernet communication for monitoring. The main characteristics and pictures of the selected solar string combiner boxes are shown below.

Technical Data	SSM-U-1615	SSM-U-2415
Input (DC)		
Rated voltage	1500 V	
Number of string inputs	16	24
Rated current per measuring input	19 A	
Output (DC)		
Rated current	315 A	
DC switch	400 A / 1500 V	
Enclosure / Ambient Parameters		
IP degree of protection	IP 54 / self-ventilated	
Enclosure material	Glass-fiber reinforced plastic / self-extinguishing, halogen-free, UV stable	
Dimensions (W / H / D)	630 / 1055 / 320 mm	
Max. weight	34 kg	
Protection class	II	
Operating temperature	-40 °C to +60 °C	
Relative humidity	0 % to 95 %, condensation possible	
Max. altitude above MSL	4000 m	

Table 13: Technical data of the selected solar string combiner box (Source: [21])



Figure 52: SMA SSM-U-1615 and SSM-U-2415 (Source: [21])

The number of solar strings combiner boxes is chosen considering that, as the number of elements increases (and therefore the price), the voltage drop decreases. Furthermore, it was decided to position the elements with inputs that were not totally exploited more distant from the inverter. In

this way, since the current is less, the voltage drop is reduced. Finally, the positioning in the central path (later called the central axis) of the installation makes them easily accessible for maintenance.

9.5. Choice of the support structure

The support structure chosen is fixed. Unlike a mobile structure, this system involves less exploitation of solar radiation, but it has its advantages. The first consideration regards the installation space: the presence of solar trackers requires a greater surface area due to the shadows. In addition to saving land, fixed structures generally involve an economic saving of investment and maintenance.

Fixed structures can be single pole or double pole. These structures can be further classified according to the number of rows and the configuration of the panels. As regards the inclination, the PVGIS solar simulation program is used to identify the optimal slope of the panels with respect to the horizon. The optimal angle of 37° is identified. Considering an average slope of the ground of 7° , an adjustable structure is necessary to allow the optimal functioning of all the panels.

A parenthesis opens on the inclination of the panels. When there is the possibility of snowfall in the place of installation, to avoid the accumulation on the panels, an inclination greater than 45° can be considered. The place of interest, being at 920 m, can be subject to snow. It was decided to use the optimal inclination of the panels as the issue is slighter and limited to a few months of the year (December/January).

From a market investigation, the most convenient and customisable option, according to the variable inclination of the ground, results in a double pole structure. The configuration chosen is two rows of panels arranged vertically. The following image shows the side view of the structure. The structure is represented in a terrain with a 7° slope and with the dimensions of the panels chosen previously.

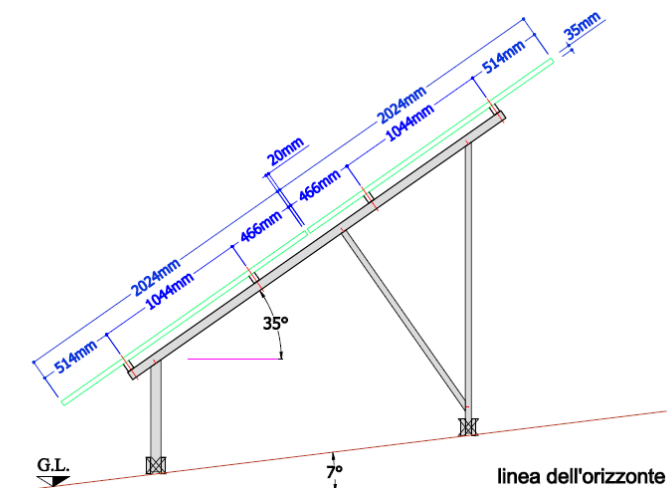


Figure 53: Double pole structure with variable inclination (Source: [8])

In total 250 structures with 50 modules each are needed. So, each structure contains two strings.

In the next chapter the layout of the system is defined.

$$d_{min} = L \cdot k \cdot \frac{\sin 37^\circ - \cos 37^\circ \cdot \tan 7^\circ}{1 + k \cdot \tan 7^\circ} \quad (49)$$

By entering the numerical values of L , which represents the length of two modules side by side vertically, and of k :

$$L = 2 \cdot 2,004 = 4,008 \text{ m} \quad (50)$$

$$d_{min} = 3,83 \text{ m} \quad (51)$$

The distance obtained is the minimum distance between the back of one row and the beginning of the following, as shown in the image. A final distance of 4,27 meters between rows of panels is considered. A distance of 4 meters between adjacent structures is counted to allow the passage to vehicles for maintenance and cleaning of the system. A greater distance (8,5 m) separates the operating zones of each inverter, obtaining a mirror photovoltaic system along this central axis. Here, there are solar string combiner boxes and inverters, so that they are easily accessible. In addition, the calculation of the minimum distance between inverter and photovoltaic panels is also reported. In fact, inverters also cause shade and must be considered. The following image schematizes the case under examination.

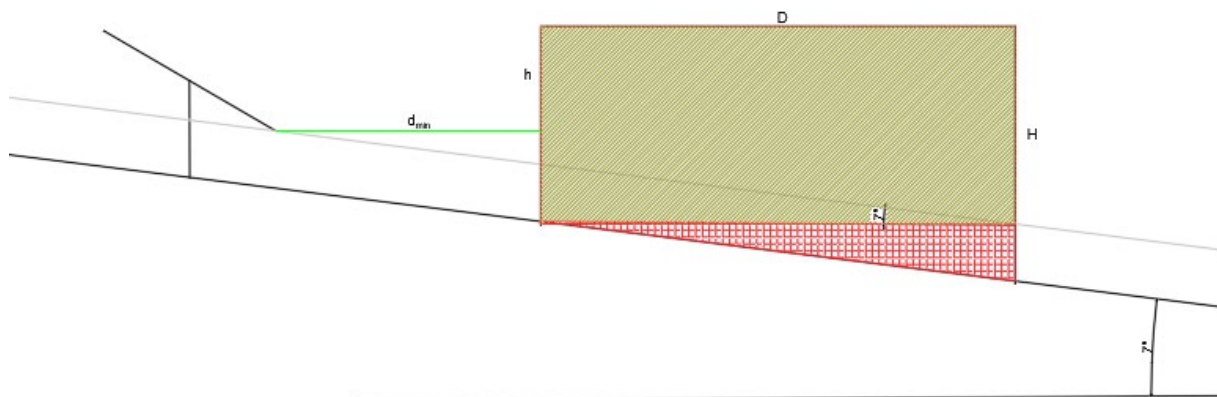


Figure 55: Calculation of the distance between inverter and modules in an inclined plane

The formula to be particularized is the following:

$$d_{min} = h \cdot k \quad (3)$$

Where:

$$k = \frac{1}{\tan(61^\circ - \text{latitude})} = \frac{1}{\tan(61^\circ - 39^\circ)} = 2,475 \quad (4)$$

The trigonometric calculations to derive the parameter h are presented

$$h = H - d_{min} \cdot \tan 7^\circ - D \cdot \tan 7^\circ$$

Substituting in formula (3):

$$d_{min} = k \cdot \frac{H - D \cdot \tan 7^\circ}{1 + k \cdot \tan 7^\circ} \quad (52)$$

By entering the numerical values of H , which represents the height of the inverter, D , which represents the depth of the inverter, and of k :

$$D = 2,438 \text{ m}$$

$$H = 2,896 \text{ m}$$

$$d_{min} = 4,93 \text{ m} \quad (53)$$

This distance is widely respected, as shown in the final configuration in the AutoCAD drawing number 4.

10.2. Identification of the strings

It was decided to identify each string with a code consisting of numbers and letters. In particular, proceeding from left to right:

- A capital letter, A or B, identifies the inverter to which the string is connected. On the AutoCAD, inverter A is on the left and inverter B on the right.
- A number, from 01 to 12, marks the combiner box to which the string is connected. On the AutoCAD, the combiner box has a progressive number from top to bottom.
- A lowercase letter between a, b, c, d, e, f, g, h, l, m, n, o. These letters have been chosen to avoid any ambiguity using similar graphic characters; they label the double pole support structure on which the string is positioned. The letters have been arranged to occupy the same relative position with respect to the combiner box.
- The last number, 1 or 2, identifies the upper or lower string

The following image is an example of strings connected to the same string box.

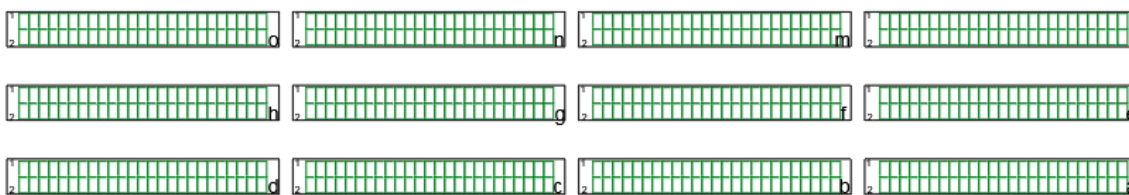


Figure 56: Identification of the strings

Another zoom is indicated in the AutoCAD drawings number 5 and 6.

10.3. Low voltage connections

This section contains three main topics: firstly, the serial connection of modules; secondly, the choice of cables between strings and string combiner box and finally, between string combiner box and inverter.

10.3.1. Connection of modules

The standard series connection of panels forming a string provides for connecting the positive terminal with the negative one of two adjacent panels. At the end of the string, the last cable goes back until it joins the first. This type of connection is called a daisy chain. The drawbacks of this method mainly concern the length of the return cable and the excess cable of the panel which must be rolled up and fixed to the structure to prevent it from hanging down. Rolling up the cables also leads to greater heating of the cables and obstruction of the passage of current.

To solve these problems, a first option provides for a connection called leapfrog wiring in which the panels are always connected in series but skipping a panel that will be used for the return, as shown in the figure.

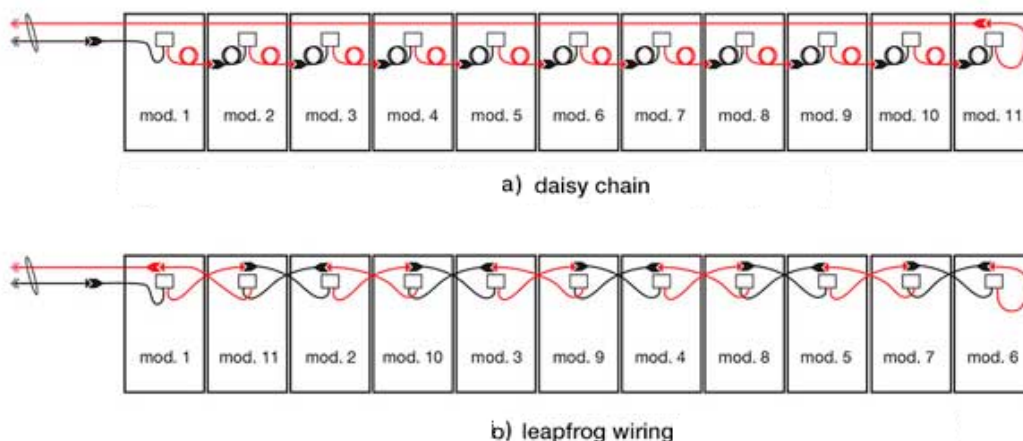


Figure 57: Series connection of modules: a) daisy chain and b) leapfrog wiring (Source: [22])

It can be observed that, with this method, the length of the panel is used to cover the entire series; besides, the absence of cable windings can be noticed. This method is mainly used in large installations

given that the cable gain is considerable. The leapfrog wiring cannot be applied in this installation because the cables of the panel have a reduced length sufficient only to connect two adjacent modules. Applying this method would involve adding cable and two connectors to each panel. The final system would therefore be more complex and more expensive. [22]

A second hypothesis is the connection with rows of inverted polarity modules. In this case, a string is divided into two files, unlike the previous cases where a string developed over the entire length of the support structure.

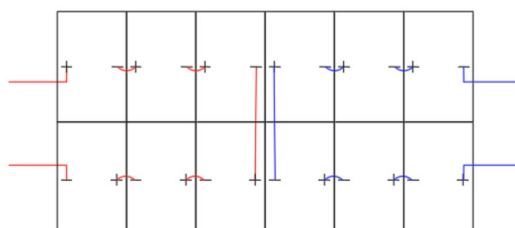


Figure 58: Connection with rows of inverted polarity modules

In this case two connectors and an extra cable for each string are necessary to connect the upper part to the lower part. This configuration is certainly the most convenient in terms of cable length, but it cannot be applied because of it presents the problem of overvoltage induced by indirect lightning strikes.

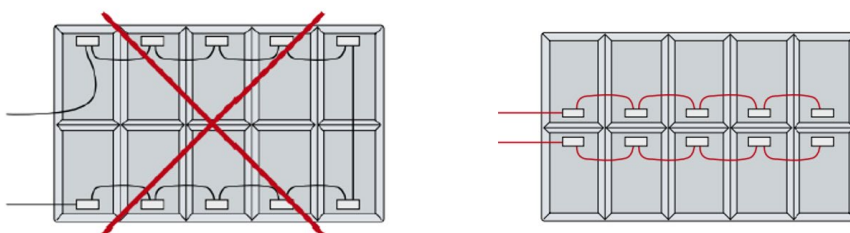


Figure 59: Examples of incorrect (left) and correct (right) connection of photovoltaic modules in series to avoid overvoltage (Source: [6])

Looking at the back of the panel considered, it can be said that it represents an intermediate situation of the two connection cases in the previous figure because it has a junction box located in the middle of the panel. However, it is preferred not to apply this method.

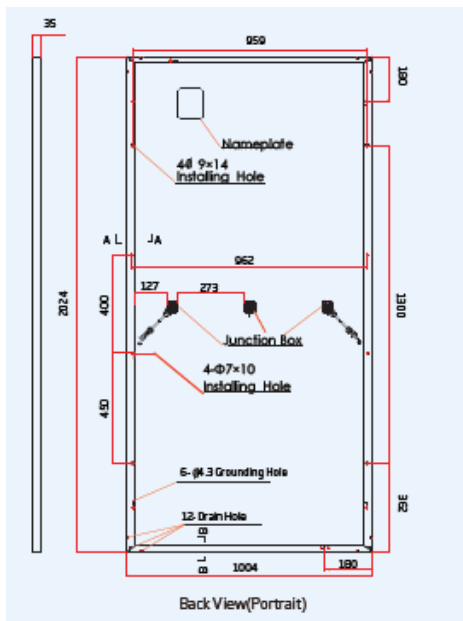


Figure 60: Trinasolar TSM-DE15H(II) panel (Source: [18])

Finally, it was decided to employ the first connection, the daisy chain, in a way to reduce the area of the loop. The return cable must therefore pass as close as possible to the series connection cables of the modules. Since the module itself has a reduced length of junction cables, this solution does not have hanging cables.

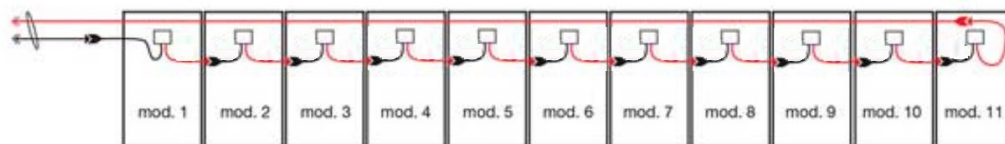


Figure 61 Series connection of modules: daisy chain without coiled cables (Source: [22])

10.3.2. Connection of modules-string combiner box

TECSUN (PV) PV1-F 0,6/1 kV AC (1,5 kV DC) cables from the Prysmian group are used. These cables are intended exclusively for photovoltaic installations and therefore fulfil the regulatory requirements of paragraph 6.3.2. They are cables with copper conductor, HEPR insulation and the outer sheath is in EVA (ethylene vinyl acetate).



Figure 62: TECSUN (PV) PV1-F 0,6/1 kV AC (1,5 kV DC) (Source: [23])

As regards the laying, reference is made to laying D1 or single-core cables in an underground pipe. The cables to be buried must have a minimum section of 6 mm² (regulation ITC-BT-07). Installation in metal conduits is not considered because these elements hinder the passage of maintenance machinery (example: lawn mowers). The depth at which the cables are located is standard, 80 cm. The advantages of pipe laying are: firstly, greater protection to the cables from water and mechanical forces. Furthermore, in case of failure the cables can be easily removed. However, installation in the air is also considered to check that the two sections in the air do not present heat dissipation problems. The first section covers the cable behind the panel until the ground and the second section from the ground to the combiner box. For these sections, reference is made to laying E, that is, single-pole cables suspended/separated from the structure. To size the cables, it is necessary consider the thermal and electrical criteria, presented below.

10.3.2.1. Thermal criterion

To confirm the criterion, you need to verify the equation:

$$I_b \leq I_z \quad (32)$$

Where:

$$I_b = m \cdot 1,25 I_{sc} \quad (31)$$

$$I_z = I_o \cdot k \quad (33)$$

$$m = 1$$

By combining the previous formulas:

$$I_o \geq \frac{I_b}{k} \quad (54)$$

This formula is implemented on an Excel sheet and the calculation is repeated for each string. By presenting the system with a symmetrical structure, the calculations of the inverter A strings are identical to those of the other inverter. This calculation is presented completely in Annex B.

Below are some considerations on the k_i coefficients referring to a string i .

For the section in the ground k is the product of the coefficients:

- $k_{1g} = 1,1$ ground thermal resistivity (clay)
- $k_{2g} = 0,93$ ground temperature other than 20 °C; in particular, it refers to 30 °C
- k_{3g} is about laying and grouping. It is used to consider cables in the same pipe
- k_{4g} is about laying and grouping. It is used to consider the interference with the combiner box-inverter connection cables in a pipe one meter away.

The k_{3g} and k_{4g} coefficients are obtained in table B.52.19-A of the UNE 60364-5 standard. They vary according to the string considered. A numerical value obtained from the I_b/k ratio is obtained. A current I_o of the next higher value is chosen from table C.52.2. in correspondence of the pose D1, 2 charged copper conductors and XLPE insulation. The section S_1 corresponding to the selected current is noted.

For the two sections in the air k is the product of the coefficients:

- $k_{1a} = 0,9$ sun exposure
- $k_{2a} = 0,58$ air temperature other than 30 °C; in particular, it refers to 70 °C
- k_{3a} is about laying and grouping

The k_{3a} coefficient is obtained in table C.52.3 of the UNE 60364-5 standard. It varies according to the string considered. For each section, a numerical value obtained from the I_b/k ratio is obtained. A current I_o of the next higher value is chosen from table C.52.1. in correspondence of the pose E, 2 charged copper conductors and XLPE insulation. The sections S_2/S_3 corresponding to the selected currents are noted.

The thermal criterion ends by choosing the larger of the three section S_1, S_2, S_3 .

10.3.2.2. *Electrical criterion*

In the general formula for voltage drop, shown below, a factor two appears because it considers the outward and return of the cable with equal parameters.

$$\Delta V = \frac{2 \cdot r \cdot L \cdot m \cdot I}{V} \cdot 100 \quad (34)$$

In the case under analysis, there are different lengths of return cables; besides, behind the panels there are 4 mm² cables and therefore a change of section, that is resistance, for almost all the strings.

Consequently, the formula for voltage drop is considered without the factor two and as the sum of the drops:

- for connecting the panels
- from the first panel of the series to the combiner box
- from the last panel of the series to the combiner box

Since the voltage drop from the panels to the point of connection to the public grid must not exceed 1,5 %, the sum of these three values, which include the voltage drop from the panels to the combiner box, must not exceed 0,5 %.

In the Excel sheet, the total voltage drop is implemented for each string as the sum of:

- ΔV_1 from the first panel to the combiner box, where the general formula can be applied because it considers cables of equal parameters, with variable sections depending on the string. The resistance is obtained from the Prysmian catalogue and reported to 90 °C. The length of this section is obtained on AutoCAD, with a 10 % increase and rounding up.

- ΔV_2 behind the panels (forward), each panel has two 4mm² cables with a total length of 425 mm. The resistance is obtained from the Prysmian catalogue and reported to 90 °C.
- ΔV_3 behind the panels (return), 30 m long and with cables of section/resistance equal to that in ΔV_1

As regards voltage and current, the parameters of the maximum power point of the string are considered:

$$I_m = 9,74 \text{ A}$$

$$V_m = 25 \cdot 41,1 = 1027,5 \text{ V}$$

The voltage drop criterion ends by determining the section of the cable S whose resistance allows it to remain below the limit of 0,5 % voltage drop.

10.3.2.3. Choice of cable: modules-string combiner box

After applying the thermal and electrical criteria, two sections are obtained for each string. Since the cable must meet both criteria, the larger section is chosen. In the module-string combiner box section, the largest section is the one needed to satisfy the voltage drop.

10.3.3. Connection of string combiner box-inverter

TECSUN (PV) S3Z2Z2-K 1,8/3 kV AC (1,5 kV DC) cables from the Prysmian group are used. These cables are suitable for photovoltaic installations and, in particular, for the box-inverter section. These cables have got copper conductor, insulation and the outer sheath in elastomeric material.



Figure 63: TECSUN (PV) S3Z2Z2-K 1,8/3 kV AC (Source: [23])

As regards the laying, reference is made to laying D1 or single-core cables in an underground pipe. The considerations discussed above are valid:

- The cables to be buried must have a minimum section of 6 mm² (regulation ITC-BT-07).
- Installation in metal conduits is not considered
- The depth at which the cables are located is standard, 80 cm.

However, installation in the air is also considered to check that the two sections in the air do not present heat dissipation problems. The first section covers the cable from the combiner box until the ground and the second section from the ground to the inverter. For these sections, reference is made to laying E, that is, single-pole cables suspended/separated from the structure. To size the cables, it is necessary consider the thermal and electrical criteria, presented below.

10.3.3.1. Thermal criterion

To verify the criterion, you need to verify the equation:

$$I_b \leq I_z \quad (32)$$

Where:

$$I_b = \frac{m}{n} \cdot 1,25 I_{sc} \quad (31)$$

$$I_z = I_o \cdot k \quad (33)$$

A different operating current is defined according to the number of strings under the combiner box. Consequently, it means that the term m is greater than unity. Parameter n indicates the presence of multiple conductors per polarity, necessary due to the high current characteristics of these cables.

By combining the previous formulas:

$$I_o \geq \frac{I_b}{n \cdot k} \quad (55)$$

This formula is implemented on an Excel sheet and the calculation is repeated for each string box. By presenting the system with a symmetrical structure, the calculations of the inverter A strings are identical to those of the other inverter. This calculation is presented completely in Annex C.

Below are some considerations on the k_i coefficients referring to a string box i . Proceed in an iterative way, assigning n a value gradually increasing and adjusting each time the coefficients that consider the presence of multiple cables.

For the section in the ground k is the product of the coefficients:

- $k_{1g} = 1,1$ ground thermal resistivity (clay)
- $k_{2g} = 0,93$ ground temperature other than 20 °C; in particular, it refers to 30 °C
- k_{3g} is about laying and grouping. It is used to consider cables in the same pipe
- k_{4g} is about laying and grouping. It is used to consider the interference with the modules-combiner box connection cables in a pipe one meter away.

The k_{3g} and k_{4g} coefficients are obtained in table B.52.19-A of the UNE 60364-5 standard. They vary according to the string considered. A numerical value obtained from the $I_b/n \cdot k$ ratio is obtained. A current I_o of the next higher value is chosen from table C.52.2. in correspondence of the pose D1, 2 charged copper conductors and XLPE insulation. The section S_1 corresponding to the selected current is noted.

For the two sections in the air k is the product of the coefficients:

- $k_{1a} = 0,9$ sun exposure

- $k_{2a} = 0,58$ air temperature other than 30 °C; in particular, it refers to 70 °C
- k_{3a} is about laying and grouping

The k_{3a} coefficient is obtained in table C.52.3 of the UNE 60364-5 standard. It varies according to the string considered. For each section, a numerical value obtained from the $I_b/n \cdot k$ ratio is obtained. Is chosen from table C.52.1. a current I_o of the next higher value in correspondence of the pose E, 2 charged copper conductors and XLPE insulation. The sections S_2/S_3 corresponding to the selected currents are noted.

The thermal criterion ends by choosing the larger (in terms of quantity and size) of the three section S_1, S_2, S_3 .

10.3.3.2. Electrical criterion

The general formula for voltage drop can be used because the outward and return of the cable have the same parameters.

$$\Delta V = \frac{2 \cdot r \cdot L \cdot m \cdot I}{V} \cdot 100 \quad (34)$$

Since the voltage drop from the panels to the point of connection to the public grid must not exceed 1,5 %, and the previous section must not exceed 0,5 %, the first indicative value is decided not to exceed 1 %.

In the Excel sheet, the total voltage drop is implemented for each box. The resistance is obtained from the Prysmian catalogue and reported to 90 °C. The length of this section is obtained on AutoCAD, with a 10 % increase and rounding up.

As regards voltage and current, the parameters of the box are considered:

$$I_{m,box} = (m \cdot 9,74) A$$

$$V_{m,box} = 25 \cdot 41,1 = 1027,5 V$$

The voltage drop criterion ends by determining the section of the cable S whose resistance allows to remain below the limit of 1 %.

10.3.3.3. Choice of cable: string combiner box-inverter

After applying the thermal and electrical criteria, two sections are obtained for each string box. Since the cable must meet both criteria, the larger section is chosen. In the string combiner box-inverter section, the largest section is the one needed to satisfy the thermal criterion. It is therefore necessary to recalculate the voltage drop with the electrical parameters of the section defined with the thermal criterion. Some sections have been increased in order to reduce energy loss by assessing the overall balance between higher cost of copper and greater energy production.

10.3.4. Calculation example

The complete calculation of the two sections (modules-string combiner box/string combiner box-inverter) is shown for a string with the greatest voltage drop, A.03.o.1. For other strings, there are the Annexes B and C.

10.3.4.1. Modules-string combiner box, thermal criterion

$$I_o \geq \frac{I_b}{k} \quad (54)$$

$$I_b = m \cdot 1,25 I_{sc} = 1 \cdot 1,25 \cdot 10,18 = 10,725 A$$

The grouping factors derive from an iterative process because cables with multiple conductors per polarity were chosen in the box-inverter section. Only the last check is presented.

For the section in the ground k is the product of the coefficients:

$$k_{1g} = 1,1$$

$$k_{2g} = 0,93$$

$$k_{3g} = 0,39$$

$$k_{4g} = 0,9$$

$$I_o \geq 35,44$$

$$I_o = 44 A$$

$$S_1 = 4 \text{ mm}^2$$

For the first section in the air (the cable behind the panel until it is buried) k is the product of the coefficients:

$$k_{1a} = 0,9$$

$$k_{2a} = 0,58$$

$$k_{3a} = 0,8$$

$$I_o \geq 30,47$$

$$I_o = 35 A$$

$$S_2 = 2,5 \text{ mm}^2$$

For the second section in the air (from the ground to the combiner box) k is the product of the coefficients:

$$k_{1a} = 0,9$$

$$k_{2a} = 0,58$$

$$k_{3a} = 0,41$$

$$I_o \geq 59,46$$

$$I_o = 63 A$$

$$S_3 = 6 \text{ mm}^2$$

The larger of the three section S_1 , S_2 , S_3 is:

$$S_3 = 6 \text{ mm}^2$$

10.3.4.2. Modules-string combiner box, electrical criterion

$$\Delta V = \frac{2 \cdot r \cdot L \cdot m \cdot I}{V} \cdot 100 \quad (34)$$

$$I_m = 9,74 A$$

$$V_m = 25 \cdot 41,1 = 1027,5 V$$

$$m = 1$$

- ΔV_1 from the first panel to the combiner box:

$$L = 115 m$$

$$r = 1,24 \Omega/km \rightarrow r_{90^\circ} = 1,58 \Omega/km$$

$$\Delta V_1 = \frac{2 \cdot r \cdot L \cdot m \cdot I}{V} \cdot 100 = \frac{2 \cdot 0,158 \cdot 115 \cdot 1 \cdot 9,74}{1027,5} = 0,3445 \%$$

- ΔV_2 behind the panels (forward):

$$L = 10,625 m$$

$$r = 5,09 \Omega/km \rightarrow r_{90^\circ} = 6,49 \Omega/km$$

$$\Delta V_2 = \frac{r \cdot L \cdot m \cdot I}{V} \cdot 100 = \frac{0,649 \cdot 10,625 \cdot 1 \cdot 9,74}{1027,5} = 0,0654 \%$$

- ΔV_3 behind the panels (return):

$$L = 30 m$$

$$r = 1,24 \Omega/km \rightarrow r_{90^\circ} = 1,58 \Omega/km$$

$$\Delta V_1 = \frac{2 \cdot r \cdot L \cdot m \cdot I}{V} \cdot 100 = \frac{0,158 \cdot 30 \cdot 1 \cdot 9,74}{1027,5} = 0,0449 \%$$

The total voltage drop and cable section are:

$$\Delta V = 0,3445 + 0,0449 + 0,0654 = 0,4548 \%$$

$$S = 16 mm^2$$

10.3.4.3. Choice of cable: modules-string combiner box

By comparing the sections that meet the criteria, the 16 mm² section is chosen. It is therefore not necessary to recalculate the voltage drop.

10.3.4.4. String combiner box-inverter, thermal criterion

$$I_o \geq \frac{I_b}{n \cdot k} \tag{55}$$

$$I_b = m \cdot 1,25 I_{sc} = 24 \cdot 1,25 \cdot 10,18 = 305,4 A$$

The grouping factors derive from an iterative process because cables with multiple conductors per polarity have been chosen. Only the verification of the worst section is presented, which requires a larger section and a greater number of cables.

For the second sections in the air (from the ground to the combiner box) k is the product of the coefficients:

$$k_{1a} = 0,9$$

$$k_{2a} = 0,58$$

$$k_{3a} = 0,4$$

$$n = 3$$

$$I_o \geq 487,548$$

$$I_o = 542 \text{ A}$$

$$S_3 = 3 \times 185 \text{ mm}^2$$

For the first sections in the air (the cable behind the panel until it is buried) k is the product of the coefficients:

$$k_{1a} = 0,9$$

$$k_{2a} = 0,58$$

$$k_{3a} = 1$$

$$n = 3$$

$$I_o \geq 195,019$$

$$S_3 = 3 \times 185 \text{ mm}^2$$

For the section in the ground k is the product of the coefficients:

$$k_{1g} = 1,1$$

$$k_{2g} = 0,93$$

$$k_{3g} = 0,65$$

$$k_{4g} = 0,83$$

$$n = 3$$

$$I_o \geq 184,45$$

$$S_3 = 3 \times 185 \text{ mm}^2$$

10.3.4.5. String combiner box-inverter, electrical criterion

$$\Delta V = \frac{2 \cdot r \cdot L \cdot m \cdot I}{V} \cdot 100 \quad (34)$$

$$I_m = 9,74 \text{ A}$$

$$V_m = 25 \cdot 41,1 = 1027,5 \text{ V}$$

$$m = 24$$

$$L = 95 \text{ m}$$

$$r = 0,164 \Omega/km \rightarrow r_{90^\circ} = 0,209 \Omega/km$$

$$\Delta V = \frac{2 \cdot r \cdot L \cdot m \cdot I}{V} \cdot 100 = \frac{2 \cdot 0,0209 \cdot 95 \cdot 24 \cdot 9,74}{1027,5} = 0,903 \%$$

$$S = 120 \text{ mm}^2$$

10.3.4.6. Choice of cable: string combiner box-inverter

By comparing the sections that meet the criteria, the 3 x 185 mm² sections are chosen. It is therefore necessary to recalculate the voltage drop. Some sections have been increased in order to reduce energy loss by assessing the overall balance between higher cost of copper and greater energy production. In this case the final sections are:

$$S = 3 \times 240 \text{ mm}^2$$

$$r = 0,082 \Omega/km \rightarrow r_{90^\circ} = 0,1045 \Omega/km$$

$$\Delta V = \frac{2 \cdot r \cdot L \cdot m \cdot I}{V} \cdot 100 = \frac{2 \cdot 0,0105 \cdot 95 \cdot 24 \cdot 9,74}{1027,5} = 0,4517 \%$$

The total voltage drop from the modules to the inverter is:

$$\Delta V = 0,4548 + 0,4517 = 0,9065 \%$$

This is the largest voltage drop among all drops in the installation in the low voltage side.

10.4. Medium voltage connections

Two underground medium voltage sections are sized. The first section connects the two medium voltage stations. Another MV cable starts from the medium voltage switchgear of the southernmost station until it reaches the overhead line outside the plant. In the drawing number 7 the point of connection to the MV line is shown. From Google maps it is observed that a hydroelectric plant is present a few kilometres from the plant lot. So, actually a branch of the MV line can reach the hypothesized point.

ARP1H5(AR)E 12/20 kV cables from the Prysmian group are used. These cables are made up of aluminium conductor, HPTE insulation and the outer sheath is in polyethylene. Three single-core cables are used for each section. The maximum permanent service temperature is 105 °C.



Figure 64: ARP1H5(AR)E cable (Source: [24])

For the sizing of the cables, the “Instrucción técnica complementaria ITC-LAT 06” is used. Analysing the technical support of the MV stations, MV cables enter/exit directly from the ground at the medium voltage switchgear. The laying is then buried in a pipe. The depth at which the cables are located is standard, 1 m. For medium voltage cables it is not sufficient to check the thermal and electrical criteria. Besides, these cables must be able to withstand a short circuit and therefore a condition is added on the section. This calculation is presented first as it is more restrictive and it is equal in the both sections.

10.4.1. Short circuit condition

The minimum section is obtained to withstand a short circuit from the formula present in ITC-LAT 06.

$$\frac{I_{cc}}{S} = \frac{K}{\sqrt{t_{cc}}} \quad (56)$$

Where:

- I_{cc} is the short circuit current
- S is the conductor's section
- K is the coefficient for short-circuit temperatures. For the cables chosen $K = 100$
- $t_{cc} = 1 \text{ s}$ is the duration of the short circuit

Knowing that the short-circuit power S_{cc} of a 20 kV grid (V_n) is 350 MVA, the current I_{cc} can be calculated:

$$I_{cc} = \frac{350 \cdot 10^6}{\sqrt{3} \cdot 20 \cdot 10^3} = 10,1 \text{ kA} \quad (57)$$

The minimum section can be calculated:

$$S = \frac{10100}{100} = 101 \text{ mm}^2 \rightarrow 120 \text{ mm}^2$$

Once the minimum section has been defined, the criteria are checked.

10.4.2. Thermal criterion

$$I_b \leq I_z \quad (32)$$

Where:

$$I_b = \frac{S'}{\sqrt{3} \cdot V_n} \quad (58)$$

It was decided to check the two sections in the same paragraph. The connection section between the MV stations has subscript 1 and the other 2.

$$I_{b1} = \frac{2,5 \cdot 10^6}{\sqrt{3} \cdot 20 \cdot 10^3} = 72,2 \text{ A}$$

$$I_{b2} = \frac{5 \cdot 10^6}{\sqrt{3} \cdot 20 \cdot 10^3} = 144,3 \text{ A}$$

$$I_z = I_o \cdot k \quad (33)$$

By combining the previous formulas:

$$I_o \geq \frac{I_b}{k} \quad (54)$$

Where k is the product of the coefficients:

- $k_{1g} = 1$ ground thermal resistivity (clay)
- $k_{2g} = 0,97$ ground temperature other than 20 °C; in particular, it refers to 30 °C
- $k_{3g} = 1$
- $k_{4g} = 0,87$ consider interference with the other MV cable 40 cm away

It is observed that the coefficients are slightly different from those for LV cables. These coefficients derived from ITC-LAT 06.

$$I_{o1} \geq 85,5 \text{ A}$$

$$I_{o2} \geq 171 \text{ A}$$

The I_o of the cable with section 120 mm² is 245 A, therefore the thermal criterion is respected.

10.4.3. Electrical criterion

Starting from the equation (36) below, with simple steps we arrive at the following formula. This formula is implemented in Excel and voltage drops are calculated

$$\Delta V = \frac{\sqrt{3} \cdot L \cdot m \cdot I \cdot (r \cdot \cos\Phi + x \cdot \sin\Phi)}{V} \cdot 100 \quad (36)$$

$$\frac{\Delta V}{V_n} = \frac{S' \cdot L \cdot (r \cdot \cos\Phi + x \cdot \sin\Phi)}{V_n^2} \cdot 100 \quad (59)$$

The following table shows the calculation for both sections and with the parameters corresponding to the cable with a section of 120 mm².

CABLES	V _n (kV)	S' (MVA)	L (m)	r ₉₀ (Ω/km)	x ₉₀ (Ω/km)	cosφ	senφ	ΔV (%)
B.A	20	2,5	35	0,333	0,12	1	0	0,007284
A.Red	20	5	160	0,333	0,12	1	0	0,0666

Table 14: Verification of the voltage drop for MV cables

With these small values, typical of medium voltage, the total DC + AC voltage drop of less than 1,5 % is respected. In the worst case, a voltage drop of 0,98 % is obtained.

The layout of all the cables of the photovoltaic system is in the AutoCAD drawing number 7. In addition, there are the ducts presented in the next paragraph.

10.5. Ducts

Reference is made to ITC-BT-21. [25] When multiple cables are provided in a duct, it is assumed that they all have the same section equivalent to the largest one. In the following table there are the minimum external diameter of the duct as a function of the number and section of the conducting cables. In the case of conductors for duct greater than 10, the section of the duct is at least equal to 4 times the section occupied by the cables. [25] To calculate the section occupied by the cables, the external radius of the cables, provided in the datasheet, is used.

Sección nominal de los conductores unipolares (mm ²)	Diámetro exterior de los tubos (mm)				
	Número de conductores				
	≤ 6	7	8	9	10
1,5	25	32	32	32	32
2,5	32	32	40	40	40
4	40	40	40	40	50
6	50	50	50	63	63
10	63	63	63	75	75
16	63	75	75	75	90
25	90	90	90	110	110
35	90	110	110	110	125
50	110	110	125	125	140
70	125	125	140	160	160
95	140	140	160	160	180
120	160	160	180	180	200
150	180	180	200	200	225
185	180	200	225	225	250
240	225	225	250	250	--

Figure 65: Minimum external diameter of the duct as a function of the number and section of the conducting cables (Source: [25])

By analysing the various possible cases in the installation, a summary table is obtained.

Number of cables	Maximum section in the duct (mm ²)	Minimum diameter (mm)	Diameter chosen (mm)
4	16	63	63
8	16	75	75
12	16	75	90
16 and 32	16	125	125
4 and 6	240	225	225
4 and 6	185	180	180
4	150	180	180

Table 15: Calculation of ducts, diameter

AutoCAD is used to count the meters for each duct, assuming appropriate diameter changes where necessary. A summary table is reported

Summary (one inverter)						
External diameter (mm)	63	75	90	125	180	225
Duct: Modul - Combiner Box (m)	826	797	767	305	0	0
Duct: Combiner Box - Inverter (m)	0	0	0	0	415	555
Total (one inverter) (m)	826	797	767	305	415	555

Table 16: Calculation of ducts, length

The last table shows the calculation for photovoltaic inter-installation with MV cables. For this calculation, the document used is MT 2.31.01. To meet the distributor's requirements, two 160 mm ducts are required. [26]

Summary (photovoltaic system)							
Diametro externo (mm)	63	75	90	125	160	180	225
Ducts: 2 inverter (m)	1652	1593	1534	610	0	830	1110
MV ducts (m)	0	0	0	0	390	0	0
Total with rounding (m)	1700	1600	1550	650	400	850	1150

Table 17: Calculation of ducts, final summary

The next chapter is about protections.

11. Protections and system grounding

This chapter contains calculations and verifications for the protections and earthing of the photovoltaic system.

11.1. Protections

The protections are included in other components. They are analysed in detail. Then, the fuse calculation is presented.

The first protection on the DC side is included in the Trinasolar TSM-DE15H(II) panel. They are the bypass diodes, described in paragraph 3.4. Their main function is to avoid the hot spot phenomenon.

On each string of the photovoltaic field there are fuses and disconnectors, incorporated in the string monitor. In the case of installations with several strings in parallel, the fuses are used to protect the strings from reverse currents from other strings. Assuming a short circuit in a string, in the worst case of the installation described in this work, we would have the sum of the currents coming from the other 23 strings in the string with fault. A reverse current can result from a double earth fault of modules/cables or from a short circuit in a module. The calculation necessary to correctly choose the fuses from the options in the datasheet is presented below.

In the UNE 60364 standard the following equations are present to derive the rated current I_n of the fuse:

$$1,25 \cdot I_{sc} \leq I_n \leq 2 \cdot I_{sc} \quad (60)$$

Detailing the equation with the installation data:

$$1,25 \cdot 10,18 \leq I_n \leq 2 \cdot 10,18$$

$$12,725 \text{ A} \leq I_n \leq 20,36 \text{ A}$$

Two fuse sizes are available in this range, 15 A and 20 A. In the fuse connector datasheet, the manufacturer provides the following equation for choosing the fuse appropriately:

$$I_n \geq \frac{I_{sc}}{S_{factor}}$$

Where:

- S_{factor} is the screening factor obtained from tables in the datasheet based on the altitude of the place. In the case considered $S_{factor} = 0,6$. Substituting the values:

$$I_n \geq \frac{10,18}{0,6} = 16,97 \text{ A}$$

It was therefore decided to choose the 20 A fuse.

The other condition to check is the fuse voltage V_n . The standard UNE EN 60269-6 states that: “La tensión asignada del cartucho fusible seleccionado debe tener en cuenta la V_{oc} de la cadena a la temperatura de aplicación mínima”.

$$V_n \geq V_{oc,string}(T_{min}) = 1391 \text{ V} \quad (61)$$

1500 V fuses are chosen.

The last check is the breaking capacity I_{CU}

$$I_{CU} \geq (m_{p,box} - 1) \cdot 1,25 \cdot I_{sc} \quad (62)$$

$$I_{CU} \geq 23 \cdot 1,25 \cdot 10,18 = 292,7 \text{ A}$$

The standard UNE EN 60269-6 states that: “El valor mínimo del poder de corte asignado es de 10 kA cc”. This current is found in the fuse datasheet as a function of altitude. In the case considered the equation is verified because $I_{CU} = 12 \text{ kA}$.

The following information are found in the datasheet of the SMA String-Monitor. The protection class is II and the IP degree is IP54. Each model is equipped with a DC switch-disconnector. Through the DC power switch-disconnector, the PV generator connected to the SMA String-Monitor can disconnect from the inverter. The SMA String-Monitor is equipped with Type II overvoltage protection.

Other protection elements are incorporated in the MV station. The IP degree is IP65. DC switch-disconnector, medium voltage circuit breaker, type I DC surge arrester are also present. The calculation of the inverter fuses is shown below. After this calculation it is assumed to size the circuit breaker, in the section between inverter and transformer (included in the MV station).

- Cables with double conductors per polarity have only one fuse, therefore the fuse is sized for the total current carried by the 2 cables. Calculations are presented for the various boxes with 10, 16 and 24 strings in parallel.

$$1,25 \cdot I_{sc,box} \leq I_n \leq 2 \cdot I_{sc,box}$$

$$m = 10 \rightarrow 127,3 \text{ A} \leq I_n \leq 203,6 \text{ A} \rightarrow I_n = 200 \text{ A}$$

$$m = 16 \rightarrow 203,6 \text{ A} \leq I_n \leq 325,1 \text{ A} \rightarrow I_n = 250 \text{ A}$$

$$m = 24 \rightarrow 305,4 \text{ A} \leq I_n \leq 488,6 \text{ A} \rightarrow I_n = 350 \text{ A}$$

- Cables with triple conductors per polarity have 2 fuses, one for 2 cables and 1one for the other cable. Therefore, the first fuse is sized for the current carried by two cables and the second fuse for the remain current. Calculations are presented for the various boxes with 24 strings in parallel.

$$m = 24 \rightarrow 101,8 A \leq I_n \leq 162,9 A \rightarrow I_n = 160 A$$

$$m = 24 \rightarrow 203,6 \leq I_n \leq 325,8 A \rightarrow I_n = 250 A$$

18 of 24 inputs (for polarity) of the inverter are therefore occupied with cables. in total there are:

- ✓ 6 fuses of 160 A
- ✓ 1 fuse of 200 A
- ✓ 9 fuses of 250 A
- ✓ 2 fuses of 350 A

The other condition to check is the fuse voltage V_n .

$$V_n \geq V_{oc,string}(T_{min}) = 1391 V$$

1500 V fuses are chosen.

The last check is the breaking capacity I_{CU}

$$I_{CU} \geq (m_{p,inverter} - m_{p,box}) \cdot 1,25 \cdot I_{sc,box} \quad (63)$$

In the worst case:

$$I_{CU} \geq (250 - 10) \cdot 1,25 \cdot 10,18 = 3,05 kA$$

The minimum breaking capacity is 10 kA, therefore this sizing is also verified.

In the hypothesis of choosing the circuit breaker, in the section between inverter and transformer (included in the MV station), the calculation is also presented.

Previously the MV short circuit current has been calculated:

$$I_{cc} = \frac{350 \cdot 10^6}{\sqrt{3} \cdot 20 \cdot 10^3} = 10,1 kA \quad (57)$$

This current must be reported to the low voltage side of the transformer and with this the rated current of the circuit-breaker is chosen.

The phase grid voltage and its impedance, supposed only reactive, are calculated:

$$E_{grid} = \frac{c \cdot Vn}{\sqrt{3}} = 12,7 \text{ kV} \quad (64)$$

$$Z_{grid} = X_{grid} = \frac{E_{grid}}{I_{cc}} = \frac{c \cdot Vn^2}{S_{cc}} = 1,26 \Omega \quad (65)$$

This value is reported to the low voltage side of the transformer:

$$Z_{gridLV} = X_{gridLV} = Z_{grid} \cdot \left(\frac{V_{nLV}}{V_n}\right)^2 = 1,26 \cdot \left(\frac{550}{20 \cdot 10^3}\right)^2 = 0,953 \text{ m}\Omega \quad (66)$$

V_{nLV} is a datasheet information (transformer). [19]

The calculation of the impedance of the transformer, supposedly reactive, is reported.

$$X_{Tcc} = \frac{V_{cc}\%}{100} \cdot \frac{V_{nLV}^2}{S_T} = \frac{6}{100} \cdot \frac{550^2}{2500000} = 7,26 \text{ m}\Omega \quad (67)$$

$V_{cc}\%$ and S_T come from the datasheet (transformer). [19]

The short circuit current at the low voltage side of the transformer can be calculated with the following formula:

$$I_{cc,LV} = \frac{V_{nLV}}{\sqrt{3} \cdot Z_{LV}} = \frac{500}{\sqrt{3} \cdot (0,953 + 7,26) \cdot 10^{-3}} = 38,7 \text{ kA} \quad (68)$$

The automatic low voltage switch has the following characteristics:

- rated current I_n greater than the maximum output current from the inverter $I_{inv,AC}$

$$I_n > 2624 \text{ A}$$

- breaking capacity I_{cu} greater than the value of $I_{cc,LV}$

$$I_{cu} > 38,7 \text{ kA}$$

For example, in Schneider products, the circuit breaker MasterPact NW32HF has the following characteristic values:

$$I_n = 3200 \text{ A} \quad 50 \text{ Hz} \quad 690 \text{ V}$$

$$I_{cu} = 85 \text{ kA}$$

The single wire diagram is in the AutoCAD 9 drawing.

11.2. System grounding

The study of grounding starts from the inverter. On the technical manual, it is clear that the connection between the inverter and the transformer is with insulated neutral (IT). [19] This means that the neutral of the LV side transformer is isolated and the masses connect directly to earth. The local distributor, i-De group Iberdrola, in the document "Condiciones técnicas de instalaciones de producción eléctrica conectadas a la red" [27], specifies that installations with a connection point greater than 1 kV will not supply neutral current in the event of earth faults in the grid. For this the neutrals of the transformers, MV side, are not connected to the ground. Finally, from the datasheet, the inverter can incorporate elements for the control of currents to earth for both poles. It was decided to insert this optional element because, as explained in the theoretical part, it is important to identify the first fault when the distribution system is it. the calculations for grounding the low voltage and the medium voltage stations masses, plus the verification calculation for a common ground are presented below.

11.2.1. Low voltage

In the "Instrucción Técnica Complementaria" ITC-RAT 13 there is a table for calculating the resistance of the most common electrodes. [28] The chosen electrode is the bare copper conductor that connects all the structures. The technical data are the section of 35 mm² and the depth of 0,5 m. For the arrangement of these conductors, see drawing 8, made on AutoCAD. The formula to be used for this electrode is:

$$R_{LV} = \frac{2 \cdot \rho}{L} \quad (69)$$

Where:

- ρ is the resistivity of the ground which depends on the nature of the terrain
- $L = 2121 \text{ m}$ is the total length of the buried conductor, measured on AutoCAD.

To obtain the resistivity of the ground, reference is always made to ITC-RAT 13:

$$\rho = 100 \Omega \cdot m$$

By substituting these values:

$$R_{LV} = \frac{2 \cdot 100}{2121} = 94,3 \text{ m}\Omega \quad (70)$$

11.2.2. Medium voltage stations

To do this calculation, reference is made to the Spanish document which can be translated as "Method of calculation and design of grounding installations for transformation centres connected to the third category grid" [29]. The configuration that provides for a 50 mm² conductor around the MV station with a rectangular perimeter shape. The conductor is 50 cm deep in the ground. If this configuration is

not sufficient, electrodes (with a diameter of 14 mm) will be inserted in increasing numbers, length and depths. Once the configuration has been chosen, the following coefficients are obtained.

- $k_r = 0,103 \Omega/\Omega \cdot m$ is the coefficient of the earth resistance
- $k_p = 0,0203 V/(\Omega \cdot m \cdot A)$ is the step voltage coefficient
- $k_c = 0,0610 V/(\Omega \cdot m \cdot A)$ is the contact voltage coefficient. This is equal to the access step voltage coefficient for this configuration.

The resistance of the configuration chosen with this formula is calculated:

$$R_{MV} = k_r \cdot \rho \quad (71)$$

$$R_{MV} = 10,3 \Omega \quad (72)$$

There are two MV stations in the installation with this resistance.

11.2.3. Common ground

To achieve a common grounding of all the masses, two conditions must be verified, expressed by the formulas (73) and (74).

$$U_{pad} > U_{p-max} = R_{commun} \cdot I_T \quad (73)$$

It means that the step voltage U_{p-max} that occurs at the passage of the maximum fault current I_T must be less than the admissible one U_{pad}

$$U_{cad} > U_{c-max} = R_{commun} \cdot I_T \quad (74)$$

It means that the contact voltage U_{c-max} that occurs at the passage of the maximum fault current I_T must be less than the admissible one U_{cad} .

There is also the following numerical relationship for the admissible applied voltages.

$$U_{A-pad} = 10 \cdot U_{A-cad} \quad (75)$$

The common resistance in this installation, if possible, is the parallel of the three ground connections calculated previously.

$$\frac{1}{R_{commun}} = \frac{1}{R_{LV}} + \frac{1}{R_{MV}} + \frac{1}{R_{MV}} \quad (76)$$

$$R_{commun} = 92,6 m\Omega \quad (77)$$

The maximum earth current must then be calculated as:

$$I_T = \frac{c \cdot V_n}{\sqrt{3} \cdot \sqrt{(R_{\text{commun}} + R_n)^2 + X_n^2}} \quad (78)$$

Where:

- $c = 1,1$
- $V_n = 20 \text{ kV}$ is the grid rated voltage
- $R_n = 0 \Omega$ is the substation grounding resistance [30]
- $X_n = 25,4 \Omega$ is the limiting reactance of the substation [30]

By particularizing equation (78):

$$I_T = 499,7 \text{ A} \quad (79)$$

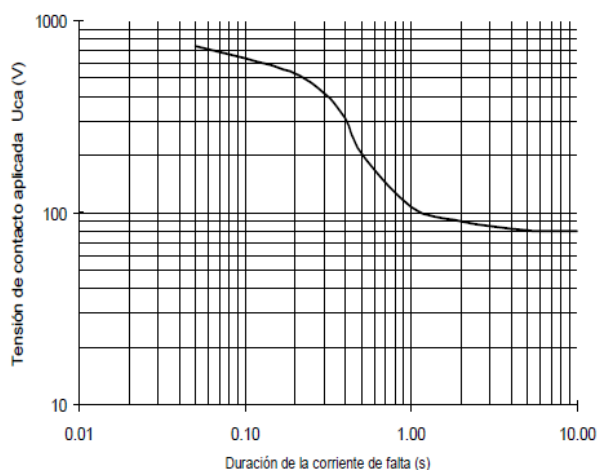
The last element is the admissible contact voltage:

$$U_{\text{cad}} = U_{A-\text{cad}} \cdot \left(1 + \frac{\frac{R_a}{2} + \frac{R_c}{2}}{Z_B} \right) \quad (80)$$

Where:

- $U_{A-\text{cad}}$ is the admissible applied contact voltage
- $R_a = 2000 \Omega$ is the shoe resistance
- $R_c = 3 \cdot \rho = 300 \Omega$ is the contact point earth resistance
- $Z_B = 1000 \Omega$ is the impedance of the human body

The value of $U_{A-\text{cad}}$ is obtained from the ITC-RAT 13.



Duración de la corriente de falta, t_f (s)	Tensión de contacto aplicada admisible, U_{ca} (V)
0.05	735
0.10	633
0.20	528
0.30	420
0.40	310
0.50	204
1.00	107
2.00	90
5.00	81
10.00	80
> 10.00	50

Figure 66: Admissible applied contact voltage values as a function of the current fault time (Source: [28])

Since the characteristics and curves of the substation protection elements are not met, it is assumed that they fulfill the requirements established by the Iberdrola distributor. In the document “Diseño de puestas a tierra en centros de transformación en edificio de otros usos de tensión nominal ≤ 30 kV” [30] is established that the time of intervention must respect the equation:

$$I_T \cdot t_F = 400 \quad (81)$$

Substituting the values:

$$t_F = \frac{400}{499,7} = 0,80 \text{ s} \quad (82)$$

With a linear interpolation of the data in Figure 65:

$$U_{A-cad} = 145,8 \text{ V} \quad (83)$$

Finally:

$$U_{cad} = 313,5 V \quad (84)$$

Equation (74) can be calculated:

$$U_{cad} > U_{c-max} = R_{commun} \cdot I_T \rightarrow 313,5 V > 46,3 V$$

For the step voltages, in the ITC-RAT 13:

$$U_{A-pad} = 10 \cdot U_{A-cad} = 1458 V$$

$$U_{pad} = U_{A-pad} \cdot \left(1 + \frac{2 \cdot R_a + 2 \cdot R_c}{Z_B}\right) \quad (85)$$

$$U_{pad} = 8164,8 V \quad (86)$$

Equation (73) can be calculated:

$$U_{pad} > U_{p-max} = R_{commun} \cdot I_T \rightarrow 8164,8 V > 46,3 V$$

Since the conditions of equations (73) and (74) have been occurred, this installation can have a common ground for all masses.

With this chapter all the elements of the photovoltaic installation have been identified and verified. The next chapters concern the producibility and economic analysis.

12. Producibility of the plant

After choosing all the elements of the photovoltaic system, the annual producibility can be calculated. The formulas for this calculation are shown below. In case of lack of data, reference is made to the values provided by the IDAE.

$$PR(\%) = (100 - A - P_{temp}) \cdot B \cdot C \cdot D \cdot E \cdot F \quad (38)$$

$$E_p = \frac{G_{dm}(\alpha, \beta) \cdot P_{MPPT-PV} \cdot PR}{G_{STC}} \quad (39)$$

The parameter A is the first calculated. A can be expressed as:

$$A = 100 \cdot (A_1 + A_2 + A_3 + A_4) \quad (87)$$

Where:

- $A_1 = 0,03$ is a parameter supplied by the manufacturer of the photovoltaic modules. [18] It is the tolerance on nominal power because photovoltaic cells are different from each other.
- $A_2 = 0,015$ considers dust and dirt. The indicative value of IDAE is halved because adequate maintenance is expected, concentrated in the little rainy months.
- $A_3 = 0,01$ considers angular and spectral reflectance. A low value is assumed because the panel is a new technology (2019) and has a high transmission.
- $A_4 = 0,03$ considers the shadow. Besides, in this case a low value is considered because the ground has been previously levelled to have a correct arrangement of the panels.

The calculation for P_{temp} is presented.

$$P_{temp} = |\gamma| \cdot (T_{cel} - 25) \quad (88)$$

Where:

- $\gamma = -0,36 \text{ } \%/^{\circ}\text{C}$ is the coefficient of variation of P_m with temperature. It is a parameter supplied by the manufacturer of the photovoltaic modules. [18]
- T_{cel} derives from formula (26) with reference to the average temperature T_{av} and average irradiance G_{av} with 37° inclination angle. T_{av} is obtained with PVGIS for each month of the year. the PVGIS-SARAH database is used. [20] The formula for T_{cel} is:

$$T_{cel} = T_{av} + G_{av} \cdot \frac{NOCT - 20}{800} \quad (89)$$

Formulas (88) and (89) are implemented in Excel and summarized in the following table:

Month	Tav (°C)	Gav (kWh/m2*month)	Tcel (°C)	Ptemp
January	6,26	134,3	9,78	-0,055
February	7,57	132,6	11,05	-0,050
March	10,09	173,7	14,65	-0,037
April	15,66	174,8	20,25	-0,017
May	19,22	193,8	24,30	-0,003
June	22,27	201,3	27,55	0,009
July	28,91	217,4	34,62	0,035
August	27,70	207,6	33,14	0,029
September	21,86	175,9	26,48	0,005
October	15,55	157,5	19,68	-0,019
November	10,16	130,9	13,60	-0,041
December	6,48	131,8	9,94	-0,054

Table 18: Calculation of Ptemp in the year

It should be noted that a positive term P_{temp} means losses while a negative one means gain.

Parameter B refers to the efficiency of the DC cables. It is calculated below.

$$P_{L-PV-DC} = \frac{N_s \cdot V_{MPPT} \cdot I_{MPPT}}{100} \cdot \sum_{i=1}^{Nstring} \Delta V_{DCi} = 36091 W \quad (90)$$

$$P_{MPPT-PV} = N_s \cdot V_{MPPT} \cdot I_{MPPT} \cdot N_p = 5003925 W \quad (91)$$

$$B = \frac{P_{MPPT-PV} - P_{L-PV-DC}}{P_{MPPT-PV}} = 0,993 \quad (92)$$

Parameter C refers to the efficiency of the AC cables. It is calculated below.

$$P_{L-PV-AC} = \frac{V_n}{100} \cdot \sum_{i=1}^2 \Delta V_{ACi} \cdot I_{Bi} = 3512 W \quad (93)$$

In this case the reference power is that of the output from the MV station. The MV station datasheet shows the maximum output power, the $P_{MV-STATION}$ shown below.

$$P_{MV-STATION} = 500000 W \quad (94)$$

$$C = \frac{P_{MV-STATION} - P_{L-PV-AC}}{P_{MPPT-PV}} = 0,999 \quad (95)$$

$D = 0,95$ is the maximum value suggested by the IDAE in order to consider periods when the plant is not in operation.

$E = 0,955$ normally considers the losses of the inverter. In this case it considers marks the losses of the components in the station (inverter, bar, auxiliaries, transformer). Consequently, in order to obtain it, an energy balance is made.

$$E = \frac{P_{MV-STATION}}{P_{MV-STATION} + 2 \cdot (P_{Tsc} + P_{Toc} + P_{bar} + P_{aux} + P_{inv})} \quad (96)$$

Where:

- P_{Tsc}, P_{Toc} are the short circuit and vacuum losses of the transformer provided by the datasheet
- P_{bar} is the power loss of the bar
- P_{aux} is the power loss of the auxiliaries
- P_{inv} is the power loss of the inverter

For the available data available, it is decided to make the product of the efficiencies.

$$E = \eta_{inv} \cdot \eta_{bar,aux} \cdot \eta_T \quad (97)$$

Where:

- $\eta_T = 0,975$ is the efficiency of the transformer which is calculated as the ratio of the output power to the input power

$$\eta_T = \frac{P_{MV-STATION}}{P_{MV-STATION} + 2 \cdot (P_{Tsc} + P_{Toc})} \quad (98)$$

The datasheet provides 33 kV losses. Vacuum losses are considered invariable and short-circuit losses are corrected.

$$P_{Tsc} = P_{Tsc,33kV} \cdot \left(\frac{I_{b,20kV}}{I_{b,33kV}} \right)^2 = 23,2 \cdot \left(\frac{72,2}{44} \right)^2 = 62,5 \text{ kW}$$

$$P_{Toc} = 2,5 \text{ kW}$$

Finally, η_T is calculated:

$$\eta_T = \frac{5 \cdot 10^6}{5 \cdot 10^6 + 2 \cdot (2,5 \cdot 10^3 + 62,5 \cdot 10^3)} = 0,975 \quad (99)$$

- $\eta_{bar,aux}$ considers the losses of the 2 bars (copper, supposedly 3 m long. The section is taken from the manual) and of the auxiliary elements (10 kW basic elements). It is calculated as the ratio of the output power (input of the transformer) to the input power

$$\eta_{bar,aux} = \frac{P_{MV-STATION} + 2 \cdot (P_{Tsc} + P_{Toc})}{P_{MV-STATION} + 2 \cdot (P_{Tsc} + P_{Toc} + P_{bar} + P_{aux})} \quad (100)$$

$$R_{bar} = \frac{\rho \cdot L}{2 \cdot S} = \frac{0,022 \cdot 3}{2 \cdot 2000} = 1,65 \cdot 10^{-5} \Omega$$

$$P_{bar} = 3 \cdot R_{bar} \cdot I_{inv,AC}^2 = 3 \cdot 1,65 \cdot 10^{-5} \cdot 2624^2 = 340,8 W$$

Finally, $\eta_{bar,aux}$ is calculated:

$$\eta_{bar,aux} = \frac{256500}{256500 + 340,8 + 10000} = 0,996 \quad (101)$$

- $\eta_{inv} = 0,983$ is the European efficiency of the inverter found in the datasheet

The values calculated can be used in equation (97)

$$E = 0,983 \cdot 0,996 \cdot 0,975 = 0,955 \quad (102)$$

$F = 0,95$ is the IDAE value for losses due to errors in the monitoring of the maximum power point.

All the elements for the calculation of the PR are calculated, its value is presented for each month because the P_{temp} parameter is monthly. Its average value is 78,24 %

Month	PR (%)
January	78,28
February	78,28
March	78,26
April	78,25
May	78,23
June	78,22
July	78,20
August	78,21
September	78,23
October	78,25
November	78,27
December	78,28

Table 19: Calculation of the PR parameter

The last calculation shown is the producibility calculation.

$$E_p = \frac{G_{dm}(\alpha, \beta) \cdot P_{MPPT-PV} \cdot PR}{G_{STC}} \quad (39)$$

It is noted that $G_{dm}(\alpha, \beta)$ is equivalent to G_{av} obtained with PVGIS.

Month	Tav (°C)	Gav (kWh/m2*month)	PR (%)	Ep (kWh/month)
January	6,26	134,3	78,28	525901
February	7,57	132,6	78,28	519373
March	10,09	173,7	78,26	680376
April	15,66	174,8	78,25	684337
May	19,22	193,8	78,23	758648
June	22,27	201,3	78,22	787987
July	28,91	217,4	78,20	850575
August	27,70	207,6	78,21	812390
September	21,86	175,9	78,23	688475
October	15,55	157,5	78,25	616732
November	10,16	130,9	78,27	512780
December	6,48	131,8	78,28	516340
TOTAL				7953913

Table 20: Calculation of monthly and annual producibility

The final annual production is around 7,9 GWh.

The same software used previously, PVGIS, provides a simulation of energy that can be produced by the plant. This is possible thanks to a database from 2005 to 2016. This simulation considers typical loss values and the optimal orientation (south) and inclination of the panels (37°). The result of the simulation is presented.

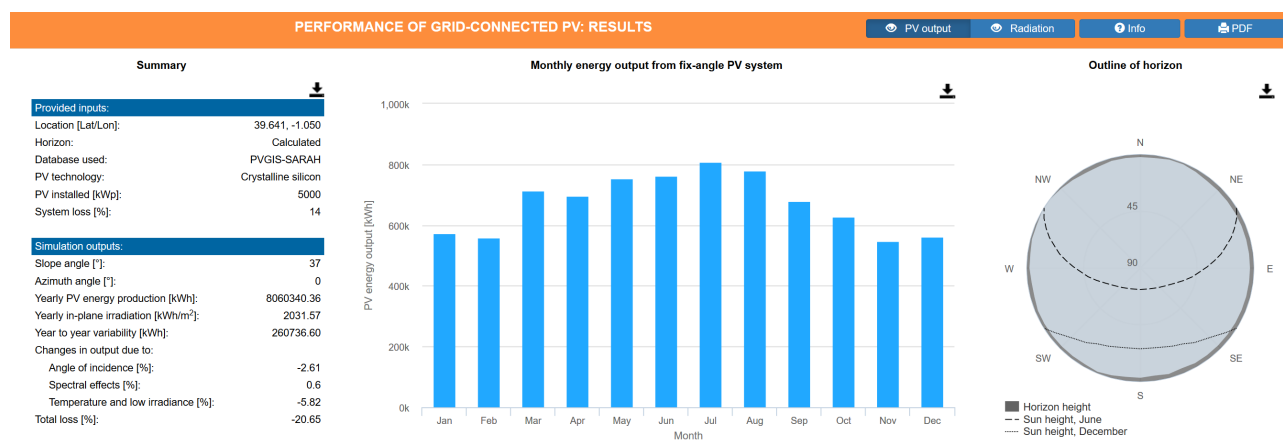


Figure 67: Monthly energy output from fix-angle PV system (Source: [20])

Furthermore, these data, although indicative, provide a good estimate of the producibility of the plant. It is observed that similar annual production is obtained considering different loss percentages. Producibility calculated with the proposed method is more precise.

PRESUPUESTO

13. Economic analysis

In this chapter there are two paragraphs that deal respectively with the economic specifications and the economic indices.

13.1. Economic specifications

The costs associated with each of the elements and equipment that form the photovoltaic installation constitute the initial investment. This parameter is essential to study the profitability of the project in term of economic indices. The following table summarizes the prices associated with each element.

Description	Quantity	Unit	Unit price (€)	Total (€)	Total investment (€)
Trinasolar TSM-DE15H(II) Panel	12500		90,00	1.125.000	3.112.592
Installation and connection of modules	5	MW	1.000,00	5.000	
SMA MV Power Station 2500	2		170.000,00	340.000	
SMA SSM-U-1615 (string monitor)	8		1.100,00	8.800	
SSM-U-2415 (string monitor)	16		1.270,00	20.320	
TreeSystem Support solution	250		1.332,00	333.000	
Transport and installation of supports	250		170,00	42.500	
Connectors	1000		1,05	1.050	
LV cables					
Line DC Cu (PV)1-F 0,6/1 kV 2x(1x4 mm2), supply and laying	240	m	4,39	1.054	
Line DC Cu (PV)1-F 0,6/1 kV 1x(1x4 mm2), supply and laying	1440	m	3,83	5.515	
Line DC Cu (PV)1-F 0,6/1 kV 2x(1x6 mm2), supply and laying	1620	m	4,82	7.808	
Line DC Cu (PV)1-F 0,6/1 kV 1x(1x6 mm2), supply and laying	2520	m	4,05	10.206	
Line DC Cu (PV)1-F 0,6/1 kV 2x(1x10 mm2), supply and laying	8940	m	5,63	50.332	
Line DC Cu (PV)1-F 0,6/1 kV 1x(1x10 mm2), supply and laying	5400	m	4,45	24.030	
Line DC Cu (PV)1-F 0,6/1 kV 2x(1x16 mm2), supply and laying	17700	m	6,87	121.599	
Line DC Cu (PV)1-F 0,6/1 kV 1x(1x16 mm2), supply and laying	5640	m	5,07	28.595	
Line DC Cu (PV)S3Z2Z2-K 0,6/1 kV 2x[2x(1x150 mm2)], supply and laying	330	m	68,62	22.645	
Line DC Cu (PV)S3Z2Z2-K 0,6/1 kV 2x[2x(1x185 mm2)], supply and laying	60	m	83,62	5.017	
Line DC Cu (PV)S3Z2Z2-K 0,6/1 kV 3x[2x(1x185 mm2)], supply and laying	440	m	123,25	54.230	
Line DC Cu (PV)S3Z2Z2-K 0,6/1 kV 2x[2x(1x240 mm2)], supply and laying	740	m	107,18	79.313	
Line DC Cu (PV)S3Z2Z2-K 0,6/1 kV 3x[2x(1x240 mm2)], supply and laying	370	m	158,59	58.678	
MV cables					
Line MT trifasica ARP1H5(AR)E 12/20 kV 3x(1x120 mm2), supply and laying	195	m	29,96	5.842	
Grounded cables					
Bare copper conductor 35 mm2, supply and laying	2121	m	6,20	13.150	
Bare copper conductor 50 mm2, supply and laying	42	m	6,73	1.285	
Ducts					
Duct with external diameter 63 mm, supply and laying	1700	m	1,52	2.584	
Duct with external diameter 75 mm, supply and laying	1600	m	1,75	2.800	
Duct with external diameter 90 mm, supply and laying	1550	m	2,25	3.488	
Duct with external diameter 125 mm, supply and laying	650	m	3,15	2.048	
Duct with external diameter 160 mm, supply and laying	200	m	3,39	678	
Duct with external diameter 180 mm, supply and laying	850	m	4,25	3.613	
Duct with external diameter 225 mm, supply and laying	1150	m	5,61	6.452	
Digging ground					
Land Purchase				99.000	
Initial preparation	267240	m ³	2,30	614.652	
Excavating ducts	2133	m ³	5,77	12.309	

Table 21: Costs of the various elements of the PV system

The total investment is:

$$I_0 = 3112592 \text{ €} \quad (103)$$

These prices derive from quotes, from the “Base de Precios de la Comunidad Valenciana” [31] and from the “Agència Tributària Valenciana” [32]. A mixed method is used for the calculation of LV cables. The prices of the cables are obtained from quotes. The total price in the table includes the laying and other costs, obtained on the “Base de Precios de la Comunidad Valenciana” [31]. An example of calculation is shown below. The other calculations are in the Appendix D.

Codigo	UM	Description	Rdto.	Precio	Importe
MOOE11a	h	Especialista electricidad	0,12	16,84	2,02
MOOE.8a	h	Oficial 1a electricidad	0,06	19,75	1,19
-	m	Cable Cu (PV)1-F 0,6/1 kV 1x4 mm ²	2,1	0,52	1,09
%		Costes directos complementarios	0,02	4,30	0,09
Line DC Cu (PV)1-F 0,6/1 kV 2x(1x4 mm²)					4,39

Table 22: Low voltage cable's price

13.2. Economic indices

Thanks to the economic indices, the feasibility of carrying out the planned project can be determined. The economic indices described in the theoretical part, NPV, IRR and DPB are calculated and analysed. The analysis was carried out with the following hypotheses:

- The selling price of energy is the same as the previous year's ended. This data is obtained from the AEGE energy barometer. In 2019 the price of energy in Spain is 47,7 €/MWh. [33]
- The investment of the photovoltaic installation is paid entirely in year zero without economic loans.
- The production of the system decreases over time due to the performance of the photovoltaic modules. Starting from the calculated producibility, the coefficients of guaranteed producibility of the modules indicated in the datasheet in graphic form are applied. This is reported in Figure 68
- The main inflows f_k^+ derive from the sale of the energy produced. Outflow f_k^- includes initial investment, purchase of the land, periodic maintenance (1 % of the initial investment),
- The discount rate is $r = 6 \%$
- Normally a plant life of 25 years is assumed.

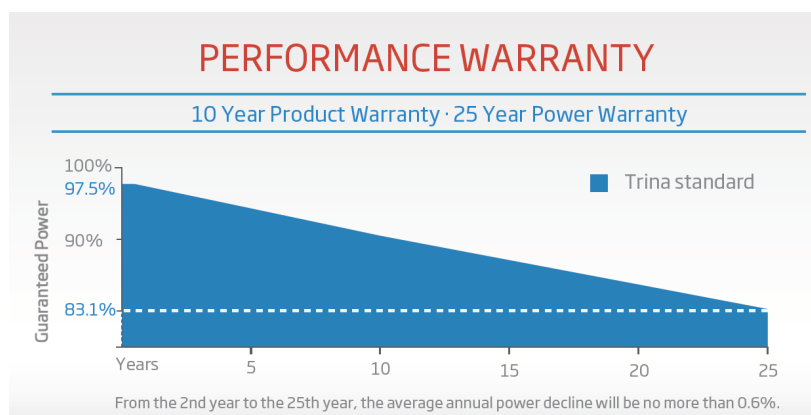


Figure 68: Performance warranty of the modules (Source: [18])

13.2.1. NPV

This economic index is calculated by considering the useful life of the plant. The calculation implemented in Excel is reported.

Year	Energy production (MWh/year)	fk+(€/year)	fk-(€/year)	fk(€/year)	Discounted fk(€/year)	NPV (€)
0	0	0	3112592	-3112592	-3112592	987166
1	7755,1	369917	31126	338791	319614	
2	7755,1	369917	31126	338791	301523	
3	7708,5	367697	31126	336571	282592	
4	7662,0	365478	31126	334352	264838	
5	7615,5	363258	31126	332132	248188	
6	7568,9	361039	31126	329913	232575	
7	7522,4	358819	31126	327693	217935	
8	7475,9	356600	31126	325474	204206	
9	7429,4	354380	31126	323254	191334	
10	7382,8	352161	31126	321035	179264	
11	7336,3	349941	31126	318815	167948	
12	7289,8	347722	31126	316596	157338	
13	7243,2	345502	31126	314376	147392	
14	7196,7	343283	31126	312157	138067	
15	7150,2	341063	31126	309937	129326	
16	7103,6	338844	31126	307718	121132	
17	7057,1	336624	31126	305498	113451	
18	7010,6	334405	31126	303279	106252	
19	6964,0	332185	31126	301059	99504	
20	6917,5	329966	31126	298840	93180	
21	6871,0	327746	31126	296620	87252	
22	6824,5	325527	31126	294401	81698	
23	6777,9	323307	31126	292181	76492	
24	6731,4	321088	31126	289962	71614	
25	6684,9	318868	31126	287742	67044	

Table 23: NPV calculation

The total value is the sum of the discounted annual values and it is:

$$NPV = 997166 \text{ €} \quad (104)$$

The positive value of this index in the planning phase indicates that the project can be carried out because there is a positive return on capital. The higher its value, the greater the benefit obtained.

13.2.2. IRR

The discount rate $r = IRR$, that makes the NPV null, is calculated for a period of 10 year.

Year	Energy production (MWh/year)	fk+(€/year)	fk-(€/year)	fk(€/year)	Discounted fk(€/year)	Total Discounted fk(€)	IRR
0	0	0	3112592	-3112592	-3112592	-3112592	1,134%
1	7755,1	369917	31126	338791	334993	-2777599	
2	7755,1	369917	31126	338791	331238	-2446362	
3	7708,5	367697	31126	336571	325379	-2120983	
4	7662,0	365478	31126	334352	319610	-1801373	
5	7615,5	363258	31126	332132	313929	-1487444	
6	7568,9	361039	31126	329913	308336	-1179108	
7	7522,4	358819	31126	327693	302828	-876280	
8	7475,9	356600	31126	325474	297405	-578875	
9	7429,4	354380	31126	323254	292066	-286809	
10	7382,8	352161	31126	321035	286809	0	

Table 24: IRR calculation

The value obtained is:

$$IRR = 1,134 \% \quad (105)$$

It is observed that the value obtained is lower than the one used in the NPV. According to this index, an investment is valid if the discount rate is greater than that used in the NPV. To obtain a value greater than 6 %, the minimum period is 15 years. This is confirmed by the DPB.

13.2.3. DPB

This economic index is calculated by considering the useful life of the plant. The calculation implemented in Excel is reported.

Year	Energy production (MWh/year)	fk+(€/year)	fk-(€/year)	Total discounted fk+(€/year)	Total discounted fk-(€/year)
0	0	0	3112592,076	3112592,076	0
1	7755	369917	31125,92076	3141956	348978
2	7755	369917	31125,92076	3169658	678202
3	7709	367697	31125,92076	3195792	986928
4	7662	365478	31125,92076	3220447	1276420
5	7615	363258	31125,92076	3243706	1547868
6	7569	361039	31125,92076	3265648	1802386
7	7522	358819	31125,92076	3286349	2041021
8	7476	356600	31125,92076	3305878	2264756
9	7429	354380	31125,92076	3324301	2474513
10	7383	352161	31125,92076	3341682	2671158
11	7336	349941	31125,92076	3358078	2855503
12	7290	347722	31125,92076	3373547	3028310
13	7243	345502	31125,92076	3388140	3190294
14	7197	343283	31125,92076	3401907	3342129
15	7150	341063	31125,92076	3414895	3484442
16	7104	338844	31125,92076	3427147	3617827
17	7057	336624	31125,92076	3438706	3742837
18	7011	334405	31125,92076	3449611	3859994
19	6964	332185	31125,92076	3459899	3969785
20	6918	329966	31125,92076	3469604	4072670
21	6871	327746	31125,92076	3478760	4169078
22	6824	325527	31125,92076	3487397	4259414
23	6778	323307	31125,92076	3495546	4344055
24	6731	321088	31125,92076	3503234	4423356
25	6685	318868	31125,92076	3510486	4497652

Table 25: DPB calculation

It is observed and confirmed that, with the discount rate used in the NPV, it takes 15 years to recover the initial investment. This is an acceptable period of time for a photovoltaic system.

Conclusions

The following steps are taken for the 5 MWp photovoltaic installation project located in Chelva, Valencian Community, Spain. The analysis of the municipality leads to the identification of a clayey soil destined for cultivation. Later, it is estimated, with cadastral information, that an area of parcel 806 is enough to accommodate the entire plant. Next, it is simulated a preparation of the soil, exposed in an optimal direction towards the south. This analysis, made with MATLAB, leads to a removal of about 270'000 m³ of soil, placed into another area of the parcel. The preparation of the land involves a total expense of 614'652 €. A further cost is the purchase of the land of 99'000 €. The next step is choosing the main elements of the system. Various technologies of photovoltaic modules currently on the market are analysed. The final choice falls on the 400 W Trinasolar TSM-DE15H (II) monocrystalline module. For a production of 5MWp, 12'500 panels are required and an investment of 1'125'000 €. The following element is the MV station, in particular two 2'500 kW units are chosen. One unit incorporates the inverter, transformer, medium voltage switch and all necessary electrical protections. The centralized configuration, widely used for installations on the ground in Spain, entails a cost of 340'000 €. The optimal configuration among those studied consists of 250 strings of 25 modules per inverter, which are 100 % exploited. 250 fixed double pole structures are chosen; each structure contains 2 strings. The total including facilities, transportation and installation is 375'500 €. To prevent the photovoltaic modules from shadow, the structures are separated by about 4 meters. Besides, since the inverter is an element that creates shadow, a central area is dedicated to this element, separated from the remaining modules and so as not to interrupt the paths between the various structures. A final element is the combiner box which has cables coming from its subfield strings at the input and larger cables in the inverter direction at the output. In this way there are fewer cables in the inverter's inputs which are limited to 24. In the plant there are 24 combiner boxes of two distinct sizes for an expense of 29'120 €. Their position on the central path, like that of the inverters, makes them easily accessible for maintenance. Moreover, inverters incorporate protective elements. To facilitate the study and correctly identify each string/cable, a nomenclature is presented. With the defined nomenclature the appropriate cables are studied to connect firstly the strings to the combiner boxes, secondly the combiner boxes to the inverter, and finally the mv stations to the medium voltage line. The total cost for cables and ducts is 496'526 €. To dig the ground where the cables are placed, 12'309 € is spent. In order to complete the technical analysis, the protective elements, (fuses and switches), and earthing are studied. It is verified that common grounding is possible. The grounding of the photovoltaic system requires 14'435 €. The total investment amounts to 3'112'592€. With the producibility study, an annual production of about 7,9 GWh is obtained. Starting from this data, the profitability of the photovoltaic system, with an estimated life of 25 years, is studied. From the analysis of the NPV, IRR, DPB economic indices it is noted that to recover the investment, with a discount rate of 6 %, it takes 15 years. Since the guaranteed life of the plant is 25 years, the remaining 10 produce profit.

Appendix A

This appendix presents in this order:

- 1) The main script “*Surface_leveling_volume*” (drawing the 3D surface, levelling and inclination of the area chosen for the photovoltaic installation, calculation of the volume to be exported, AutoCAD export).
- 2) The first auxiliary functions “*importfile*” necessary to import profiles data from excel to MATLAB.
- 3) The second auxiliary functions “*Datapreparation_perimeter*” transfers the soil profile and perimeter data of the plot into three spatial vectors x, y, z.
- 4) The third auxiliary functions “*Datapreparation_liveling*” transfers the perimeter data of area of interest into three spatial vectors x, y, z.

1) “*Surface_leveling_volume*”

```
clear all
close all
clc

load("Dataprofile_perimeter")

figure(1), plot3(x,y,z, '.')
xlabel('Latitude (m)');
ylabel('Longitude (m)');
zlabel('Elevation (m)');
title('Profiles');
delta_x=2.5; % meters
delta_y=2.5; % meters

xv = [
(floor(min(x)/delta_x)*delta_x):delta_x:(ceil(max(x)/delta_x)*delta_x)
];
yv = [
(floor(min(y)/delta_y)*delta_y):delta_y:(ceil(max(y)/delta_y)*delta_y)
];
[X,Y] = meshgrid(xv, yv);
Z = griddata(x,y,z,X,Y);

ridx=5;
ridy=5;
index1 = [1:ridx:size(X,1), size(X,1)];
index2 = [1:ridy:size(X,2), size(X,2)];
X_1 = X(index1,index2);
Y_1 = Y(index1,index2);
```

```
Z_1 = Z(index1,index2);

figure(2)
hold on
grid on
xlabel('Latitude (m)');
ylabel('Longitude (m)');
zlabel('Elevation (m)');
title('Plot number 806');
set(gca, 'ZLim',[0.99*min(z) 1.01*max(z)])

superficie1 = surf(X, Y, Z);
superficie1.EdgeColor = 'none';

superficie2 = surf(X_1, Y_1, Z_1);
superficie2.FaceColor = 'none';
superficie2.FaceLighting = 'none';

parcelEdge = plot3([x_c;x_c(1)], [y_c;y_c(1)], [z_c;z_c(1)], 'r');
parcelEdge.LineWidth = 5;

%% Livelining

load('Profile_data_1.mat')

dir=2; % '1' along a line ||| '2' along a column

[in,on] = inpolygon(X,Y,x_cl,y_cl);
inon=in|on;

figure(5), close(5)
figure(5), hold on
xlabel('Latitude (m)');
ylabel('Longitude (m)');
zlabel('Elevation (m)');
title('No leveled area')
superficie7 = surf(X, Y, Z);
superficie7.EdgeColor = 'none';

superficie8 = surf(X_1, Y_1, Z_1);
superficie8.FaceColor = 'none';
superficie8.FaceLighting = 'none';

parcelEdge = plot3([x_c;x_c(1)], [y_c;y_c(1)], [z_c;z_c(1)], 'r');
parcelEdge.LineWidth = 5;
parcelEdge =
plot3([x_cl;x_cl(1)], [y_cl;y_cl(1)], [z_cl;z_cl(1)], 'y');
parcelEdge.LineWidth = 5;
```

```

for k=1:size(Z,1)
    for h=1:size(Z,2)
        if inon(k,h) == 1
            Zcl(k,h) = Z(k,h);
        else
            Zcl(k,h) = NaN;
        end
    end
end

if dir == 1
    for k=1:size(Z,1)
        r=[0 0];
        for h=1:size(Z,2)
            if (isnan(Zcl(k,h)) == 0) && (r(1) == 0)
                r(1)=h;
            end
            if r(1) ~= 0
                if isnan(Zcl(k,h)) == 1
                    r(2)=h-1;
                end
            end
            if r(2) ~= 0
                Zcl(k,[r(1):r(2)]) = linspace( Zcl(k,r(1)),
Zcl(k,r(2)), r(2)-r(1)+1);
                inclinazione_x(k,1) = rad2deg(atan((Zcl(r(2),h) -
Zcl(r(1),h))./(r(2)-r(1))));
                r=[0 0];
            end
        end
        if (r(1) ~= 0) && (r(2) == 0)
            r(2)=h;
            Zcl(k,[r(1):r(2)]) = linspace( Zcl(k,r(1)), Zcl(k,r(2)),
r(2)-r(1)+1);
            inclinazione_x(k,1) = rad2deg(atan((Zcl(r(2),h) -
Zcl(r(1),h))./(r(2)-r(1))));
            r=[0 0];
        end
    end
elseif dir == 2
    for h=1:size(Z,2)
        r=[0 0];
        for k=1:size(Z,1)
            if (isnan(Zcl(k,h)) == 0) && (r(1) == 0)
                r(1)=k;
            end
            if r(1) ~= 0
                if isnan(Zcl(k,h)) == 1
                    r(2)=k-1;
                end
            end
        end
        if r(2) ~= 0

```

```

                Zcl([r(1):r(2)],h) = linspace( Zcl(r(1),h),
Zcl(r(2),h), r(2)-r(1)+1)';
                inclinazione_y(k,1) = rad2deg(atan((Zcl(r(2),h) -
Zcl(r(1),h))./(r(2)-r(1))));
                r=[0 0];
            end

        end
        if (r(1) ~= 0) && (r(2) == 0)
            r(2)=k;
            Zcl([r(1):r(2)],h) = linspace( Zcl(r(1),h), Zcl(r(2),h),
r(2)-r(1)+1)';
            inclinazione_y(k,1) = rad2deg(atan((Zcl(r(2),h) -
Zcl(r(1),h))./(r(2)-r(1))));
            r=[0 0];
        end
    end
end

Zcl_1 = Zcl(index1,index2);

figure(3), close(3)
figure(3), hold on
xlabel('Latitude (m)');
ylabel('Longitude (m)');
zlabel('Elevation (m)');
title('Leveled area');
superficie3 = surf(X, Y, Zcl);
superficie3.EdgeColor = 'none';

superficie4 = surf(X_1, Y_1, Zcl_1);
superficie4.FaceColor = 'none';
superficie4.FaceLighting = 'none';

parcelEdge =
plot3([x_cl;x_cl(1)],[y_cl;y_cl(1)],[z_cl;z_cl(1)],'y');
parcelEdge.LineWidth = 5;

Z1=NaN(size(Z));
for k=1:size(Z,1)
    for h=1:size(Z,2)
        if isnan(Zcl(k,h)) == 1
            Z1(k,h) = Z(k,h);
        else
            Z1(k,h) = Zcl(k,h);
        end
    end
end
end

Z1_1 = Z1(index1,index2);

figure(4), close(4)

```

```
figure(4), hold on
xlabel('Latitude (m)');
ylabel('Longitude (m)');
zlabel('Elevation (m)');
title('Leveled area')
superficie5 = surf(X, Y, Z1);
superficie5.EdgeColor = 'none';

superficie6 = surf(X_1, Y_1, Z1_1);
superficie6.FaceColor = 'none';
superficie6.FaceLighting = 'none';

parcelEdge = plot3([x_c;x_c(1)], [y_c;y_c(1)], [z_c;z_c(1)], 'r');
parcelEdge.LineWidth = 5;
parcelEdge =
plot3([x_cl;x_cl(1)], [y_cl;y_cl(1)], [z_cl;z_cl(1)], 'y');
parcelEdge.LineWidth = 5;

%% Volume calculation

% original surface
for k=1:size(Z,1)
    for h=1:size(Z,2)
        if isnan(Z(k,h)) == 0
            Zv(k,h) = Z(k,h);
        else
            Zv(k,h) = 0;
        end
    end
end
end
Volume_old = trapz(yv, trapz(xv, Zv, 2), 1)

% leveled surface
for k=1:size(Z1,1)
    for h=1:size(Z1,2)
        if isnan(Z1(k,h)) == 0
            Zv1(k,h) = Z1(k,h);
        else
            Zv1(k,h) = 0;
        end
    end
end
end
Volume_new = trapz(yv, trapz(xv, Zv1, 2), 1)

DeltaVolume = Volume_new - Volume_old

%% polilinea autocad

Aa=[x_cl;x_cl(1)];
```

```

Bb=[y_cl;y_cl(1)];
Cc=zeros(size(Aa));%[z_cl;z_cl(1)];

FID = dxf_open('polilinea2D.dxf');
dxf_polyline(FID,Aa,Bb,Cc);
dxf_close(FID);

```

2) “importfile”

```

function datosperfil0 = importfile(filename, startRow, endRow)
%IMPORTFILE1 Import numeric data from a text file as a matrix.
% DATOSPERFIL0 = IMPORTFILE1(FILENAME) Reads data from text file
FILENAME
% for the default selection.
%
% DATOSPERFIL0 = IMPORTFILE1(FILENAME, STARTROW, ENDROW) Reads
data from
% rows STARTROW through ENDROW of text file FILENAME.
%
% Example:
% datosperfil0 = importfile1('datos_perfil(0).csv', 2, 202);
%
% See also TEXTSCAN.

% Auto-generated by MATLAB on 2020/02/08 16:41:31

%% Initialize variables.
delimiter = {' ',';'};
if nargin<=2
    startRow = 2;
    endRow = inf;
end

%% Read columns of data as text:
% For more information, see the TEXTSCAN documentation.
formatSpec = '%*q%q%q%q%q%q%[\n\r]';

%% Open the text file.
fileID = fopen(filename,'r','n','UTF-8');
% Skip the BOM (Byte Order Mark).
fseek(fileID, 3, 'bof');

%% Read columns of data according to the format.
% This call is based on the structure of the file used to generate
this
% code. If an error occurs for a different file, try regenerating
the code
% from the Import Tool.
dataArray = textscan(fileID, formatSpec, endRow(1)-startRow(1)+1,
'Delimiter', delimiter, 'TextType', 'string', 'HeaderLines',
startRow(1)-1, 'ReturnOnError', false, 'EndOfLine', '\r\n');

```

```

for block=2:length(startRow)
    frewind(fileID);
    dataArrayBlock = textscan(fileID, formatSpec, endRow(block)-
startRow(block)+1, 'Delimiter', delimiter, 'TextType', 'string',
'HeaderLines', startRow(block)-1, 'ReturnOnError', false,
'EndOfLine', '\r\n');
    for col=1:length(dataArray)
        dataArray{col} = [dataArray{col};dataArrayBlock{col}];
    end
end

%% Close the text file.
fclose(fileID);

%% Convert the contents of columns containing numeric text to
numbers.
% Replace non-numeric text with NaN.
raw = repmat({''},length(dataArray{1}),length(dataArray)-1);
for col=1:length(dataArray)-1
    raw(1:length(dataArray{col}),col) = mat2cell(dataArray{col},
ones(length(dataArray{col}), 1));
end
numericData = NaN(size(dataArray{1},1),size(dataArray,2));

for col=[1,2,3,4]
    % Converts text in the input cell array to numbers. Replaced
non-numeric
    % text with NaN.
    rawData = dataArray{col};
    for row=1:size(rawData, 1)
        % Create a regular expression to detect and remove non-
numeric prefixes and
        % suffixes.
        regexstr = '(?<prefix>.*?)(?<numbers>([-
]*(\d+(\.)*)+[\,]{0,1}\d*[eEdD]{0,1}[-+]*\d*[i]{0,1})|([-
]*(\d+(\.)*)*[\,]{1,1}\d+[eEdD]{0,1}[-
+]*\d*[i]{0,1})) (?<suffix>.*)';
        try
            result = regexp(rawData(row), regexstr, 'names');
            numbers = result.numbers;

            % Detected commas in non-thousand locations.
            invalidThousandsSeparator = false;
            if numbers.contains('.')
                thousandsRegExp = '^([-
/+]*\d+?(\. \d{3})*\, {0,1}\d*$';
                if isempty(regexp(numbers, thousandsRegExp, 'once'))
                    numbers = NaN;
                    invalidThousandsSeparator = true;
                end
            end
        end
        % Convert numeric text to numbers.
        if ~invalidThousandsSeparator

```

```

        numbers = strrep(numbers, '.', '');
        numbers = strrep(numbers, ',', '.');
        numbers = textscan(char(numbers), '%f');
        numericData(row, col) = numbers{1};
        raw{row, col} = numbers{1};
    end
catch
    raw{row, col} = rawData{row};
end
end
end
end

```

```

%% Create output variable
datosperfil0 = table;
datosperfil0.x_25830 = cell2mat(raw(:, 1));
datosperfil0.y_25830 = cell2mat(raw(:, 2));
datosperfil0.dist_origen_m = cell2mat(raw(:, 3));
datosperfil0.altura_m = cell2mat(raw(:, 4));

```

3) "Datapreparation_perimeter"

```

clear all
close all
clc

temp_import = importfile("datos_perfil.csv",2,inf)

x = temp_import.x_25830;
y = temp_import.y_25830;
z = temp_import.altura_m;
x_c = temp_import.x_25830;
y_c = temp_import.y_25830;
z_c = temp_import.altura_m;

for k=1:36
    clear temp_import
    num = int2str(k);
    filename = strcat("datos_perfil(",num,").csv")
    temp_import = importfile(filename,2,inf)

    x = [x ; temp_import.x_25830];
    y = [y ; temp_import.y_25830];
    z = [z ; temp_import.altura_m];

end

save Dataprofile_perimeter x y z x_c y_c z_c

```

4) "Datapreparation_liveling"

```
clear all
close all
clc

temp_import = importfile("Profile_data.csv",2,inf)

x_cl = temp_import.x_25830;
y_cl = temp_import.y_25830;
z_cl = temp_import.altura_m;

save Profile_data_1 x_cl y_cl z_cl
```

Appendix B

This appendix shows the calculations necessary for the choice of electrical cables in the module-combiner box section.

To calculate the resistance value, reported to 90 °C, the following formula is used:

$$r_{90} = r_{20}(1 + \alpha \cdot \Delta T) \quad (106)$$

Where:

- r_{20} is the resistance of the cable, at 20 °C
- $\alpha = 0,00393 K^{-1}$
- $\Delta T = 70 K$

It is verified that the maximum open circuit voltage of the string is lower than the maximum tension of the cables:

$$1391 V < 1800 V$$

1. Electrical criterion

STRINGS		I _{mppt} (A)	V _{mppt} (V)	N (modules)	L1 (m)	S1 (mm ²)	r (Ω/km)	r ₉₀ (Ω/km)	ΔV ₁ (%)	L2 (m)	ΔV ₂ (%)	L3 (m)	ΔV ₃ (%)	ΔV (%)
A.01.a.1	B.01.a.1	9,74	41,1	25	5	4	5,09	6,49	0,062	10,625	0,065	30	0,185	0,311
A.01.a.2	B.01.a.2	9,74	41,1	25	5	4	5,09	6,49	0,062	10,625	0,065	30	0,185	0,311
A.01.b.1	B.01.b.1	9,74	41,1	25	35	10	1,95	2,49	0,165	10,625	0,065	30	0,071	0,301
A.01.b.2	B.01.b.2	9,74	41,1	25	35	10	1,95	2,49	0,165	10,625	0,065	30	0,071	0,301
A.01.c.1	B.01.c.1	9,74	41,1	25	65	10	1,95	2,49	0,306	10,625	0,065	30	0,071	0,442
A.01.c.2	B.01.c.2	9,74	41,1	25	65	10	1,95	2,49	0,306	10,625	0,065	30	0,071	0,442
A.01.e.1	B.01.e.1	9,74	41,1	25	15	6	3,39	4,32	0,123	10,625	0,065	30	0,123	0,311
A.01.e.2	B.01.e.2	9,74	41,1	25	15	6	3,39	4,32	0,123	10,625	0,065	30	0,123	0,311
A.01.f.1	B.01.f.1	9,74	41,1	25	45	10	1,95	2,49	0,212	10,625	0,065	30	0,071	0,348
A.01.f.2	B.01.f.2	9,74	41,1	25	45	10	1,95	2,49	0,212	10,625	0,065	30	0,071	0,348
A.01.g.1	B.01.g.1	9,74	41,1	25	75	16	1,24	1,58	0,225	10,625	0,065	30	0,045	0,335
A.01.g.2	B.01.g.2	9,74	41,1	25	75	16	1,24	1,58	0,225	10,625	0,065	30	0,045	0,335
A.01.l.1	B.01.l.1	9,74	41,1	25	25	6	3,39	4,32	0,205	10,625	0,065	30	0,123	0,393
A.01.l.2	B.01.l.2	9,74	41,1	25	25	6	3,39	4,32	0,205	10,625	0,065	30	0,123	0,393
A.01.m.1	B.01.m.1	9,74	41,1	25	55	10	1,95	2,49	0,259	10,625	0,065	30	0,071	0,395
A.01.m.2	B.01.m.2	9,74	41,1	25	55	10	1,95	2,49	0,259	10,625	0,065	30	0,071	0,395
A.02.a.1	B.02.a.1	9,74	41,1	25	5	4	5,09	6,49	0,062	10,625	0,065	30	0,185	0,311
A.02.a.2	B.02.a.2	9,74	41,1	25	5	4	5,09	6,49	0,062	10,625	0,065	30	0,185	0,311
A.02.b.1	B.02.b.1	9,74	41,1	25	35	10	1,95	2,49	0,165	10,625	0,065	30	0,071	0,301
A.02.b.2	B.02.b.2	9,74	41,1	25	35	10	1,95	2,49	0,165	10,625	0,065	30	0,071	0,301
A.02.c.1	B.02.c.1	9,74	41,1	25	65	10	1,95	2,49	0,306	10,625	0,065	30	0,071	0,442
A.02.c.2	B.02.c.2	9,74	41,1	25	65	10	1,95	2,49	0,306	10,625	0,065	30	0,071	0,442
A.02.d.1	B.02.d.1	9,74	41,1	25	95	16	1,24	1,58	0,285	10,625	0,065	30	0,045	0,395
A.02.d.2	B.02.d.2	9,74	41,1	25	95	16	1,24	1,58	0,285	10,625	0,065	30	0,045	0,395
A.02.e.1	B.02.e.1	9,74	41,1	25	15	6	3,39	4,32	0,123	10,625	0,065	30	0,123	0,311
A.02.e.2	B.02.e.2	9,74	41,1	25	15	6	3,39	4,32	0,123	10,625	0,065	30	0,123	0,311
A.02.f.1	B.02.f.1	9,74	41,1	25	45	10	1,95	2,49	0,212	10,625	0,065	30	0,071	0,348
A.02.f.2	B.02.f.2	9,74	41,1	25	45	10	1,95	2,49	0,212	10,625	0,065	30	0,071	0,348
A.02.g.1	B.02.g.1	9,74	41,1	25	75	16	1,24	1,58	0,225	10,625	0,065	30	0,045	0,335
A.02.g.2	B.02.g.2	9,74	41,1	25	75	16	1,24	1,58	0,225	10,625	0,065	30	0,045	0,335
A.02.h.1	B.02.h.1	9,74	41,1	25	105	16	1,24	1,58	0,315	10,625	0,065	30	0,045	0,425
A.02.h.2	B.02.h.2	9,74	41,1	25	105	16	1,24	1,58	0,315	10,625	0,065	30	0,045	0,425

Trabajo Fin de Máster – Appendix B

STRINGS		I _{mppt} (A)	V _{mppt} (V)	N (modules)	L1 (m)	S1 (mm ²)	r (Ω/km)	r ₉₀ (Ω/km)	ΔV ₁ (%)	L2 (m)	ΔV ₂ (%)	L3 (m)	ΔV ₃ (%)	ΔV (%)
A.03.a.1	B.03.a.1	9,74	41,1	25	5	4	5,09	6,49	0,062	10,625	0,065	30	0,185	0,311
A.03.a.2	B.03.a.2	9,74	41,1	25	5	4	5,09	6,49	0,062	10,625	0,065	30	0,185	0,311
A.03.b.1	B.03.b.1	9,74	41,1	25	35	10	1,95	2,49	0,165	10,625	0,065	30	0,071	0,301
A.03.b.2	B.03.b.2	9,74	41,1	25	35	10	1,95	2,49	0,165	10,625	0,065	30	0,071	0,301
A.03.c.1	B.03.c.1	9,74	41,1	25	65	10	1,95	2,49	0,306	10,625	0,065	30	0,071	0,442
A.03.c.2	B.03.c.2	9,74	41,1	25	65	10	1,95	2,49	0,306	10,625	0,065	30	0,071	0,442
A.03.d.1	B.03.d.1	9,74	41,1	25	95	16	1,24	1,58	0,285	10,625	0,065	30	0,045	0,395
A.03.d.2	B.03.d.2	9,74	41,1	25	95	16	1,24	1,58	0,285	10,625	0,065	30	0,045	0,395
A.03.e.1	B.03.e.1	9,74	41,1	25	15	6	3,39	4,32	0,123	10,625	0,065	30	0,123	0,311
A.03.e.2	B.03.e.2	9,74	41,1	25	15	6	3,39	4,32	0,123	10,625	0,065	30	0,123	0,311
A.03.f.1	B.03.f.1	9,74	41,1	25	45	10	1,95	2,49	0,212	10,625	0,065	30	0,071	0,348
A.03.f.2	B.03.f.2	9,74	41,1	25	45	10	1,95	2,49	0,212	10,625	0,065	30	0,071	0,348
A.03.g.1	B.03.g.1	9,74	41,1	25	75	16	1,24	1,58	0,225	10,625	0,065	30	0,045	0,335
A.03.g.2	B.03.g.2	9,74	41,1	25	75	16	1,24	1,58	0,225	10,625	0,065	30	0,045	0,335
A.03.h.1	B.03.h.1	9,74	41,1	25	105	16	1,24	1,58	0,315	10,625	0,065	30	0,045	0,425
A.03.h.2	B.03.h.2	9,74	41,1	25	105	16	1,24	1,58	0,315	10,625	0,065	30	0,045	0,425
A.03.l.1	B.03.l.1	9,74	41,1	25	25	6	3,39	4,32	0,205	10,625	0,065	30	0,123	0,393
A.03.l.2	B.03.l.2	9,74	41,1	25	25	6	3,39	4,32	0,205	10,625	0,065	30	0,123	0,393
A.03.m.1	B.03.m.1	9,74	41,1	25	55	10	1,95	2,49	0,259	10,625	0,065	30	0,071	0,395
A.03.m.2	B.03.m.2	9,74	41,1	25	55	10	1,95	2,49	0,259	10,625	0,065	30	0,071	0,395
A.03.n.1	B.03.n.1	9,74	41,1	25	85	16	1,24	1,58	0,255	10,625	0,065	30	0,045	0,365
A.03.n.2	B.03.n.2	9,74	41,1	25	85	16	1,24	1,58	0,255	10,625	0,065	30	0,045	0,365
A.03.o.1	B.03.o.1	9,74	41,1	25	115	16	1,24	1,58	0,345	10,625	0,065	30	0,045	0,455
A.03.o.2	B.03.o.2	9,74	41,1	25	115	16	1,24	1,58	0,345	10,625	0,065	30	0,045	0,455
A.04.a.1	B.04.a.1	9,74	41,1	25	5	4	5,09	6,49	0,062	10,625	0,065	30	0,185	0,311
A.04.a.2	B.04.a.2	9,74	41,1	25	5	4	5,09	6,49	0,062	10,625	0,065	30	0,185	0,311
A.04.b.1	B.04.b.1	9,74	41,1	25	35	10	1,95	2,49	0,165	10,625	0,065	30	0,071	0,301
A.04.b.2	B.04.b.2	9,74	41,1	25	35	10	1,95	2,49	0,165	10,625	0,065	30	0,071	0,301
A.04.c.1	B.04.c.1	9,74	41,1	25	65	10	1,95	2,49	0,306	10,625	0,065	30	0,071	0,442
A.04.c.2	B.04.c.2	9,74	41,1	25	65	10	1,95	2,49	0,306	10,625	0,065	30	0,071	0,442
A.04.d.1	B.04.d.1	9,74	41,1	25	95	16	1,24	1,58	0,285	10,625	0,065	30	0,045	0,395
A.04.d.2	B.04.d.2	9,74	41,1	25	95	16	1,24	1,58	0,285	10,625	0,065	30	0,045	0,395
A.04.e.1	B.04.e.1	9,74	41,1	25	15	6	3,39	4,32	0,123	10,625	0,065	30	0,123	0,311
A.04.e.2	B.04.e.2	9,74	41,1	25	15	6	3,39	4,32	0,123	10,625	0,065	30	0,123	0,311
A.04.f.1	B.04.f.1	9,74	41,1	25	45	10	1,95	2,49	0,212	10,625	0,065	30	0,071	0,348
A.04.f.2	B.04.f.2	9,74	41,1	25	45	10	1,95	2,49	0,212	10,625	0,065	30	0,071	0,348
A.04.g.1	B.04.g.1	9,74	41,1	25	75	16	1,24	1,58	0,225	10,625	0,065	30	0,045	0,335
A.04.g.2	B.04.g.2	9,74	41,1	25	75	16	1,24	1,58	0,225	10,625	0,065	30	0,045	0,335
A.04.h.1	B.04.h.1	9,74	41,1	25	105	16	1,24	1,58	0,315	10,625	0,065	30	0,045	0,425
A.04.h.2	B.04.h.2	9,74	41,1	25	105	16	1,24	1,58	0,315	10,625	0,065	30	0,045	0,425
A.04.l.1	B.04.l.1	9,74	41,1	25	25	6	3,39	4,32	0,205	10,625	0,065	30	0,123	0,393
A.04.l.2	B.04.l.2	9,74	41,1	25	25	6	3,39	4,32	0,205	10,625	0,065	30	0,123	0,393
A.04.m.1	B.04.m.1	9,74	41,1	25	55	10	1,95	2,49	0,259	10,625	0,065	30	0,071	0,395
A.04.m.2	B.04.m.2	9,74	41,1	25	55	10	1,95	2,49	0,259	10,625	0,065	30	0,071	0,395
A.04.n.1	B.04.n.1	9,74	41,1	25	85	16	1,24	1,58	0,255	10,625	0,065	30	0,045	0,365
A.04.n.2	B.04.n.2	9,74	41,1	25	85	16	1,24	1,58	0,255	10,625	0,065	30	0,045	0,365
A.04.o.1	B.04.o.1	9,74	41,1	25	115	16	1,24	1,58	0,345	10,625	0,065	30	0,045	0,455
A.04.o.2	B.04.o.2	9,74	41,1	25	115	16	1,24	1,58	0,345	10,625	0,065	30	0,045	0,455

Trabajo Fin de Máster – Appendix B

STRINGS		I _{mppt} (A)	V _{mppt} (V)	N (modules)	L1 (m)	S1 (mm ²)	r (Ω/km)	r ₉₀ (Ω/km)	ΔV ₁ (%)	L2 (m)	ΔV ₂ (%)	L3 (m)	ΔV ₃ (%)	ΔV (%)
A.05.a.1	B.05.a.1	9,74	41,1	25	5	4	5,09	6,49	0,062	10,625	0,065	30	0,185	0,311
A.05.a.2	B.05.a.2	9,74	41,1	25	5	4	5,09	6,49	0,062	10,625	0,065	30	0,185	0,311
A.05.b.1	B.05.b.1	9,74	41,1	25	35	10	1,95	2,49	0,165	10,625	0,065	30	0,071	0,301
A.05.b.2	B.05.b.2	9,74	41,1	25	35	10	1,95	2,49	0,165	10,625	0,065	30	0,071	0,301
A.05.c.1	B.05.c.1	9,74	41,1	25	65	10	1,95	2,49	0,306	10,625	0,065	30	0,071	0,442
A.05.c.2	B.05.c.2	9,74	41,1	25	65	10	1,95	2,49	0,306	10,625	0,065	30	0,071	0,442
A.05.d.1	B.05.d.1	9,74	41,1	25	95	16	1,24	1,58	0,285	10,625	0,065	30	0,045	0,395
A.05.d.2	B.05.d.2	9,74	41,1	25	95	16	1,24	1,58	0,285	10,625	0,065	30	0,045	0,395
A.05.e.1	B.05.e.1	9,74	41,1	25	15	6	3,39	4,32	0,123	10,625	0,065	30	0,123	0,311
A.05.e.2	B.05.e.2	9,74	41,1	25	15	6	3,39	4,32	0,123	10,625	0,065	30	0,123	0,311
A.05.f.1	B.05.f.1	9,74	41,1	25	45	10	1,95	2,49	0,212	10,625	0,065	30	0,071	0,348
A.05.f.2	B.05.f.2	9,74	41,1	25	45	10	1,95	2,49	0,212	10,625	0,065	30	0,071	0,348
A.05.g.1	B.05.g.1	9,74	41,1	25	75	16	1,24	1,58	0,225	10,625	0,065	30	0,045	0,335
A.05.g.2	B.05.g.2	9,74	41,1	25	75	16	1,24	1,58	0,225	10,625	0,065	30	0,045	0,335
A.05.h.1	B.05.h.1	9,74	41,1	25	105	16	1,24	1,58	0,315	10,625	0,065	30	0,045	0,425
A.05.h.2	B.05.h.2	9,74	41,1	25	105	16	1,24	1,58	0,315	10,625	0,065	30	0,045	0,425
A.05.l.1	B.05.l.1	9,74	41,1	25	25	6	3,39	4,32	0,205	10,625	0,065	30	0,123	0,393
A.05.l.2	B.05.l.2	9,74	41,1	25	25	6	3,39	4,32	0,205	10,625	0,065	30	0,123	0,393
A.05.m.1	B.05.m.1	9,74	41,1	25	55	10	1,95	2,49	0,259	10,625	0,065	30	0,071	0,395
A.05.m.2	B.05.m.2	9,74	41,1	25	55	10	1,95	2,49	0,259	10,625	0,065	30	0,071	0,395
A.05.n.1	B.05.n.1	9,74	41,1	25	85	16	1,24	1,58	0,255	10,625	0,065	30	0,045	0,365
A.05.n.2	B.05.n.2	9,74	41,1	25	85	16	1,24	1,58	0,255	10,625	0,065	30	0,045	0,365
A.05.o.1	B.05.o.1	9,74	41,1	25	115	16	1,24	1,58	0,345	10,625	0,065	30	0,045	0,455
A.05.o.2	B.05.o.2	9,74	41,1	25	115	16	1,24	1,58	0,345	10,625	0,065	30	0,045	0,455
A.06.a.1	B.06.a.1	9,74	41,1	25	5	4	5,09	6,49	0,062	10,625	0,065	30	0,185	0,311
A.06.a.2	B.06.a.2	9,74	41,1	25	5	4	5,09	6,49	0,062	10,625	0,065	30	0,185	0,311
A.06.b.1	B.06.b.1	9,74	41,1	25	35	10	1,95	2,49	0,165	10,625	0,065	30	0,071	0,301
A.06.b.2	B.06.b.2	9,74	41,1	25	35	10	1,95	2,49	0,165	10,625	0,065	30	0,071	0,301
A.06.c.1	B.06.c.1	9,74	41,1	25	65	10	1,95	2,49	0,306	10,625	0,065	30	0,071	0,442
A.06.c.2	B.06.c.2	9,74	41,1	25	65	10	1,95	2,49	0,306	10,625	0,065	30	0,071	0,442
A.06.d.1	B.06.d.1	9,74	41,1	25	95	16	1,24	1,58	0,285	10,625	0,065	30	0,045	0,395
A.06.d.2	B.06.d.2	9,74	41,1	25	95	16	1,24	1,58	0,285	10,625	0,065	30	0,045	0,395
A.06.e.1	B.06.e.1	9,74	41,1	25	15	6	3,39	4,32	0,123	10,625	0,065	30	0,123	0,311
A.06.e.2	B.06.e.2	9,74	41,1	25	15	6	3,39	4,32	0,123	10,625	0,065	30	0,123	0,311
A.06.f.1	B.06.f.1	9,74	41,1	25	45	10	1,95	2,49	0,212	10,625	0,065	30	0,071	0,348
A.06.f.2	B.06.f.2	9,74	41,1	25	45	10	1,95	2,49	0,212	10,625	0,065	30	0,071	0,348
A.06.g.1	B.06.g.1	9,74	41,1	25	75	16	1,24	1,58	0,225	10,625	0,065	30	0,045	0,335
A.06.g.2	B.06.g.2	9,74	41,1	25	75	16	1,24	1,58	0,225	10,625	0,065	30	0,045	0,335
A.06.h.1	B.06.h.1	9,74	41,1	25	105	16	1,24	1,58	0,315	10,625	0,065	30	0,045	0,425
A.06.h.2	B.06.h.2	9,74	41,1	25	105	16	1,24	1,58	0,315	10,625	0,065	30	0,045	0,425
A.06.l.1	B.06.l.1	9,74	41,1	25	25	6	3,39	4,32	0,205	10,625	0,065	30	0,123	0,393
A.06.l.2	B.06.l.2	9,74	41,1	25	25	6	3,39	4,32	0,205	10,625	0,065	30	0,123	0,393
A.06.m.1	B.06.m.1	9,74	41,1	25	55	10	1,95	2,49	0,259	10,625	0,065	30	0,071	0,395
A.06.m.2	B.06.m.2	9,74	41,1	25	55	10	1,95	2,49	0,259	10,625	0,065	30	0,071	0,395
A.06.n.1	B.06.n.1	9,74	41,1	25	85	16	1,24	1,58	0,255	10,625	0,065	30	0,045	0,365
A.06.n.2	B.06.n.2	9,74	41,1	25	85	16	1,24	1,58	0,255	10,625	0,065	30	0,045	0,365
A.06.o.1	B.06.o.1	9,74	41,1	25	115	16	1,24	1,58	0,345	10,625	0,065	30	0,045	0,455
A.06.o.2	B.06.o.2	9,74	41,1	25	115	16	1,24	1,58	0,345	10,625	0,065	30	0,045	0,455

Trabajo Fin de Máster – Appendix B

STRINGS		I _{mppt} (A)	V _{mppt} (V)	N (modules)	L1 (m)	S1 (mm ²)	r (Ω/km)	r ₉₀ (Ω/km)	ΔV ₁ (%)	L2 (m)	ΔV ₂ (%)	L3 (m)	ΔV ₃ (%)	ΔV (%)
A.07.a.1	B.07.a.1	9,74	41,1	25	5	4	5,09	6,49	0,062	10,625	0,065	30	0,185	0,311
A.07.a.2	B.07.a.2	9,74	41,1	25	5	4	5,09	6,49	0,062	10,625	0,065	30	0,185	0,311
A.07.b.1	B.07.b.1	9,74	41,1	25	35	10	1,95	2,49	0,165	10,625	0,065	30	0,071	0,301
A.07.b.2	B.07.b.2	9,74	41,1	25	35	10	1,95	2,49	0,165	10,625	0,065	30	0,071	0,301
A.07.c.1	B.07.c.1	9,74	41,1	25	65	10	1,95	2,49	0,306	10,625	0,065	30	0,071	0,442
A.07.c.2	B.07.c.2	9,74	41,1	25	65	10	1,95	2,49	0,306	10,625	0,065	30	0,071	0,442
A.07.d.1	B.07.d.1	9,74	41,1	25	95	16	1,24	1,58	0,285	10,625	0,065	30	0,045	0,395
A.07.d.2	B.07.d.2	9,74	41,1	25	95	16	1,24	1,58	0,285	10,625	0,065	30	0,045	0,395
A.07.e.1	B.07.e.1	9,74	41,1	25	15	6	3,39	4,32	0,123	10,625	0,065	30	0,123	0,311
A.07.e.2	B.07.e.2	9,74	41,1	25	15	6	3,39	4,32	0,123	10,625	0,065	30	0,123	0,311
A.07.f.1	B.07.f.1	9,74	41,1	25	45	10	1,95	2,49	0,212	10,625	0,065	30	0,071	0,348
A.07.f.2	B.07.f.2	9,74	41,1	25	45	10	1,95	2,49	0,212	10,625	0,065	30	0,071	0,348
A.07.g.1	B.07.g.1	9,74	41,1	25	75	16	1,24	1,58	0,225	10,625	0,065	30	0,045	0,335
A.07.g.2	B.07.g.2	9,74	41,1	25	75	16	1,24	1,58	0,225	10,625	0,065	30	0,045	0,335
A.07.h.1	B.07.h.1	9,74	41,1	25	105	16	1,24	1,58	0,315	10,625	0,065	30	0,045	0,425
A.07.h.2	B.07.h.2	9,74	41,1	25	105	16	1,24	1,58	0,315	10,625	0,065	30	0,045	0,425
A.07.l.1	B.07.l.1	9,74	41,1	25	25	6	3,39	4,32	0,205	10,625	0,065	30	0,123	0,393
A.07.l.2	B.07.l.2	9,74	41,1	25	25	6	3,39	4,32	0,205	10,625	0,065	30	0,123	0,393
A.07.m.1	B.07.m.1	9,74	41,1	25	55	10	1,95	2,49	0,259	10,625	0,065	30	0,071	0,395
A.07.m.2	B.07.m.2	9,74	41,1	25	55	10	1,95	2,49	0,259	10,625	0,065	30	0,071	0,395
A.07.n.1	B.07.n.1	9,74	41,1	25	85	16	1,24	1,58	0,255	10,625	0,065	30	0,045	0,365
A.07.n.2	B.07.n.2	9,74	41,1	25	85	16	1,24	1,58	0,255	10,625	0,065	30	0,045	0,365
A.07.o.1	B.07.o.1	9,74	41,1	25	115	16	1,24	1,58	0,345	10,625	0,065	30	0,045	0,455
A.07.o.2	B.07.o.2	9,74	41,1	25	115	16	1,24	1,58	0,345	10,625	0,065	30	0,045	0,455
A.08.a.1	B.08.a.1	9,74	41,1	25	5	4	5,09	6,49	0,062	10,625	0,065	30	0,185	0,311
A.08.a.2	B.08.a.2	9,74	41,1	25	5	4	5,09	6,49	0,062	10,625	0,065	30	0,185	0,311
A.08.b.1	B.08.b.1	9,74	41,1	25	35	10	1,95	2,49	0,165	10,625	0,065	30	0,071	0,301
A.08.b.2	B.08.b.2	9,74	41,1	25	35	10	1,95	2,49	0,165	10,625	0,065	30	0,071	0,301
A.08.c.1	B.08.c.1	9,74	41,1	25	65	10	1,95	2,49	0,306	10,625	0,065	30	0,071	0,442
A.08.c.2	B.08.c.2	9,74	41,1	25	65	10	1,95	2,49	0,306	10,625	0,065	30	0,071	0,442
A.08.d.1	B.08.d.1	9,74	41,1	25	95	16	1,24	1,58	0,285	10,625	0,065	30	0,045	0,395
A.08.d.2	B.08.d.2	9,74	41,1	25	95	16	1,24	1,58	0,285	10,625	0,065	30	0,045	0,395
A.08.e.1	B.08.e.1	9,74	41,1	25	15	6	3,39	4,32	0,123	10,625	0,065	30	0,123	0,311
A.08.e.2	B.08.e.2	9,74	41,1	25	15	6	3,39	4,32	0,123	10,625	0,065	30	0,123	0,311
A.08.f.1	B.08.f.1	9,74	41,1	25	45	10	1,95	2,49	0,212	10,625	0,065	30	0,071	0,348
A.08.f.2	B.08.f.2	9,74	41,1	25	45	10	1,95	2,49	0,212	10,625	0,065	30	0,071	0,348
A.08.g.1	B.08.g.1	9,74	41,1	25	75	16	1,24	1,58	0,225	10,625	0,065	30	0,045	0,335
A.08.g.2	B.08.g.2	9,74	41,1	25	75	16	1,24	1,58	0,225	10,625	0,065	30	0,045	0,335
A.08.h.1	B.08.h.1	9,74	41,1	25	105	16	1,24	1,58	0,315	10,625	0,065	30	0,045	0,425
A.08.h.2	B.08.h.2	9,74	41,1	25	105	16	1,24	1,58	0,315	10,625	0,065	30	0,045	0,425
A.08.l.1	B.08.l.1	9,74	41,1	25	25	6	3,39	4,32	0,205	10,625	0,065	30	0,123	0,393
A.08.l.2	B.08.l.2	9,74	41,1	25	25	6	3,39	4,32	0,205	10,625	0,065	30	0,123	0,393
A.08.m.1	B.08.m.1	9,74	41,1	25	55	10	1,95	2,49	0,259	10,625	0,065	30	0,071	0,395
A.08.m.2	B.08.m.2	9,74	41,1	25	55	10	1,95	2,49	0,259	10,625	0,065	30	0,071	0,395
A.08.n.1	B.08.n.1	9,74	41,1	25	85	16	1,24	1,58	0,255	10,625	0,065	30	0,045	0,365
A.08.n.2	B.08.n.2	9,74	41,1	25	85	16	1,24	1,58	0,255	10,625	0,065	30	0,045	0,365
A.08.o.1	B.08.o.1	9,74	41,1	25	115	16	1,24	1,58	0,345	10,625	0,065	30	0,045	0,455
A.08.o.2	B.08.o.2	9,74	41,1	25	115	16	1,24	1,58	0,345	10,625	0,065	30	0,045	0,455

Trabajo Fin de Máster – Appendix B

STRINGS		I _{mppt} (A)	V _{mppt} (V)	N (modules)	L1 (m)	S1 (mm ²)	r (Ω/km)	r ₉₀ (Ω/km)	ΔV ₁ (%)	L2 (m)	ΔV ₂ (%)	L3 (m)	ΔV ₃ (%)	ΔV (%)
A.09.a.1	B.09.a.1	9,74	41,1	25	5	4	5,09	6,49	0,062	10,625	0,065	30	0,185	0,311
A.09.a.2	B.09.a.2	9,74	41,1	25	5	4	5,09	6,49	0,062	10,625	0,065	30	0,185	0,311
A.09.b.1	B.09.b.1	9,74	41,1	25	35	10	1,95	2,49	0,165	10,625	0,065	30	0,071	0,301
A.09.b.2	B.09.b.2	9,74	41,1	25	35	10	1,95	2,49	0,165	10,625	0,065	30	0,071	0,301
A.09.c.1	B.09.c.1	9,74	41,1	25	65	10	1,95	2,49	0,306	10,625	0,065	30	0,071	0,442
A.09.c.2	B.09.c.2	9,74	41,1	25	65	10	1,95	2,49	0,306	10,625	0,065	30	0,071	0,442
A.09.d.1	B.09.d.1	9,74	41,1	25	95	16	1,24	1,58	0,285	10,625	0,065	30	0,045	0,395
A.09.d.2	B.09.d.2	9,74	41,1	25	95	16	1,24	1,58	0,285	10,625	0,065	30	0,045	0,395
A.09.e.1	B.09.e.1	9,74	41,1	25	15	6	3,39	4,32	0,123	10,625	0,065	30	0,123	0,311
A.09.e.2	B.09.e.2	9,74	41,1	25	15	6	3,39	4,32	0,123	10,625	0,065	30	0,123	0,311
A.09.f.1	B.09.f.1	9,74	41,1	25	45	10	1,95	2,49	0,212	10,625	0,065	30	0,071	0,348
A.09.f.2	B.09.f.2	9,74	41,1	25	45	10	1,95	2,49	0,212	10,625	0,065	30	0,071	0,348
A.09.g.1	B.09.g.1	9,74	41,1	25	75	16	1,24	1,58	0,225	10,625	0,065	30	0,045	0,335
A.09.g.2	B.09.g.2	9,74	41,1	25	75	16	1,24	1,58	0,225	10,625	0,065	30	0,045	0,335
A.09.h.1	B.09.h.1	9,74	41,1	25	105	16	1,24	1,58	0,315	10,625	0,065	30	0,045	0,425
A.09.h.2	B.09.h.2	9,74	41,1	25	105	16	1,24	1,58	0,315	10,625	0,065	30	0,045	0,425
A.09.l.1	B.09.l.1	9,74	41,1	25	25	6	3,39	4,32	0,205	10,625	0,065	30	0,123	0,393
A.09.l.2	B.09.l.2	9,74	41,1	25	25	6	3,39	4,32	0,205	10,625	0,065	30	0,123	0,393
A.09.m.1	B.09.m.1	9,74	41,1	25	55	10	1,95	2,49	0,259	10,625	0,065	30	0,071	0,395
A.09.m.2	B.09.m.2	9,74	41,1	25	55	10	1,95	2,49	0,259	10,625	0,065	30	0,071	0,395
A.09.n.1	B.09.n.1	9,74	41,1	25	85	16	1,24	1,58	0,255	10,625	0,065	30	0,045	0,365
A.09.n.2	B.09.n.2	9,74	41,1	25	85	16	1,24	1,58	0,255	10,625	0,065	30	0,045	0,365
A.09.o.1	B.09.o.1	9,74	41,1	25	115	16	1,24	1,58	0,345	10,625	0,065	30	0,045	0,455
A.09.o.2	B.09.o.2	9,74	41,1	25	115	16	1,24	1,58	0,345	10,625	0,065	30	0,045	0,455
A.10.a.1	B.10.a.1	9,74	41,1	25	5	4	5,09	6,49	0,062	10,625	0,065	30	0,185	0,311
A.10.a.2	B.10.a.2	9,74	41,1	25	5	4	5,09	6,49	0,062	10,625	0,065	30	0,185	0,311
A.10.b.1	B.10.b.1	9,74	41,1	25	35	10	1,95	2,49	0,165	10,625	0,065	30	0,071	0,301
A.10.b.2	B.10.b.2	9,74	41,1	25	35	10	1,95	2,49	0,165	10,625	0,065	30	0,071	0,301
A.10.c.1	B.10.c.1	9,74	41,1	25	65	10	1,95	2,49	0,306	10,625	0,065	30	0,071	0,442
A.10.c.2	B.10.c.2	9,74	41,1	25	65	10	1,95	2,49	0,306	10,625	0,065	30	0,071	0,442
A.10.d.1	B.10.d.1	9,74	41,1	25	95	16	1,24	1,58	0,285	10,625	0,065	30	0,045	0,395
A.10.d.2	B.10.d.2	9,74	41,1	25	95	16	1,24	1,58	0,285	10,625	0,065	30	0,045	0,395
A.10.e.1	B.10.e.1	9,74	41,1	25	15	6	3,39	4,32	0,123	10,625	0,065	30	0,123	0,311
A.10.e.2	B.10.e.2	9,74	41,1	25	15	6	3,39	4,32	0,123	10,625	0,065	30	0,123	0,311
A.10.f.1	B.10.f.1	9,74	41,1	25	45	10	1,95	2,49	0,212	10,625	0,065	30	0,071	0,348
A.10.f.2	B.10.f.2	9,74	41,1	25	45	10	1,95	2,49	0,212	10,625	0,065	30	0,071	0,348
A.10.g.1	B.10.g.1	9,74	41,1	25	75	16	1,24	1,58	0,225	10,625	0,065	30	0,045	0,335
A.10.g.2	B.10.g.2	9,74	41,1	25	75	16	1,24	1,58	0,225	10,625	0,065	30	0,045	0,335
A.10.h.1	B.10.h.1	9,74	41,1	25	105	16	1,24	1,58	0,315	10,625	0,065	30	0,045	0,425
A.10.h.2	B.10.h.2	9,74	41,1	25	105	16	1,24	1,58	0,315	10,625	0,065	30	0,045	0,425
A.10.l.1	B.10.l.1	9,74	41,1	25	25	6	3,39	4,32	0,205	10,625	0,065	30	0,123	0,393
A.10.l.2	B.10.l.2	9,74	41,1	25	25	6	3,39	4,32	0,205	10,625	0,065	30	0,123	0,393
A.10.m.1	B.10.m.1	9,74	41,1	25	55	10	1,95	2,49	0,259	10,625	0,065	30	0,071	0,395
A.10.m.2	B.10.m.2	9,74	41,1	25	55	10	1,95	2,49	0,259	10,625	0,065	30	0,071	0,395
A.10.n.1	B.10.n.1	9,74	41,1	25	85	16	1,24	1,58	0,255	10,625	0,065	30	0,045	0,365
A.10.n.2	B.10.n.2	9,74	41,1	25	85	16	1,24	1,58	0,255	10,625	0,065	30	0,045	0,365
A.10.o.1	B.10.o.1	9,74	41,1	25	115	16	1,24	1,58	0,345	10,625	0,065	30	0,045	0,455
A.10.o.2	B.10.o.2	9,74	41,1	25	115	16	1,24	1,58	0,345	10,625	0,065	30	0,045	0,455

STRINGS		I _{mppt} (A)	V _{mppt} (V)	N (modules)	L1 (m)	S1 (mm ²)	r (Ω/km)	r ₉₀ (Ω/km)	ΔV ₁ (%)	L2 (m)	ΔV ₂ (%)	L3 (m)	ΔV ₃ (%)	ΔV (%)
A.11.a.1	B.11.a.1	9,74	41,1	25	5	4	5,09	6,49	0,062	10,625	0,065	30	0,185	0,311
A.11.a.2	B.11.a.2	9,74	41,1	25	5	4	5,09	6,49	0,062	10,625	0,065	30	0,185	0,311
A.11.b.1	B.11.b.1	9,74	41,1	25	35	10	1,95	2,49	0,165	10,625	0,065	30	0,071	0,301
A.11.b.2	B.11.b.2	9,74	41,1	25	35	10	1,95	2,49	0,165	10,625	0,065	30	0,071	0,301
A.11.c.1	B.11.c.1	9,74	41,1	25	65	10	1,95	2,49	0,306	10,625	0,065	30	0,071	0,442
A.11.c.2	B.11.c.2	9,74	41,1	25	65	10	1,95	2,49	0,306	10,625	0,065	30	0,071	0,442
A.11.d.1	B.11.d.1	9,74	41,1	25	95	16	1,24	1,58	0,285	10,625	0,065	30	0,045	0,395
A.11.d.2	B.11.d.2	9,74	41,1	25	95	16	1,24	1,58	0,285	10,625	0,065	30	0,045	0,395
A.11.e.1	B.11.e.1	9,74	41,1	25	15	6	3,39	4,32	0,123	10,625	0,065	30	0,123	0,311
A.11.e.2	B.11.e.2	9,74	41,1	25	15	6	3,39	4,32	0,123	10,625	0,065	30	0,123	0,311
A.11.f.1	B.11.f.1	9,74	41,1	25	45	10	1,95	2,49	0,212	10,625	0,065	30	0,071	0,348
A.11.f.2	B.11.f.2	9,74	41,1	25	45	10	1,95	2,49	0,212	10,625	0,065	30	0,071	0,348
A.11.g.1	B.11.g.1	9,74	41,1	25	75	16	1,24	1,58	0,225	10,625	0,065	30	0,045	0,335
A.11.g.2	B.11.g.2	9,74	41,1	25	75	16	1,24	1,58	0,225	10,625	0,065	30	0,045	0,335
A.11.h.1	B.11.h.1	9,74	41,1	25	105	16	1,24	1,58	0,315	10,625	0,065	30	0,045	0,425
A.11.h.2	B.11.h.2	9,74	41,1	25	105	16	1,24	1,58	0,315	10,625	0,065	30	0,045	0,425
A.12.a.1	B.12.a.1	9,74	41,1	25	5	4	5,09	6,49	0,062	10,625	0,065	30	0,185	0,311
A.12.a.2	B.12.a.2	9,74	41,1	25	5	4	5,09	6,49	0,062	10,625	0,065	30	0,185	0,311
A.12.b.1	B.12.b.1	9,74	41,1	25	35	10	1,95	2,49	0,165	10,625	0,065	30	0,071	0,301
A.12.b.2	B.12.b.2	9,74	41,1	25	35	10	1,95	2,49	0,165	10,625	0,065	30	0,071	0,301
A.12.c.1	B.12.c.1	9,74	41,1	25	65	10	1,95	2,49	0,306	10,625	0,065	30	0,071	0,442
A.12.c.2	B.12.c.2	9,74	41,1	25	65	10	1,95	2,49	0,306	10,625	0,065	30	0,071	0,442
A.12.e.1	B.12.e.1	9,74	41,1	25	15	6	3,39	4,32	0,123	10,625	0,065	30	0,123	0,311
A.12.e.2	B.12.e.2	9,74	41,1	25	15	6	3,39	4,32	0,123	10,625	0,065	30	0,123	0,311
A.12.f.1	B.12.f.1	9,74	41,1	25	45	10	1,95	2,49	0,212	10,625	0,065	30	0,071	0,348
A.12.f.2	B.12.f.2	9,74	41,1	25	45	10	1,95	2,49	0,212	10,625	0,065	30	0,071	0,348

3. Choice of cable: modules-string combiner box

STRINGS		S_CDT (mm2)	S_thermal (mm2)	S_final (mm2)	I-catalog (A)
A.01.a.1	B.01.a.1	4	2,5	4	55
A.01.a.2	B.01.a.2	4	2,5	4	55
A.01.b.1	B.01.b.1	10	4	10	96
A.01.b.2	B.01.b.2	10	4	10	96
A.01.c.1	B.01.c.1	10	4	10	96
A.01.c.2	B.01.c.2	10	4	10	96
A.01.e.1	B.01.e.1	6	6	6	70
A.01.e.2	B.01.e.2	6	6	6	70
A.01.f.1	B.01.f.1	10	6	10	96
A.01.f.2	B.01.f.2	10	6	10	96
A.01.g.1	B.01.g.1	16	6	16	132
A.01.g.2	B.01.g.2	16	6	16	132
A.01.l.1	B.01.l.1	6	6	6	70
A.01.l.2	B.01.l.2	6	6	6	70
A.01.m.1	B.01.m.1	10	6	10	96
A.01.m.2	B.01.m.2	10	6	10	96
A.02.a.1	B.02.a.1	4	2,5	4	55
A.02.a.2	B.02.a.2	4	2,5	4	55
A.02.b.1	B.02.b.1	10	4	10	96
A.02.b.2	B.02.b.2	10	4	10	96
A.02.c.1	B.02.c.1	10	4	10	96
A.02.c.2	B.02.c.2	10	4	10	96
A.02.d.1	B.02.d.1	16	4	16	132
A.02.d.2	B.02.d.2	16	4	16	132
A.02.e.1	B.02.e.1	6	4	6	70
A.02.e.2	B.02.e.2	6	4	6	70
A.02.f.1	B.02.f.1	10	4	10	96
A.02.f.2	B.02.f.2	10	4	10	96
A.02.g.1	B.02.g.1	16	4	16	132
A.02.g.2	B.02.g.2	16	4	16	132
A.02.h.1	B.02.h.1	16	4	16	132
A.02.h.2	B.02.h.2	16	4	16	132
A.03.a.1	B.03.a.1	4	2,5	4	55
A.03.a.2	B.03.a.2	4	2,5	4	55
A.03.b.1	B.03.b.1	10	4	10	96
A.03.b.2	B.03.b.2	10	4	10	96
A.03.c.1	B.03.c.1	10	4	10	96
A.03.c.2	B.03.c.2	10	4	10	96
A.03.d.1	B.03.d.1	16	4	16	132
A.03.d.2	B.03.d.2	16	4	16	132
A.03.e.1	B.03.e.1	6	6	6	70
A.03.e.2	B.03.e.2	6	6	6	70
A.03.f.1	B.03.f.1	10	6	10	96
A.03.f.2	B.03.f.2	10	6	10	96
A.03.g.1	B.03.g.1	16	6	16	132
A.03.g.2	B.03.g.2	16	6	16	132
A.03.h.1	B.03.h.1	16	6	16	132
A.03.h.2	B.03.h.2	16	6	16	132
A.03.l.1	B.03.l.1	6	6	6	70
A.03.l.2	B.03.l.2	6	6	6	70
A.03.m.1	B.03.m.1	10	6	10	96
A.03.m.2	B.03.m.2	10	6	10	96
A.03.n.1	B.03.n.1	16	6	16	132
A.03.n.2	B.03.n.2	16	6	16	132
A.03.o.1	B.03.o.1	16	6	16	132
A.03.o.2	B.03.o.2	16	6	16	132

STRINGS		S_CDT (mm2)	S_thermal (mm2)	S_final (mm2)	I-catalog (A)
A.04.a.1	B.04.a.1	4	2,5	4	55
A.04.a.2	B.04.a.2	4	2,5	4	55
A.04.b.1	B.04.b.1	10	4	10	96
A.04.b.2	B.04.b.2	10	4	10	96
A.04.c.1	B.04.c.1	10	4	10	96
A.04.c.2	B.04.c.2	10	4	10	96
A.04.d.1	B.04.d.1	16	4	16	132
A.04.d.2	B.04.d.2	16	4	16	132
A.04.e.1	B.04.e.1	6	6	6	70
A.04.e.2	B.04.e.2	6	6	6	70
A.04.f.1	B.04.f.1	10	6	10	96
A.04.f.2	B.04.f.2	10	6	10	96
A.04.g.1	B.04.g.1	16	6	16	132
A.04.g.2	B.04.g.2	16	6	16	132
A.04.h.1	B.04.h.1	16	6	16	132
A.04.h.2	B.04.h.2	16	6	16	132
A.04.l.1	B.04.l.1	6	6	6	70
A.04.l.2	B.04.l.2	6	6	6	70
A.04.m.1	B.04.m.1	10	6	10	96
A.04.m.2	B.04.m.2	10	6	10	96
A.04.n.1	B.04.n.1	16	6	16	132
A.04.n.2	B.04.n.2	16	6	16	132
A.04.o.1	B.04.o.1	16	6	16	132
A.04.o.2	B.04.o.2	16	6	16	132
A.05.a.1	B.05.a.1	4	2,5	4	55
A.05.a.2	B.05.a.2	4	2,5	4	55
A.05.b.1	B.05.b.1	10	4	10	96
A.05.b.2	B.05.b.2	10	4	10	96
A.05.c.1	B.05.c.1	10	4	10	96
A.05.c.2	B.05.c.2	10	4	10	96
A.05.d.1	B.05.d.1	16	4	16	132
A.05.d.2	B.05.d.2	16	4	16	132
A.05.e.1	B.05.e.1	6	6	6	70
A.05.e.2	B.05.e.2	6	6	6	70
A.05.f.1	B.05.f.1	10	6	10	96
A.05.f.2	B.05.f.2	10	6	10	96
A.05.g.1	B.05.g.1	16	6	16	132
A.05.g.2	B.05.g.2	16	6	16	132
A.05.h.1	B.05.h.1	16	6	16	132
A.05.h.2	B.05.h.2	16	6	16	132
A.05.l.1	B.05.l.1	6	6	6	70
A.05.l.2	B.05.l.2	6	6	6	70
A.05.m.1	B.05.m.1	10	6	10	96
A.05.m.2	B.05.m.2	10	6	10	96
A.05.n.1	B.05.n.1	16	6	16	132
A.05.n.2	B.05.n.2	16	6	16	132
A.05.o.1	B.05.o.1	16	6	16	132
A.05.o.2	B.05.o.2	16	6	16	132

STRINGS		S_CDT (mm2)	S_thermal (mm2)	S_final (mm2)	I-catalog (A)
A.06.a.1	B.06.a.1	4	2,5	4	55
A.06.a.2	B.06.a.2	4	2,5	4	55
A.06.b.1	B.06.b.1	10	4	10	96
A.06.b.2	B.06.b.2	10	4	10	96
A.06.c.1	B.06.c.1	10	4	10	96
A.06.c.2	B.06.c.2	10	4	10	96
A.06.d.1	B.06.d.1	16	4	16	132
A.06.d.2	B.06.d.2	16	4	16	132
A.06.e.1	B.06.e.1	6	6	6	70
A.06.e.2	B.06.e.2	6	6	6	70
A.06.f.1	B.06.f.1	10	6	10	96
A.06.f.2	B.06.f.2	10	6	10	96
A.06.g.1	B.06.g.1	16	6	16	132
A.06.g.2	B.06.g.2	16	6	16	132
A.06.h.1	B.06.h.1	16	6	16	132
A.06.h.2	B.06.h.2	16	6	16	132
A.06.l.1	B.06.l.1	6	6	6	70
A.06.l.2	B.06.l.2	6	6	6	70
A.06.m.1	B.06.m.1	10	6	10	96
A.06.m.2	B.06.m.2	10	6	10	96
A.06.n.1	B.06.n.1	16	6	16	132
A.06.n.2	B.06.n.2	16	6	16	132
A.06.o.1	B.06.o.1	16	6	16	132
A.06.o.2	B.06.o.2	16	6	16	132
A.07.a.1	B.07.a.1	4	2,5	4	55
A.07.a.2	B.07.a.2	4	2,5	4	55
A.07.b.1	B.07.b.1	10	4	10	96
A.07.b.2	B.07.b.2	10	4	10	96
A.07.c.1	B.07.c.1	10	4	10	96
A.07.c.2	B.07.c.2	10	4	10	96
A.07.d.1	B.07.d.1	16	4	16	132
A.07.d.2	B.07.d.2	16	4	16	132
A.07.e.1	B.07.e.1	6	6	6	70
A.07.e.2	B.07.e.2	6	6	6	70
A.07.f.1	B.07.f.1	10	6	10	96
A.07.f.2	B.07.f.2	10	6	10	96
A.07.g.1	B.07.g.1	16	6	16	132
A.07.g.2	B.07.g.2	16	6	16	132
A.07.h.1	B.07.h.1	16	6	16	132
A.07.h.2	B.07.h.2	16	6	16	132
A.07.l.1	B.07.l.1	6	6	6	70
A.07.l.2	B.07.l.2	6	6	6	70
A.07.m.1	B.07.m.1	10	6	10	96
A.07.m.2	B.07.m.2	10	6	10	96
A.07.n.1	B.07.n.1	16	6	16	132
A.07.n.2	B.07.n.2	16	6	16	132
A.07.o.1	B.07.o.1	16	6	16	132
A.07.o.2	B.07.o.2	16	6	16	132

STRINGS		S_CDT (mm2)	S_thermal (mm2)	S_final (mm2)	I-catalog (A)
A.08.a.1	B.08.a.1	4	2,5	4	55
A.08.a.2	B.08.a.2	4	2,5	4	55
A.08.b.1	B.08.b.1	10	4	10	96
A.08.b.2	B.08.b.2	10	4	10	96
A.08.c.1	B.08.c.1	10	4	10	96
A.08.c.2	B.08.c.2	10	4	10	96
A.08.d.1	B.08.d.1	16	4	16	132
A.08.d.2	B.08.d.2	16	4	16	132
A.08.e.1	B.08.e.1	6	6	6	70
A.08.e.2	B.08.e.2	6	6	6	70
A.08.f.1	B.08.f.1	10	6	10	96
A.08.f.2	B.08.f.2	10	6	10	96
A.08.g.1	B.08.g.1	16	6	16	132
A.08.g.2	B.08.g.2	16	6	16	132
A.08.h.1	B.08.h.1	16	6	16	132
A.08.h.2	B.08.h.2	16	6	16	132
A.08.l.1	B.08.l.1	6	6	6	70
A.08.l.2	B.08.l.2	6	6	6	70
A.08.m.1	B.08.m.1	10	6	10	96
A.08.m.2	B.08.m.2	10	6	10	96
A.08.n.1	B.08.n.1	16	6	16	132
A.08.n.2	B.08.n.2	16	6	16	132
A.08.o.1	B.08.o.1	16	6	16	132
A.08.o.2	B.08.o.2	16	6	16	132
A.09.a.1	B.09.a.1	4	2,5	4	55
A.09.a.2	B.09.a.2	4	2,5	4	55
A.09.b.1	B.09.b.1	10	4	10	96
A.09.b.2	B.09.b.2	10	4	10	96
A.09.c.1	B.09.c.1	10	4	10	96
A.09.c.2	B.09.c.2	10	4	10	96
A.09.d.1	B.09.d.1	16	4	16	132
A.09.d.2	B.09.d.2	16	4	16	132
A.09.e.1	B.09.e.1	6	6	6	70
A.09.e.2	B.09.e.2	6	6	6	70
A.09.f.1	B.09.f.1	10	6	10	96
A.09.f.2	B.09.f.2	10	6	10	96
A.09.g.1	B.09.g.1	16	6	16	132
A.09.g.2	B.09.g.2	16	6	16	132
A.09.h.1	B.09.h.1	16	6	16	132
A.09.h.2	B.09.h.2	16	6	16	132
A.09.l.1	B.09.l.1	6	6	6	70
A.09.l.2	B.09.l.2	6	6	6	70
A.09.m.1	B.09.m.1	10	6	10	96
A.09.m.2	B.09.m.2	10	6	10	96
A.09.n.1	B.09.n.1	16	6	16	132
A.09.n.2	B.09.n.2	16	6	16	132
A.09.o.1	B.09.o.1	16	6	16	132
A.09.o.2	B.09.o.2	16	6	16	132

STRINGS		S_CDT (mm2)	S_thermal (mm2)	S_final (mm2)	I-catalog (A)
A.10.a.1	B.10.a.1	4	2,5	4	55
A.10.a.2	B.10.a.2	4	2,5	4	55
A.10.b.1	B.10.b.1	10	4	10	96
A.10.b.2	B.10.b.2	10	4	10	96
A.10.c.1	B.10.c.1	10	4	10	96
A.10.c.2	B.10.c.2	10	4	10	96
A.10.d.1	B.10.d.1	16	4	16	132
A.10.d.2	B.10.d.2	16	4	16	132
A.10.e.1	B.10.e.1	6	6	6	70
A.10.e.2	B.10.e.2	6	6	6	70
A.10.f.1	B.10.f.1	10	6	10	96
A.10.f.2	B.10.f.2	10	6	10	96
A.10.g.1	B.10.g.1	16	6	16	132
A.10.g.2	B.10.g.2	16	6	16	132
A.10.h.1	B.10.h.1	16	6	16	132
A.10.h.2	B.10.h.2	16	6	16	132
A.10.l.1	B.10.l.1	6	6	6	70
A.10.l.2	B.10.l.2	6	6	6	70
A.10.m.1	B.10.m.1	10	6	10	96
A.10.m.2	B.10.m.2	10	6	10	96
A.10.n.1	B.10.n.1	16	6	16	132
A.10.n.2	B.10.n.2	16	6	16	132
A.10.o.1	B.10.o.1	16	6	16	132
A.10.o.2	B.10.o.2	16	6	16	132
A.11.a.1	B.11.a.1	4	2,5	4	55
A.11.a.2	B.11.a.2	4	2,5	4	55
A.11.b.1	B.11.b.1	10	4	10	96
A.11.b.2	B.11.b.2	10	4	10	96
A.11.c.1	B.11.c.1	10	4	10	96
A.11.c.2	B.11.c.2	10	4	10	96
A.11.d.1	B.11.d.1	16	4	16	132
A.11.d.2	B.11.d.2	16	4	16	132
A.11.e.1	B.11.e.1	6	4	6	70
A.11.e.2	B.11.e.2	6	4	6	70
A.11.f.1	B.11.f.1	10	4	10	96
A.11.f.2	B.11.f.2	10	4	10	96
A.11.g.1	B.11.g.1	16	4	16	132
A.11.g.2	B.11.g.2	16	4	16	132
A.11.h.1	B.11.h.1	16	4	16	132
A.11.h.2	B.11.h.2	16	4	16	132
A.12.a.1	B.12.a.1	4	2,5	4	55
A.12.a.2	B.12.a.2	4	2,5	4	55
A.12.b.1	B.12.b.1	10	4	10	96
A.12.b.2	B.12.b.2	10	4	10	96
A.12.c.1	B.12.c.1	10	4	10	96
A.12.c.2	B.12.c.2	10	4	10	96
A.12.e.1	B.12.e.1	6	4	6	70
A.12.e.2	B.12.e.2	6	4	6	70
A.12.f.1	B.12.f.1	10	4	10	96
A.12.f.2	B.12.f.2	10	4	10	96

Appendix C

This appendix shows the calculations necessary for the choice of electrical cables in the combiner box-inverter section.

To calculate the resistance value, reported to 90 °C, the following formula is used:

$$r_{90} = r_{20}(1 + \alpha \cdot \Delta T) \quad (106)$$

Where:

- r_{20} is the resistance of the cable, at 20 °C
- $\alpha = 0,00393 K^{-1}$
- $\Delta T = 70 K$

It is verified that the maximum open circuit voltage of the string is lower than the maximum tension of the cables:

$$1391 V < 5400 V$$

1. Electrical criterion

CABLES		V_box,mppt(V)	I_mppt (A)	m (paralel)	I_box,mppt (A)	L (m)	S (mm2)	r (Ω/km)	r_90 (Ω/km)	ΔV (%)
A.01	B.01	1027,5	9,74	16	155,8	135	2x240	0,082	0,105	0,428
A.02	B.02	1027,5	9,74	16	155,8	120	2x240	0,082	0,105	0,381
A.03	B.03	1027,5	9,74	24	233,8	95	3x240	0,082	0,105	0,452
A.04	B.04	1027,5	9,74	24	233,8	70	3x185	0,108	0,138	0,439
A.05	B.05	1027,5	9,74	24	233,8	45	3x185	0,108	0,138	0,282
A.06	B.06	1027,5	9,74	24	233,8	35	2x150	0,132	0,168	0,268
A.07	B.07	1027,5	9,74	24	233,8	30	2x185	0,108	0,138	0,188
A.08	B.08	1027,5	9,74	24	233,8	40	3x185	0,108	0,138	0,251
A.09	B.09	1027,5	9,74	24	233,8	65	3x185	0,108	0,138	0,407
A.10	B.10	1027,5	9,74	24	233,8	90	3x240	0,082	0,105	0,428
A.11	B.11	1027,5	9,74	16	155,8	115	2x240	0,082	0,105	0,365
A.12	B.12	1027,5	9,74	10	97,4	130	2x150	0,132	0,168	0,415

It should be noted that the resistance indicated in the table is the value reported in the datasheet, valid for a cable

2. Thermal criterion

CABLES		I _{SC} (A)	I _B (A)	m (paralel)	I _{B,box} (A)	n (multiple cables)	I _{B,cable} (A)	k _{1g}	k _{2g}	k _{3g}	k _{4g}	Io _{min} (A)	IoSTTC (A)	S ₁ (mm ²)
A.01	B.01	10,18	12,725	16	203,6	2	101,8	1,1	0,93	0,65	0,83	184,5	419	240
A.02	B.02	10,18	12,725	16	203,6	2	101,8	1,1	0,93	0,65	0,83	184,5	419	240
A.03	B.03	10,18	12,725	24	305,4	3	101,8	1,1	0,93	0,65	0,83	184,5	419	240
A.04	B.04	10,18	12,725	24	305,4	3	101,8	1,1	0,93	0,65	0,83	184,5	363	185
A.05	B.05	10,18	12,725	24	305,4	3	101,8	1,1	0,93	0,65	1	153,1	363	185
A.06	B.06	10,18	12,725	24	305,4	2	152,7	1,1	0,93	0,85	1	175,6	324	150
A.07	B.07	10,18	12,725	24	305,4	2	152,7	1,1	0,93	0,85	1	175,6	363	185
A.08	B.08	10,18	12,725	24	305,4	3	101,8	1,1	0,93	0,65	1	153,1	363	185
A.09	B.09	10,18	12,725	24	305,4	3	101,8	1,1	0,93	0,65	0,83	184,5	363	185
A.10	B.10	10,18	12,725	24	305,4	3	101,8	1,1	0,93	0,65	0,83	184,5	419	240
A.11	B.11	10,18	12,725	16	203,6	2	101,8	1,1	0,93	0,65	0,83	184,5	419	240
A.12	B.12	10,18	12,725	10	127,3	2	63,6	1,1	0,93	0,65	0,83	115,3	324	150

CABLES		I _{SC} (A)	I _B (A)	m (paralel)	I _{B,box} (A)	n (multiple cables)	I _{B,cable} (A)	k _{1a}	k _{2a}	k _{3a}	Io _{min} (A)	IoSTTC (A)	S ₂ (mm ²)
A.01	B.01	10,18	12,725	16	203,6	2	101,8	0,9	0,58	1	195,0	641	240
A.02	B.02	10,18	12,725	16	203,6	2	101,8	0,9	0,58	1	195,0	641	240
A.03	B.03	10,18	12,725	24	305,4	3	101,8	0,9	0,58	1	195,0	641	240
A.04	B.04	10,18	12,725	24	305,4	3	101,8	0,9	0,58	1	195,0	542	185
A.05	B.05	10,18	12,725	24	305,4	3	101,8	0,9	0,58	1	195,0	542	185
A.06	B.06	10,18	12,725	24	305,4	2	152,7	0,9	0,58	1	292,5	473	150
A.07	B.07	10,18	12,725	24	305,4	2	152,7	0,9	0,58	1	292,5	542	185
A.08	B.08	10,18	12,725	24	305,4	3	101,8	0,9	0,58	1	195,0	542	185
A.09	B.09	10,18	12,725	24	305,4	3	101,8	0,9	0,58	1	195,0	542	185
A.10	B.10	10,18	12,725	24	305,4	3	101,8	0,9	0,58	1	195,0	641	240
A.11	B.11	10,18	12,725	16	203,6	2	101,8	0,9	0,58	1	195,0	641	240
A.12	B.12	10,18	12,725	10	127,3	2	63,6	0,9	0,58	1	121,9	473	150

Trabajo Fin de Máster – Appendix C

CABLES		I_SC (A)	I_B (A)	m (paralel)	I_B,box (A)	n (multiple cables)	I_B,cable (A)	k_1a	k_2a	k_3a	Io_min (A)	IoSTTC (A)	S_3 (mm2)
A.01	B.01	10,18	12,725	16	203,6	2	101,8	0,9	0,58	0,4	487,5	641	240
A.02	B.02	10,18	12,725	16	203,6	2	101,8	0,9	0,58	0,4	487,5	641	240
A.03	B.03	10,18	12,725	24	305,4	3	101,8	0,9	0,58	0,4	487,5	641	240
A.04	B.04	10,18	12,725	24	305,4	3	101,8	0,9	0,58	0,4	487,5	542	185
A.05	B.05	10,18	12,725	24	305,4	3	101,8	0,9	0,58	0,4	487,5	542	185
A.06	B.06	10,18	12,725	24	305,4	2	152,7	0,9	0,58	0,65	450,0	473	150
A.07	B.07	10,18	12,725	24	305,4	2	152,7	0,9	0,58	0,65	450,0	542	185
A.08	B.08	10,18	12,725	24	305,4	3	101,8	0,9	0,58	0,4	487,5	542	185
A.09	B.09	10,18	12,725	24	305,4	3	101,8	0,9	0,58	0,4	487,5	542	185
A.10	B.10	10,18	12,725	24	305,4	3	101,8	0,9	0,58	0,4	487,5	641	240
A.11	B.11	10,18	12,725	16	203,6	2	101,8	0,9	0,58	0,4	487,5	641	240
A.12	B.12	10,18	12,725	10	127,3	2	63,6	0,9	0,58	0,4	304,7	473	150

Appendix D

This appendix shows the Excel tables with the calculation of the low voltage cables' prices.

Codigo	UM	Description	Rdto.	Precio	Importe
MOOE11a	h	Especialista electricidad	0,12	16,84	2,02
MOOE.8a	h	Oficial 1a electricidad	0,06	19,75	1,19
-	m	Cable Cu (PV)1-F 0,6/1 kV 1x4 mm ²	2,1	0,52	1,09
%		Costes directos complementarios	0,02	4,30	0,09
Line DC Cu (PV)1-F 0,6/1 kV 2x(1x4 mm²)					4,39
Codigo	UM	Description	Rdto.	Precio	Importe
MOOE11a	h	Especialista electricidad	0,12	16,84	2,02
MOOE.8a	h	Oficial 1a electricidad	0,06	19,75	1,19
-	m	Cable Cu (PV)1-F 0,6/1 kV 1x6 mm ²	2,1	0,72	1,51
%		Costes directos complementarios	0,02	4,72	0,09
Line DC Cu (PV)1-F 0,6/1 kV 2x(1x6 mm²)					4,82
Codigo	UM	Description	Rdto.	Precio	Importe
MOOE11a	h	Especialista electricidad	0,12	16,84	2,02
MOOE.8a	h	Oficial 1a electricidad	0,06	19,75	1,19
-	m	Cable Cu (PV)1-F 0,6/1 kV 1x10 mm ²	2,1	1,1	2,31
%		Costes directos complementarios	0,02	5,52	0,11
Line DC Cu (PV)1-F 0,6/1 kV 2x(1x10 mm²)					5,63
Codigo	UM	Description	Rdto.	Precio	Importe
MOOE11a	h	Especialista electricidad	0,12	16,84	2,02
MOOE.8a	h	Oficial 1a electricidad	0,06	19,75	1,19
-	m	Cable Cu (PV)1-F 0,6/1 kV 1x16 mm ²	2,1	1,68	3,53
%		Costes directos complementarios	0,02	6,73	0,13
Line DC Cu (PV)1-F 0,6/1 kV 2x(1x16 mm²)					6,87

Codigo	UM	Description	Rdto.	Precio	Importe
MOOE11a	h	Especialista electricidad	0,12	16,84	2,02
MOOE.8a	h	Oficial 1a electricidad	0,06	19,75	1,19
-	m	Cable Cu (PV)1-F 0,6/1 kV 1x4 mm ²	1,05	0,52	0,55
%		Costes directos complementarios	0,02	3,75	0,08
Line DC Cu (PV)1-F 0,6/1 kV 1x(1x4 mm²)					3,83
Codigo	UM	Description	Rdto.	Precio	Importe
MOOE11a	h	Especialista electricidad	0,12	16,84	2,02
MOOE.8a	h	Oficial 1a electricidad	0,06	19,75	1,19
-	m	Cable Cu (PV)1-F 0,6/1 kV 1x6 mm ²	1,05	0,72	0,76
%		Costes directos complementarios	0,02	3,96	0,08
Line DC Cu (PV)1-F 0,6/1 kV 1x(1x6 mm²)					4,05
Codigo	UM	Description	Rdto.	Precio	Importe
MOOE11a	h	Especialista electricidad	0,12	16,84	2,02
MOOE.8a	h	Oficial 1a electricidad	0,06	19,75	1,19
-	m	Cable Cu (PV)1-F 0,6/1 kV 1x10 mm ²	1,05	1,1	1,16
%		Costes directos complementarios	0,02	4,36	0,09
Line DC Cu (PV)1-F 0,6/1 kV 1x(1x10 mm²)					4,45
Codigo	UM	Description	Rdto.	Precio	Importe
MOOE11a	h	Especialista electricidad	0,12	16,84	2,02
MOOE.8a	h	Oficial 1a electricidad	0,06	19,75	1,19
-	m	Cable Cu (PV)1-F 0,6/1 kV 1x16 mm ²	1,05	1,68	1,76
%		Costes directos complementarios	0,02	4,97	0,10
Line DC Cu (PV)1-F 0,6/1 kV 1x(1x16 mm²)					5,07

Codigo	UM	Description	Rdto.	Precio	Importe
MOOE11a	h	Especialista electricidad	0,16	16,84	2,69
MOOE.8a	h	Oficial 1a electricidad	0,08	19,75	1,58
-	m	Cable Cu (PV)S3Z2Z2-K 0,6/1 kV 1x150 mm ²	4,2	15	63,00
%		Costes directos complementarios	0,02	67,27	1,35
Line DC Cu (PV)S3Z2Z2-K 0,6/1 kV 2x[2x(1x150 mm²)]					68,62
Codigo	UM	Description	Rdto.	Precio	Importe
MOOE11a	h	Especialista electricidad	0,16	16,84	2,69
MOOE.8a	h	Oficial 1a electricidad	0,08	19,75	1,58
-	m	Cable Cu (PV)S3Z2Z2-K 0,6/1 kV 1x185 mm ²	4,2	18,5	77,70
%		Costes directos complementarios	0,02	81,97	1,64
Line DC Cu (PV)S3Z2Z2-K 0,6/1 kV 2x[2x(1x185 mm²)]					83,62
Codigo	UM	Description	Rdto.	Precio	Importe
MOOE11a	h	Especialista electricidad	0,16	16,84	2,69
MOOE.8a	h	Oficial 1a electricidad	0,08	19,75	1,58
-	m	Cable Cu (PV)S3Z2Z2-K 0,6/1 kV 1x185 mm ²	6,3	18,5	116,55
%		Costes directos complementarios	0,02	120,82	2,42
Line DC Cu (PV)S3Z2Z2-K 0,6/1 kV 3x[2x(1x185 mm²)]					123,25
Codigo	UM	Description	Rdto.	Precio	Importe
MOOE11a	h	Especialista electricidad	0,16	16,84	2,69
MOOE.8a	h	Oficial 1a electricidad	0,08	19,75	1,58
-	m	Cable Cu (PV)S3Z2Z2-K 0,6/1 kV 1x240 mm ²	4,2	24	100,80
%		Costes directos complementarios	0,02	105,07	2,10
Line DC Cu (PV)S3Z2Z2-K 0,6/1 kV 2x[2x(1x240 mm²)]					107,18
Codigo	UM	Description	Rdto.	Precio	Importe
MOOE11a	h	Especialista electricidad	0,16	16,84	2,69
MOOE.8a	h	Oficial 1a electricidad	0,08	19,75	1,58
-	m	Cable Cu (PV)S3Z2Z2-K 0,6/1 kV 1x240 mm ²	6,3	24	151,20
%		Costes directos complementarios	0,02	155,47	3,11
Line DC Cu (PV)S3Z2Z2-K 0,6/1 kV 3x[2x(1x240 mm²)]					158,59

Bibliography

- [1] M. Barrio and M. Casa, Instalaciones solares fotovoltaicas, MARCOMBO S.A., 2012.
- [2] M. Dorothal, «White paper Spain 2020, The road ahead for solar,» SOLARPLAZA, 2020.
- [3] M. Alonso, Sistemas fotovoltaicos, Introducción al diseño y dimensionado de instalaciones de energía solar fotovoltaica, ERA SOLAR, 2005.
- [4] E. Lorenzo, Electricidad solar fotovoltaica, Ingeniería fotovoltaica Volumen III, PROGNSA , 2014.
- [5] IDAE, *Instalaciones de energía solar fotovoltaica. Pliego de condiciones técnicas de instalaciones aisladas de red.*
- [6] P. Di Leo e F. Spertino, *Course material "Electric plant design" and "Photovoltaic and wind systems for electricity production".*
- [7] SMA, «Información técnica SMA STRING-MONITOR SSM-U-XX10/SSM-U-XX15».
- [8] TreeSystem, «TreeSystem support solution».
- [9] V. Mangoni e G. Carpinelli, *Introduzione ai sistemi elettrici per l'energia*, UNIVERSITÀ DI CASSINO, 2001.
- [10] *Standards UNE 60364 and ICT BT 40.*
- [11] E. Bompard, *Course material "Power system economics and operation".*
- [12] «Wikipedia,» [Online]. Available: <https://it.wikipedia.org/wiki/Chelva>.
- [13] [Online]. Available: <http://meteo.navarra.es/definiciones/koppen.cfm#B>.
- [14] [Online]. Available: <https://es.climate-data.org/europe/espana/comunidad-valenciana/chelva-274765/#climatetable>.
- [15] «SEDE CATASTRO,» [Online]. Available: <https://www1.sedecatastro.gob.es>.
- [16] «VISORE CARTOGRAFICO,» [Online]. Available: <https://visor.gva.es>.
- [17] «IGME,» [Online]. Available: <http://mapas.igme.es>.
- [18] TrinaSolar, «Datasheet, TrinaSolar_TSM-DE15H».
- [19] SMA, «Datasheet, SMA MV Power Station, Inverter SC2500-EV, Transformer 2500 kVA».

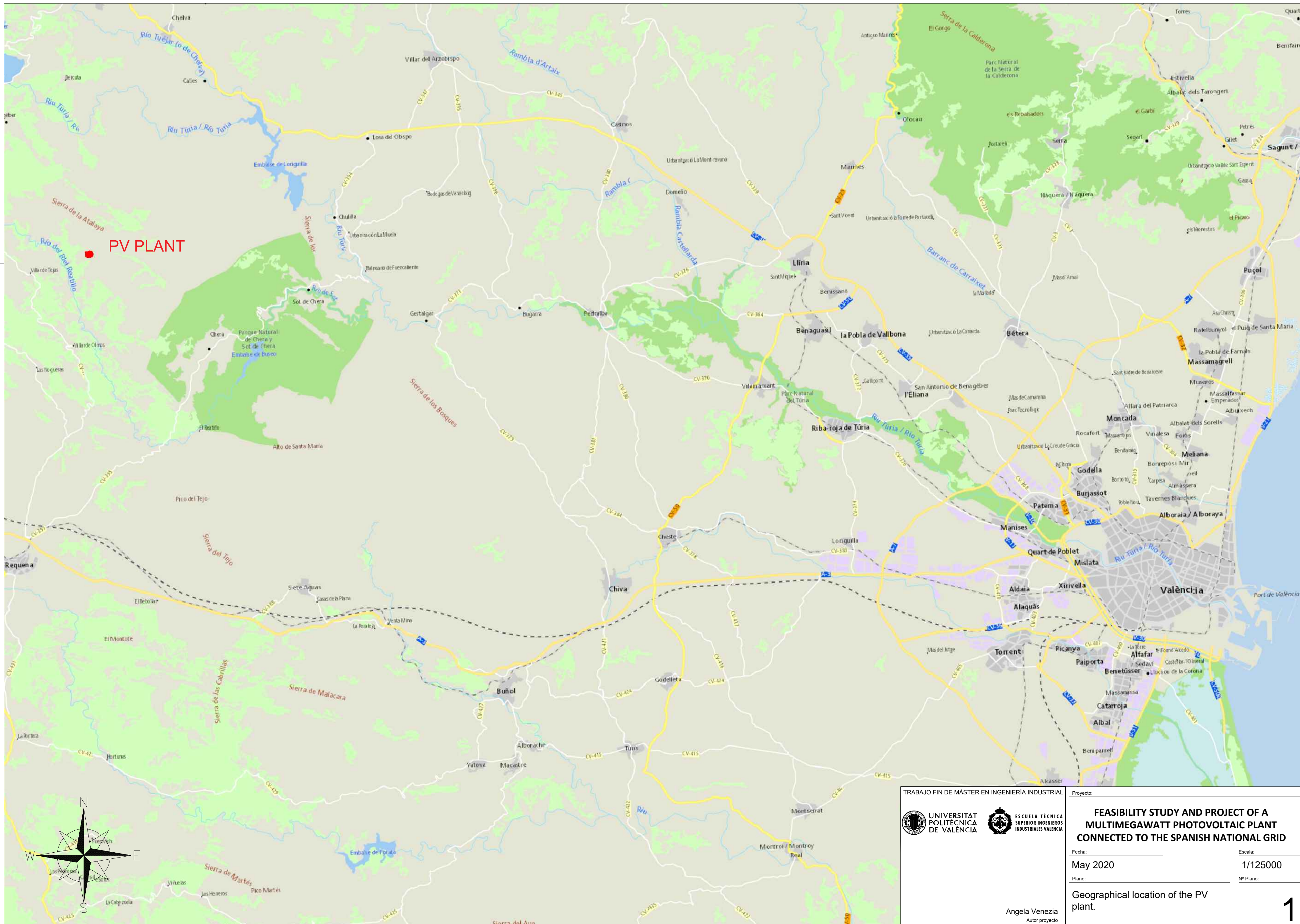
- [20] «PVGIS,» [Online]. Available: <https://ec.europa.eu/jrc/en/pvgis>.
- [21] SMA, «Datasheet, SMA String monitor SSM-U-DEN1834-V13».
- [22] [Online]. Available: <https://www.monsolar.com/blog/conexion-serie-de-paneles-solares-leapfrog-wiring-o-salto-dela->.
- [23] PRYSMIAN, «Datasheet, TECSUN(PV) PV1-F and TECSUN(PV) S3Z2Z2-K».
- [24] PRYSMIAN, «Datasheet, low and medium voltage cables and accessories».
- [25] ITC-BT-21, *Guía técnica de aplicación: instalaciones interiores tubos y canales protectoras*, 2003.
- [26] *Manual técnico de distribución, proyecto tipo de línea subterránea de AT hasta 30 kV*, Iberdrola.
- [27] i-De, «Condiciones técnicas de instalaciones de producción eléctrica conectadas a la red».
- [28] ITC-RAT 13, 2014.
- [29] *Metodo de calculo y proyecto de instalaciones de puesta a tierra para centros de trasmormacion conectados a redes de tercera categoria*.
- [30] i-De, «Diseño de puestas a tierra en centros de transformación en edificio de otros usos de tensión nominal ≤ 30 kV».
- [31] «Base de precios,» [Online]. Available: <https://menfis.info/baseprecios.html>.
- [32] «Agència Tributària Valenciana,» [Online]. Available: <http://atv.gva.es/va/>.
- [33] «AEGE,» [Online]. Available: <https://www.aege.es/>.
- [34] R. Cuervo e J. Méndez, *Energía solar fotovoltaica*. 4a edición, FC EDITORIAL.

Software

To develop this work have been used:

- MathWorks MATLAB
- Autodesk AutoCAD
- Microsoft Office

PLANOS



PV PLANT

TRABAJO FIN DE MÁSTER EN INGENIERÍA INDUSTRIAL



Proyecto:

FEASIBILITY STUDY AND PROJECT OF A MULTIMEGAWATT PHOTOVOLTAIC PLANT CONNECTED TO THE SPANISH NATIONAL GRID

Fecha: May 2020

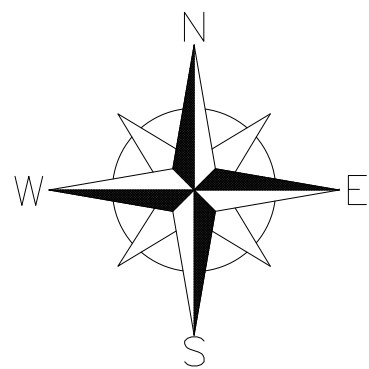
Escala: 1/125000

Plano:

Nº Plano:

Geographical location of the PV plant.

Angela Venezia
Autor proyecto



TRABAJO FIN DE MÁSTER EN INGENIERÍA INDUSTRIAL



Angela Venezia
Autor proyecto

Proyecto:

**FEASIBILITY STUDY AND PROJECT OF A
MULTIMEGAWATT PHOTOVOLTAIC PLANT
CONNECTED TO THE SPANISH NATIONAL GRID**

Fecha:

May 2020

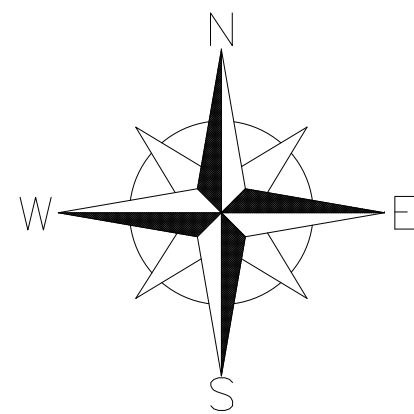
Plano:

Geographical location of the PV
plant. Plot number 806.

Escala:

1/3000

Nº Plano:



TRABAJO FIN DE MÁSTER EN INGENIERÍA INDUSTRIAL



UNIVERSITAT
POLITÀCNICA
DE VALÈNCIA



ESCUOLA TÈCNICA
SUPERIOR INGENIEROS
INDUSTRIALES VALÈNCIA

Proyecto:

**FEASIBILITY STUDY AND PROJECT OF A
MULTIMEGAWATT PHOTOVOLTAIC PLANT
CONNECTED TO THE SPANISH NATIONAL GRID**

Fecha:

May 2020

Escala:

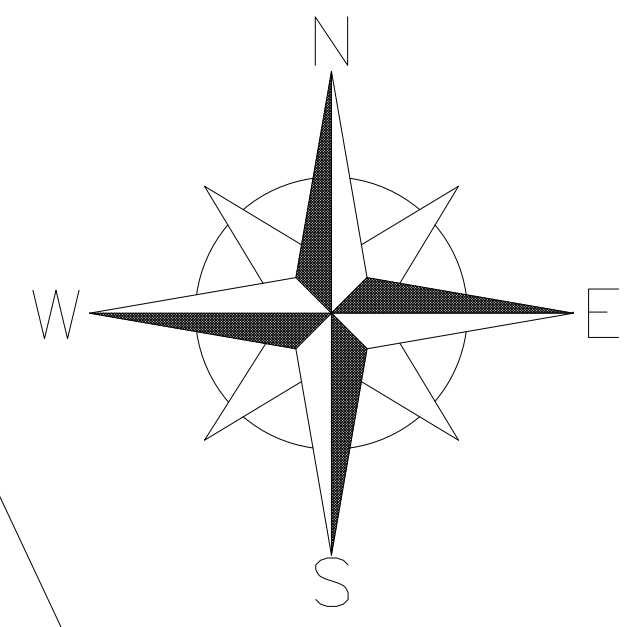
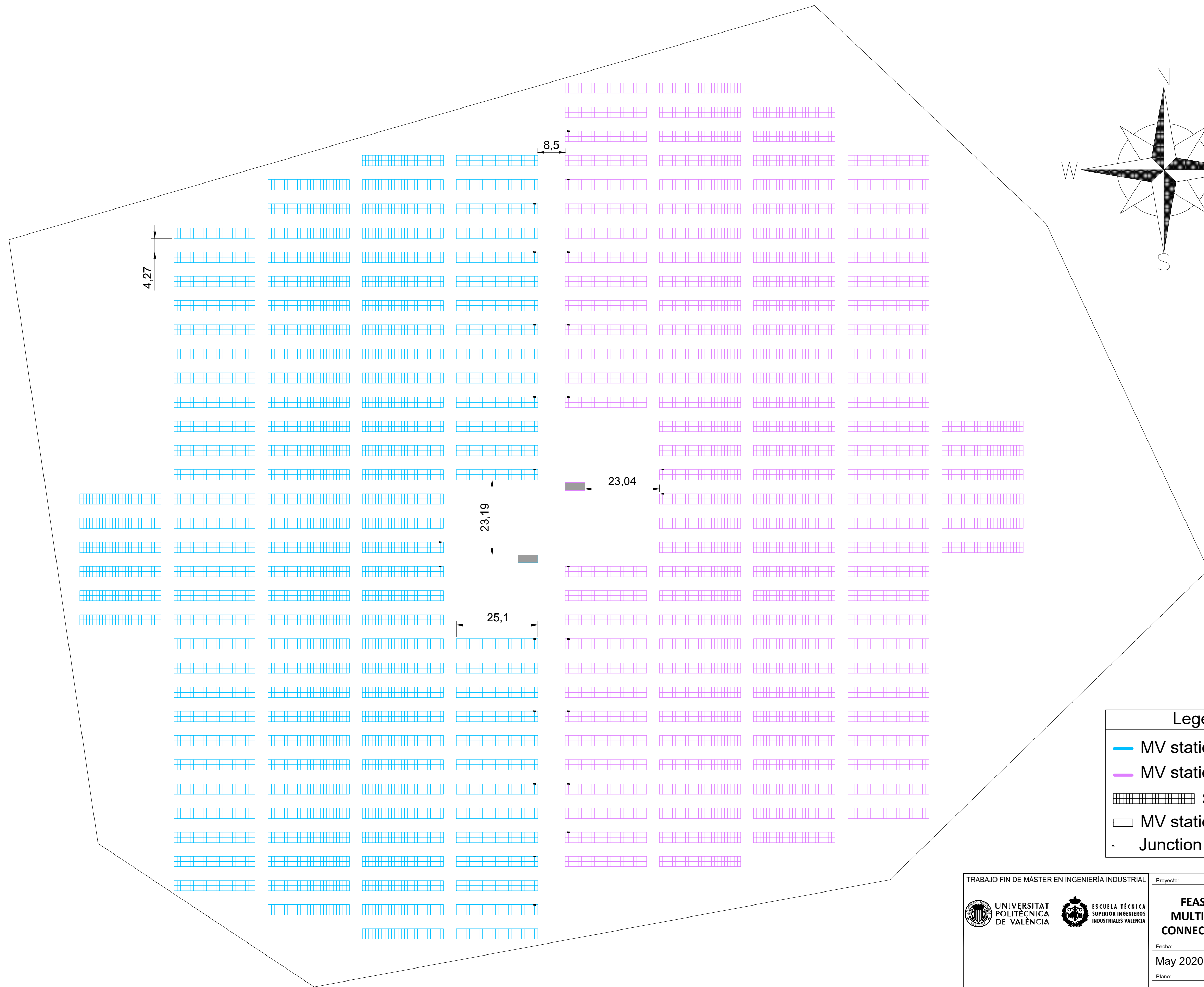
1/1000

Plano:

Nº Plano:

Geographical location of the PV
plant. Area of interest.

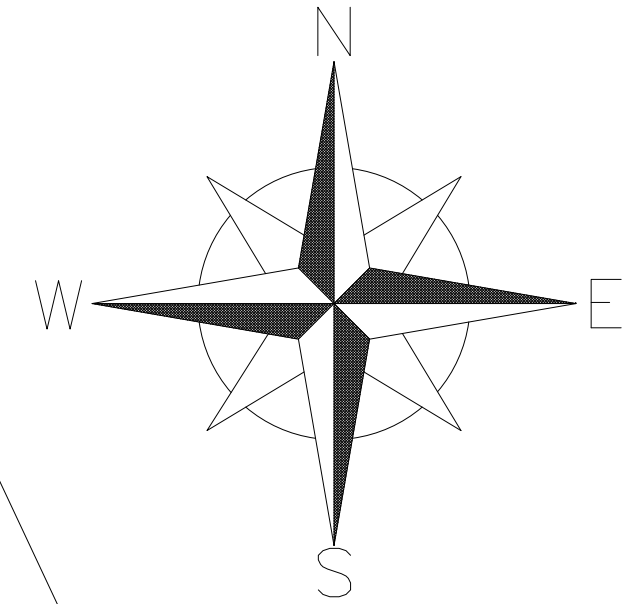
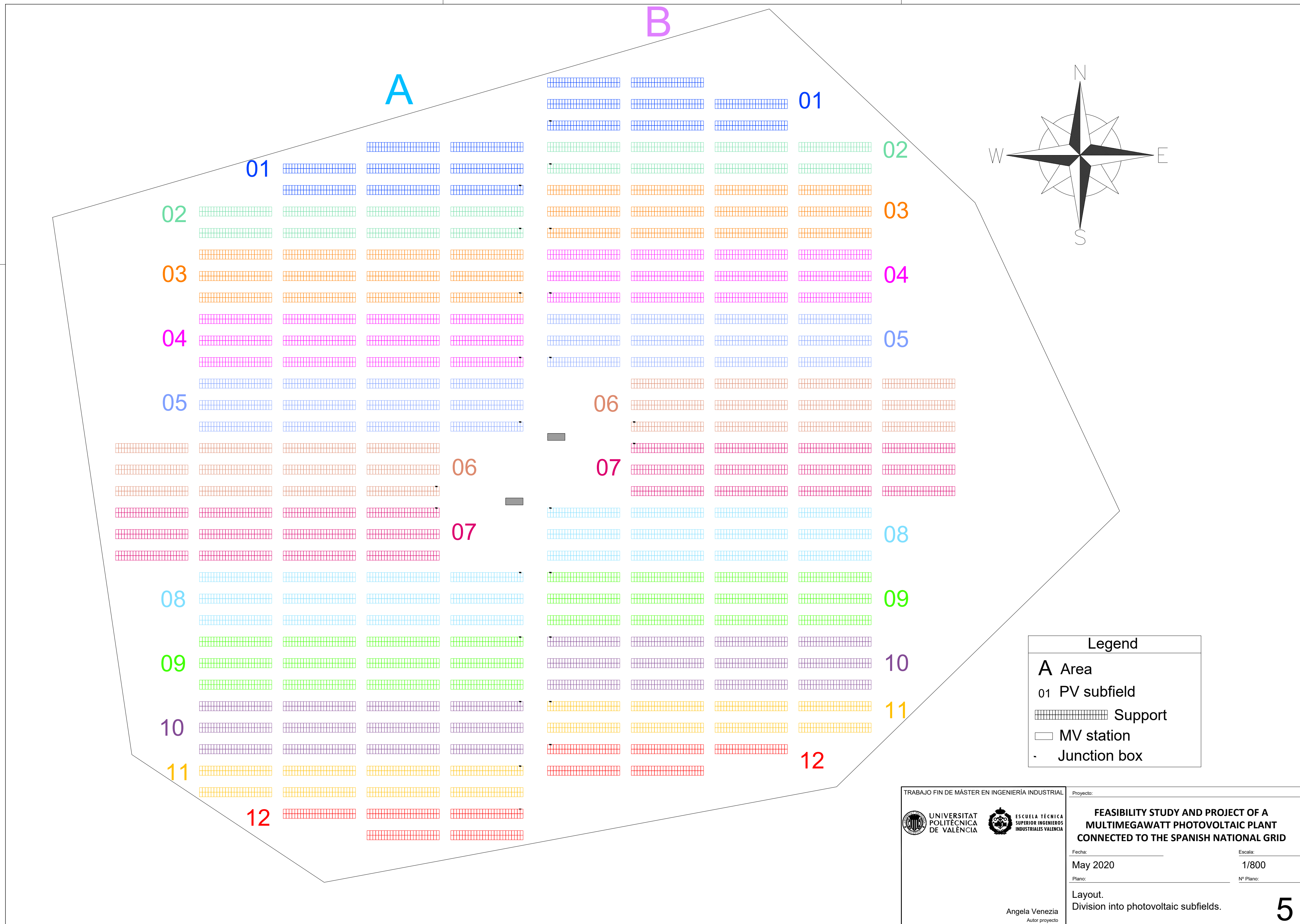
Angela Venezia
Autor proyecto



Legend

- MV station A
- MV station B
- Support
- MV station
- Junction box

TRABAJO FIN DE MÁSTER EN INGENIERÍA INDUSTRIAL		Proyecto:	
UNIVERSITAT POLITÈCNICA DE VALÈNCIA	ESCUELA TÉCNICA SUPERIOR INGENIEROS INDUSTRIALES VALENCIA	FEASIBILITY STUDY AND PROJECT OF A MULTIMEGAWATT PHOTOVOLTAIC PLANT CONNECTED TO THE SPANISH NATIONAL GRID	
Fecha:		Escala:	
May 2020		1/800	
Plano:		Nº Plano:	
Layout.		Area of competence of each MV	
station.		4	
Angela Venezia <small>Autor proyecto</small>			



Legend	
A	Area
01	PV subfield
	Support
	MV station
	Junction box

TRABAJO FIN DE MÁSTER EN INGENIERÍA INDUSTRIAL

UNIVERSITAT POLITÈCNICA DE VALÈNCIA
ESCUOLA TÉCNICA SUPERIOR INGENIEROS INDUSTRIALES VALENCIA

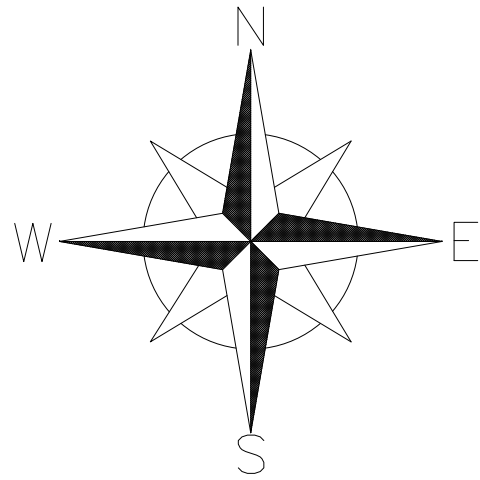
Angela Venezia
Autor proyecto

Proyecto: **FEASIBILITY STUDY AND PROJECT OF A MULTIMEGAWATT PHOTOVOLTAIC PLANT CONNECTED TO THE SPANISH NATIONAL GRID**

Fecha: **May 2020** Escala: **1/800**

Plano: **Layout.** Nº Plano: **5**

Division into photovoltaic subfields.

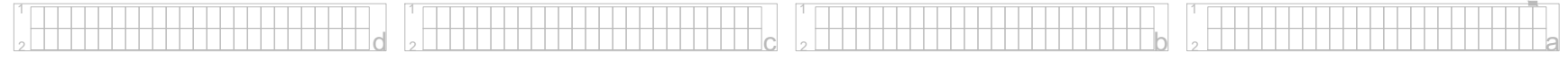
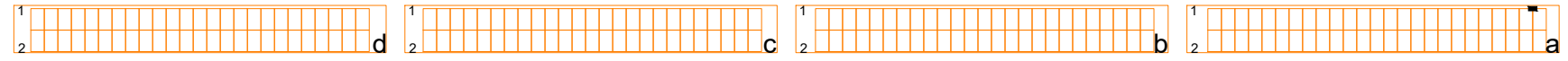
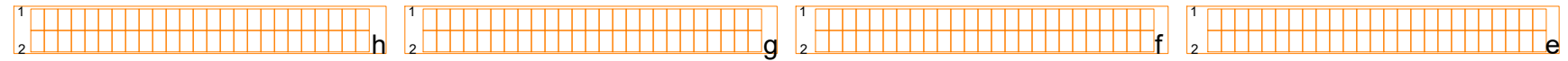
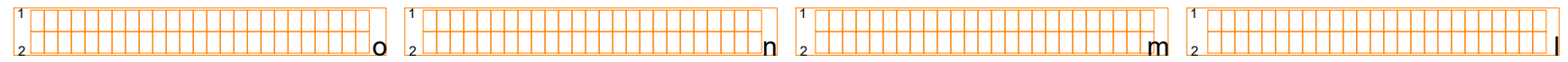
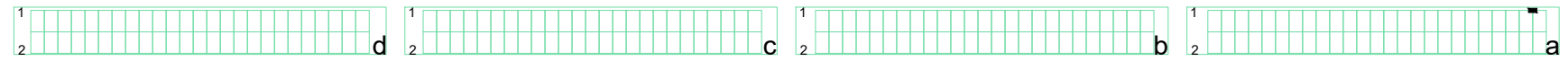
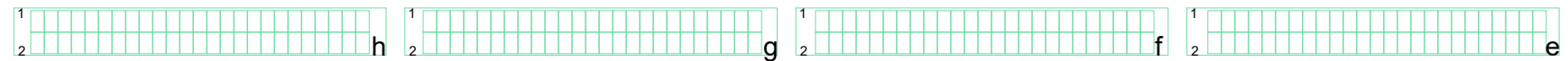


A

01

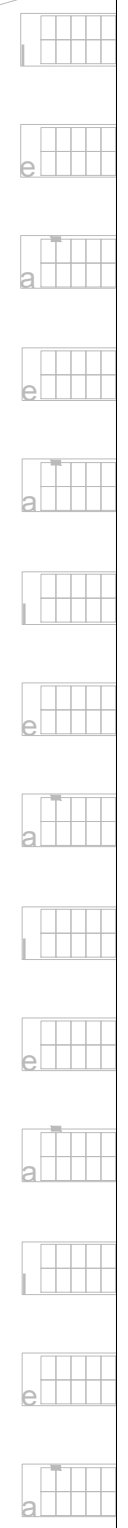
02

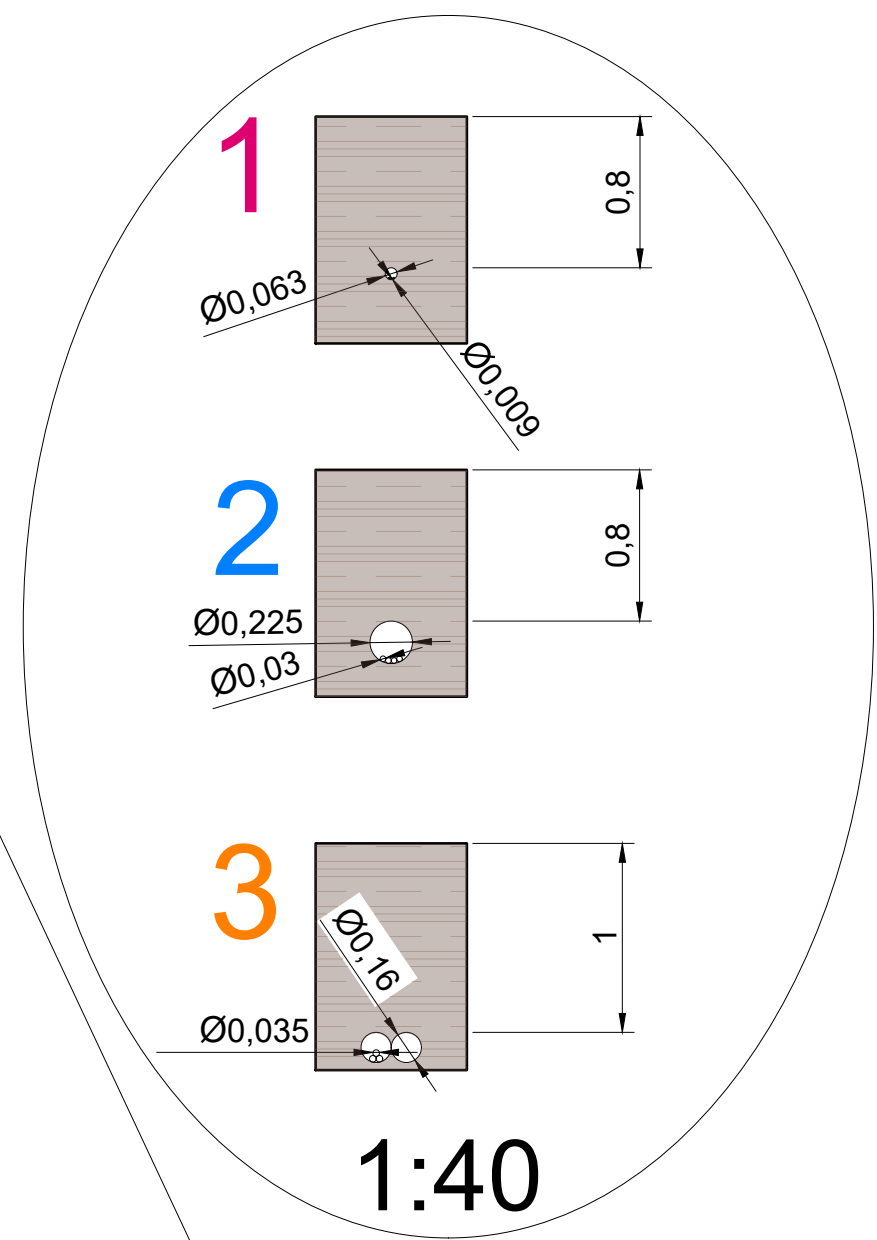
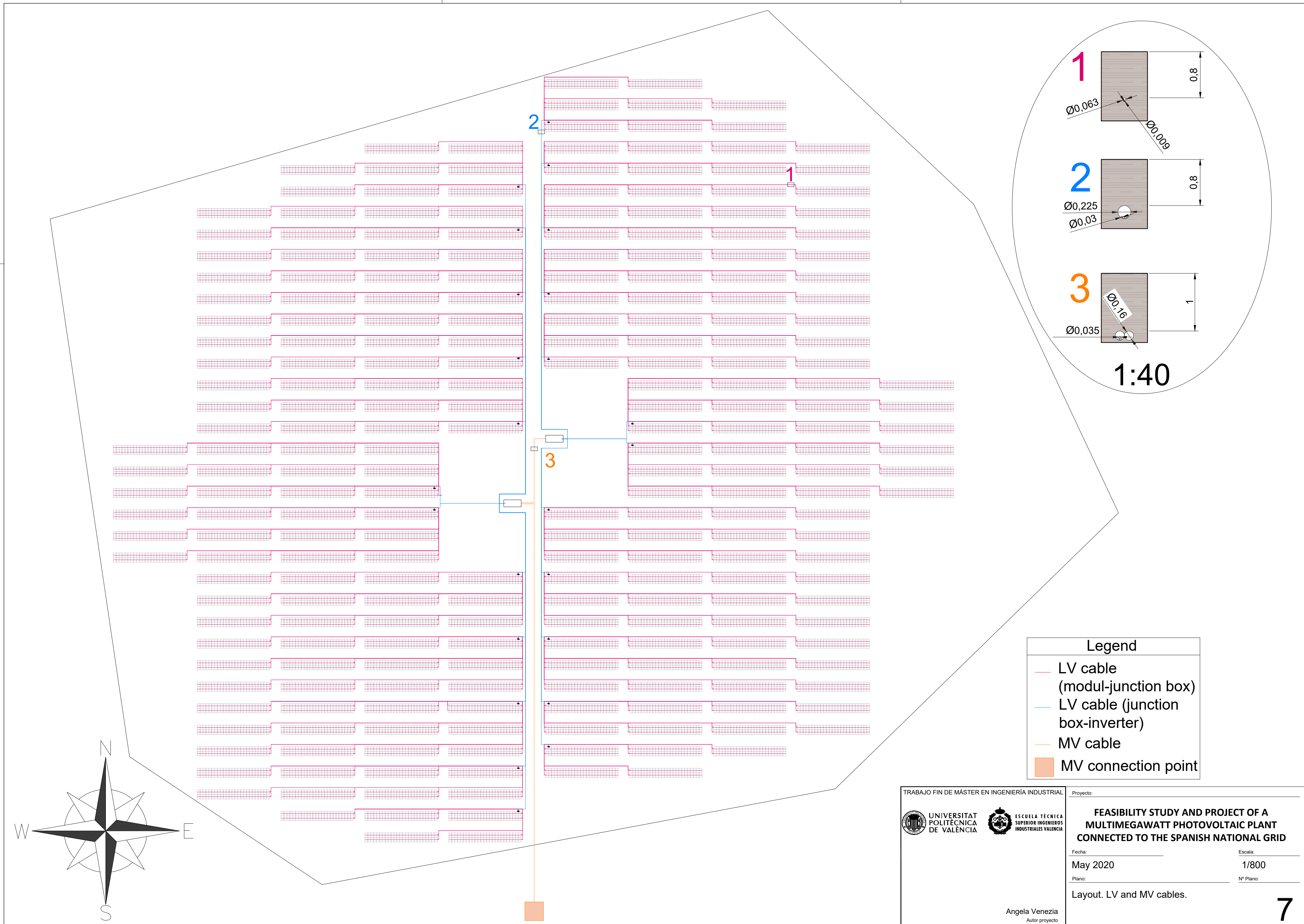
03



Legend

- A** Area
- 01 PV subfield
- a Position of support
- ¹ Upper string
- ² Lower string
- Support
- Junction box





Legend	
	LV cable (modul-junction box)
	LV cable (junction box-inverter)
	MV cable
	MV connection point

TRABAJO FIN DE MÁSTER EN INGENIERÍA INDUSTRIAL



Proyecto:

FEASIBILITY STUDY AND PROJECT OF A MULTIMEGAWATT PHOTOVOLTAIC PLANT CONNECTED TO THE SPANISH NATIONAL GRID

Fecha:

May 2020

Escala:

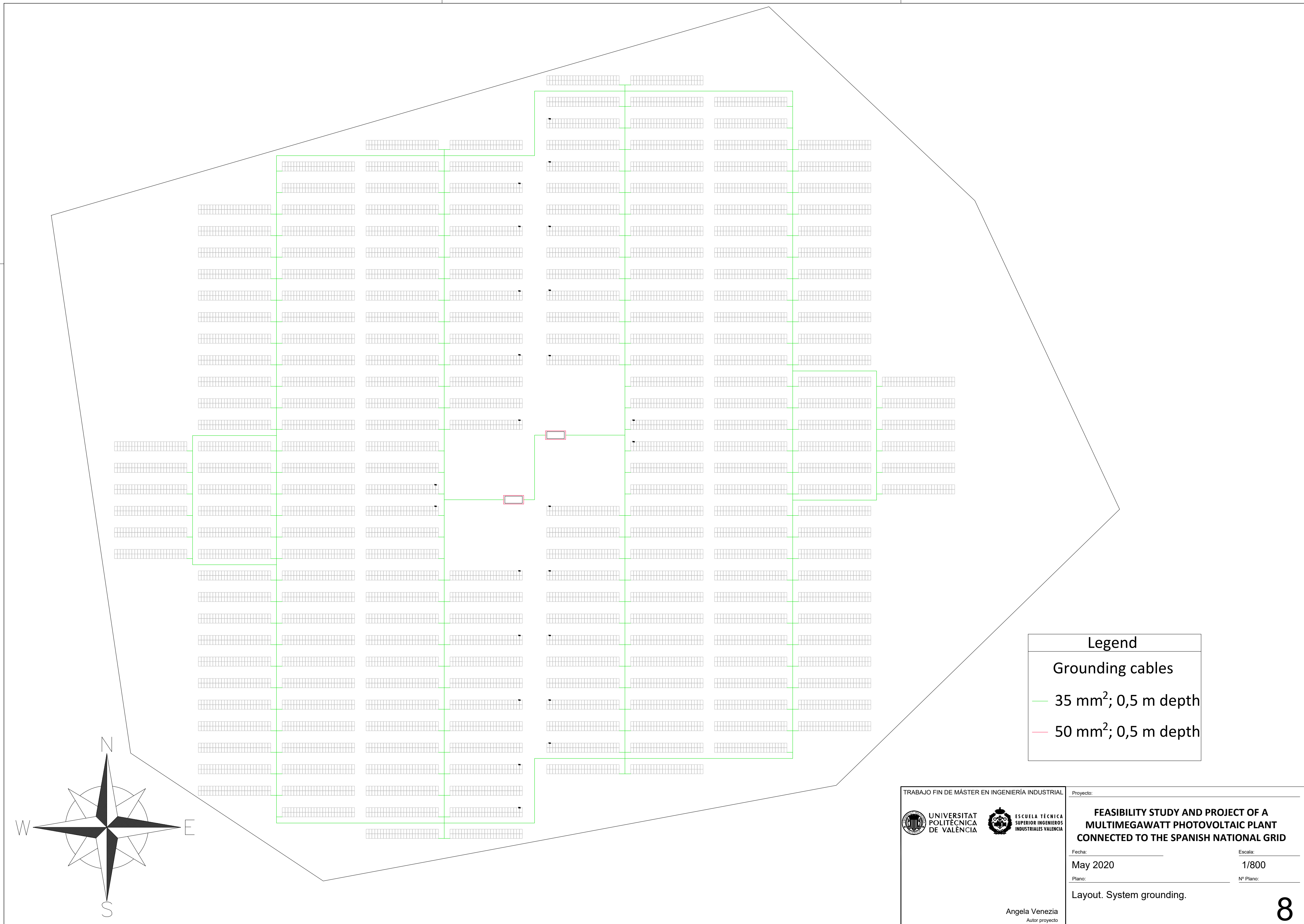
1/800

Plano:

Layout. LV and MV cables.

Nº Plano:

Angela Venezia
Autor proyecto



Legend

Grounding cables

- 35 mm²; 0,5 m depth
- 50 mm²; 0,5 m depth

TRABAJO FIN DE MÁSTER EN INGENIERÍA INDUSTRIAL



UNIVERSITAT
POLITÈCNICA
DE VALÈNCIA



ESCUELA TÉCNICA
SUPERIOR INGENIEROS
INDUSTRIALES VALÈNCIA

Proyecto:

**FEASIBILITY STUDY AND PROJECT OF A
MULTIMEGAWATT PHOTOVOLTAIC PLANT
CONNECTED TO THE SPANISH NATIONAL GRID**

Fecha:

May 2020

Escala:

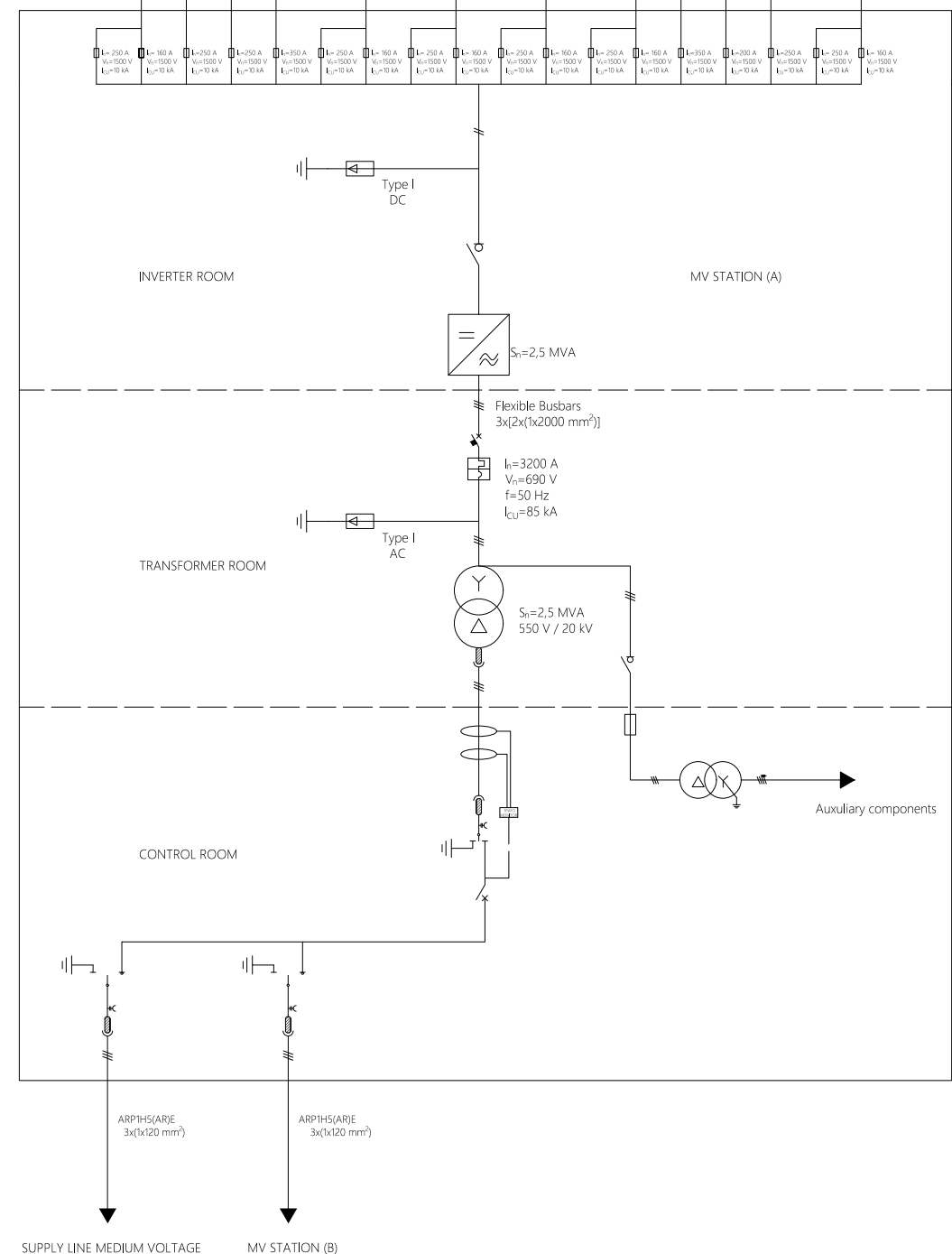
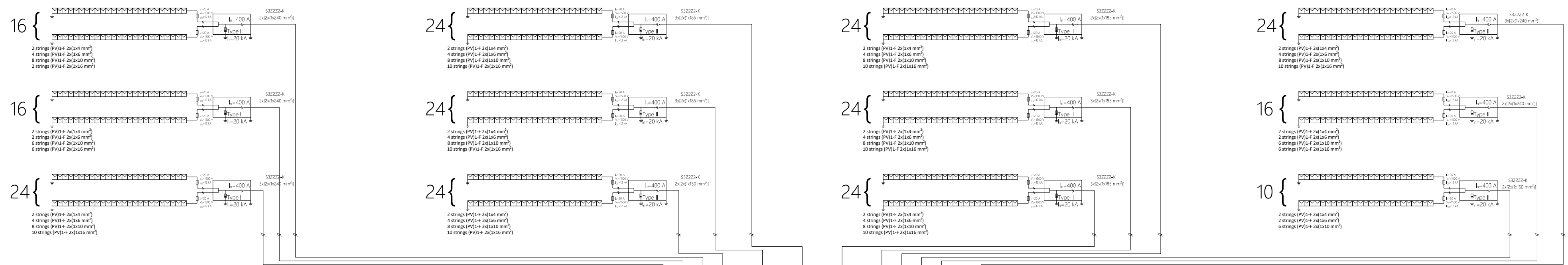
1/800

Plano:

Layout. System grounding.

Nº Plano:

Angela Venezia
Autor proyecto



Legend	
	Modul
	Fuse
	Overvoltage protection (DC/AC sides)
	Switch disconnector
	Grounding
	Circuit breaker
	Inverter
	Trasformador
	Connector
	Capacitive voltage indicator
	Two-way switch

TRABAJO FIN DE MÁSTER EN INGENIERÍA INDUSTRIAL

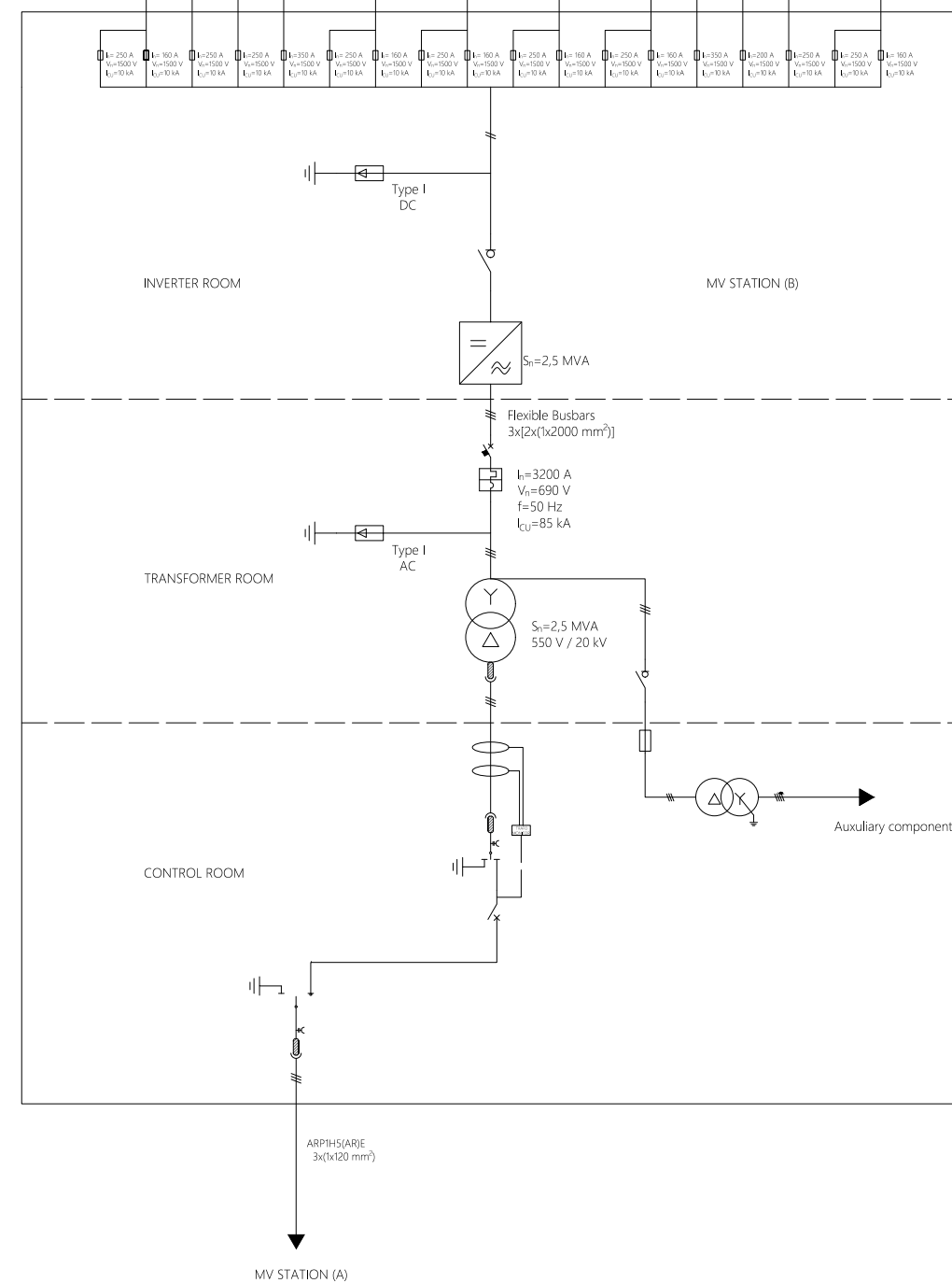
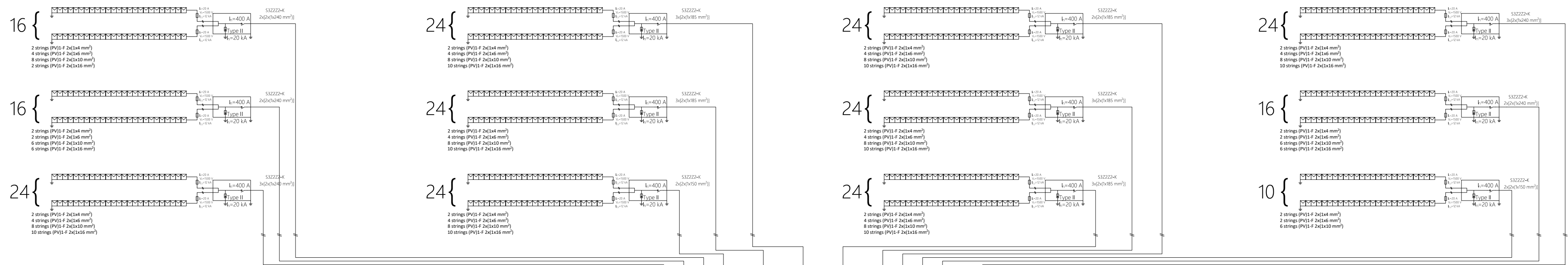


Proyecto: **FEASIBILITY STUDY AND PROJECT OF A MULTIMEGAWATT PHOTOVOLTAIC PLANT CONNECTED TO THE SPANISH NATIONAL GRID**

Fecha: **May 2020** Escala: -

Plano: **Single wire diagram. MV station A.** Nº Plano: -

Angela Venezia
Autor proyecto



Legend	
	Modul
	Fuse
	Overvoltage protection (DC/AC sides)
	Switch disconnector
	Grounding
	Circuit breaker
	Inverter
	Trasformador
	Connector
	Capacitive voltage indicator
	Two-way switch

TRABAJO FIN DE MÁSTER EN INGENIERÍA INDUSTRIAL

UNIVERSITAT POLITÈCNICA DE VALÈNCIA

ESCUOLA TÉCNICA SUPERIOR INGENIEROS INDUSTRIALES VALENCIA

Proyecto: **FEASIBILITY STUDY AND PROJECT OF A MULTIMEGAWATT PHOTOVOLTAIC PLANT CONNECTED TO THE SPANISH NATIONAL GRID**

Fecha: **May 2020**

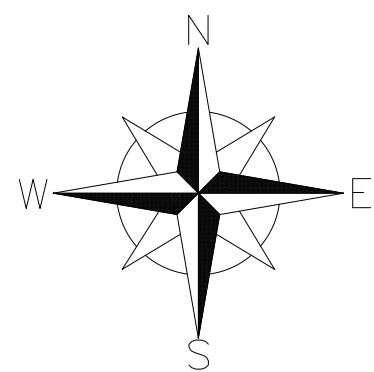
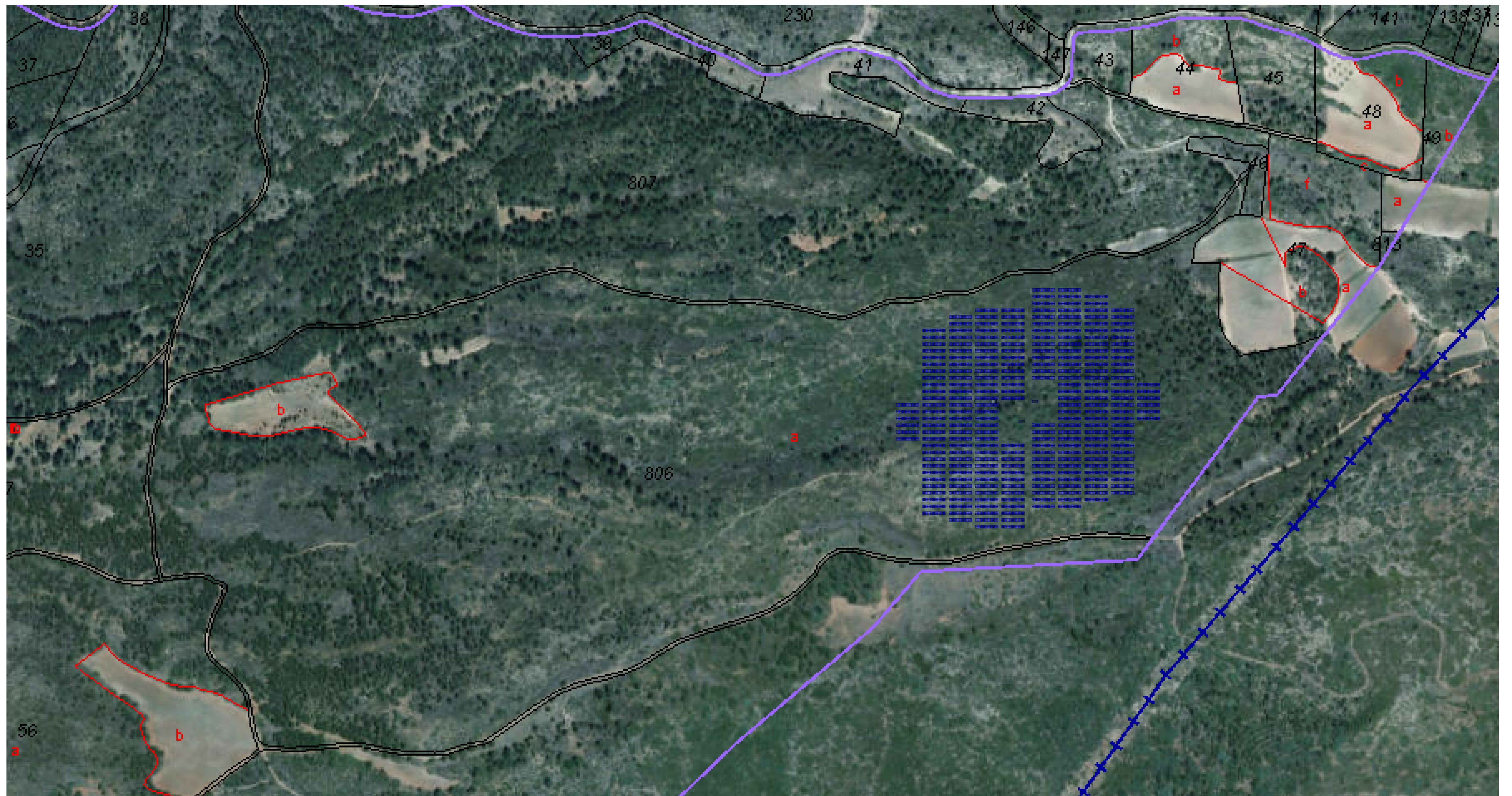
Plano: **Single wire diagram. MV station B.**

Escala: **-**

Nº Plano: **-**

Angela Venezia
Autor proyecto

10



TRABAJO FIN DE MÁSTER EN INGENIERÍA INDUSTRIAL



Proyecto:

FEASIBILITY STUDY AND PROJECT OF A MULTIMEGAWATT PHOTOVOLTAIC PLANT CONNECTED TO THE SPANISH NATIONAL GRID

Fecha:

May 2020

Escala:

1/3000

Plano:

Layout. PV plant in the plot number 806.

Nº Plano:

11

Angela Venezia
Autor proyecto